FOSSIL

DOE/PC/80016-T10
(DE92010947)

IMPROVED FISCHER-TROPSCH CATALYSTS FOR INDIRECT COAL LIQUEFACTION

Final Report

By
R. B. Wilson, Jr.
G. T. Tong
Y. W. Chan
H. W. Huang
J. G. McCarty

February 1989

Work Performed Under Contract No. AC22-85PC80016

For
U.S. Department of Energy
Pittsburgh Energy Technology Center
Pittsburgh, Pennsylvania

By
SRI International
Menlo Park, California

DISCLAIMER

Printed in the United States of America, Office of Scientific and Technical Information, Oak Ridge , Tennessee

DOE/PC/80016--T10

DE92 010947

SRI International

IMPROVED FISCHER-TROPSCH CATALYSTS FOR INDIRECT COAL LIQUEFACTION

February 1989

Final Report

By: R. B. Wilson Jr., G. T. Tong, Y. W. Chan, H. W. Huang, and J. G. McCarty

Prepared for:

UNITED STATES DEPARTMENT OF ENERGY
Pittsburgh Energy Technology Center
P.O. Box 10940
Pittsburgh, Pennsylvania

Attn: Mr. Edgar B. Klunder

Contract No.DE-AC22-85PC80016

SRI Project PYU 1245

Approved by:

D. D. Macdonald, Laboratory Director
Materials Research Laboratory

G. R. Abrahamson
Senior Vice President
Sciences Group

SRI International®

CONTENTS

CONTENTS (continued)

LIST OF FIGURES

LIST OF FIGURES (continued)

LIST OF FIGURES (continued)

LIST OF TABLES

EXECUTIVE SUMMARY

The Fischer-Tropsch synthesis (FTS) reaction is the established technology for the production of liquid fuels from coal by an indirect route using coal-derived syngas ($CO + H_2$). Modern FTS catalysts are potassium- and copper-promoted iron preparations. These catalysts exhibit moderate activity with carbon monoxide-rich feedstocks such as the syngas produced by advanced coal gasification processes. However, the relatively large yields of by-product methane and high-molecular-weight hydrocarbon waxes detract from the production of desired liquid products in the C_5-C_{16} range needed for motor and aviation fuel.

The goal of this program was to decrease undesirable portions of the FTS hydrocarbon yield by altering the Schultz-Flory polymerization product distribution through design and formulation of improved catalysts. Two approaches were taken: (1) reducing the yield of high-molecular-weight hydrocarbon waxes by using highly dispersed catalysts produced from surface-confined multiatomic clusters on acid supports and (2) suppressing methane production by uniformly pretreating active, selective conventional FTS catalysts with submonolayer levels of sulfur.

The objective of the first approach was to produce non-ASF distributions from the FTS reaction by developing ruthenium cluster catalysts that produce "living polymers" and at the same time limit chain growth so that the majority of products fall within the normal motor fuel range (C_6 through C_{15}). We also hoped to achieve this goal by using Ru catalysts and supporting them within zeolites at high pressures to give the "living polymers" and to furthur limit chain growth and stabilize the catalyst metal particle size. In all cases, the metal particle size was to be maintained in the highly dispersed state by strongly anchoring the cluster catalyst precursors to the supports using strong covalent bonds.

Nine supported atomic and multiatomic ruthenium catalysts were prepared via organometallic reactions of tetra- and hexaruthenium hydridocarbonyls and allyl monoruthenium carbonyl complexes with acid sites on three support materials: alumina, sodium Y zeolite, and molecular sieve (Linde 5A). FTS performance was measured for each catalyst in a fixed-bed microreactor under the following reaction conditions: 523 K, 1:1 and 2:1 H_2:CO, and 100 kPa. The activity of these catalysts varied from 2.3 to 21 nanomoles of product per second per gram of catalyst (nmol/s/g cat.). Conventional ruthenium on alumina had activity of 11.5 nmol/s/g cat. under these conditions. The tetraruthenium cluster catalyst supported on alumina had the highest FTS activity but had a methane selectivity of 61%. The hexaruthenium cluster catalyst supported on sodium-Y zeolite had the lowest methane selectivity (36%) and the highest olefin selectivity (ethylene/ethane > 20). The Schulz-Flory-Anderson product distribution and chain growth factors for all ruthenium cluster catalysts through C_8 were nearly independent of support type and cluster size.

Substantial changes in selectivity of potassium-promoted fused iron catalysts were found following treatment to uniformly chemisorb submonolayer quantities of sulfur. After reduction and passivation by accumulation of a surface layer of carbon and chemisorbed CO, approximately 40% of a monolayer of sulfur was slowly adsorbed at 473 K on the fused iron catalyst. The passivating layer was removed and the sulfur locally dispersed by heating to 1000 K in hydrogen. The treated catalyst had a three-fold reduction in methane selectivity relative to the untreated reduced fused iron in 2:1 H_2:CO syngas at 573 K and 100 kPa. The C_2 olefin selectivity approached 100% (C_2H_4/C_2H_6 > 20). The sulfur treatment decreased the C_{2+} production rate at 573 K to only about half the rate of the untreated catalyst per unit area and was comparable to the stationary-stable activity of the fused iron at 523 K.

A low-level sulfur-treated fused iron catalyst (20% monolayer sulfur coverage) was also prepared and tested for FTS activity and selectivity. This sulfur-treated catalyst showed almost a twofold reduction in methane

yield compared with clean fused iron catalyst. The sulfur-treated catalyst also demonstrated good stability, showing no sign of deactivation throughout a 24-h synthesis run. A similar examination was conducted for a fused iron catalyst with 80% of a monolayer of sulfur coverage. This catalyst had comparable FTS selectivity but an order of magnitude loss of activity relative to the low-level sulfur treated catalyst. These results indicate that the alkane production rate was roughly proportional to the cube of the density of the uncovered site, whereas the olefin production rate varied proportionately with the density of the uncovered site.

The medium-level sulfur-treated (50% monolayer sulfur coverage) iron and cobalt catalysts were tested for FTS activity, and the clean-fused iron catalyst was tested as a comparative standard for the fixed-bed reactor operated at high pressure (2 MPa). Of the four catalysts tested for FTS activity at high pressure, the medium-level sulfur-treated fused iron catalyst seems most promising, with a 50% reduction in methane yield, a narrower product distribution (chain growth probability factor, α, was 20% less than that of the clean catalyst under the same reaction conditions), and a threefold increase in olefin selectivity. The sulfur-treated catalyst exhibited behavior at 2 MPa similar to that of the 100-kPa synthesis run; however, olefin selectivity decreased with increasing pressure or temperature.

The monoruthenium supported on molecular sieve and the tetra-ruthenium supported on sodium-Y zeolite had been chosen for slurry reactor study, and the conventional ruthenium supported on alumina and clean-fused iron catalysts was tested for comparison. Of the four catalysts tested for FTS synthesis at high pressure (6.9 MPa), only the conventional ruthenium catalyst exhibited a chain growth factor of 0.88 and a methane selectivity of 6.6%; these findings are typical of slurry reactor results reported under similar conditions. The other three catalysts tested showed chain growth factors from 0.44 to 0.57 and methane selectivity from 20% to 32%. We were not able to determine a chain growth probability factor for these catalysts in the wax range

because the field ionization mass spectrometry (FIMS) results were inconclusive.

A potassium and copper, doubly-promoted precipitated iron catalyst was prepared for evaluation of the effect of sulfur treatment on the methane selectivity and olefin-to-paraffin ratio of light hydrocarbons. Lack of reproducible surface area after reduction and difficulty in measuring metal surface areas complicated efforts to synthesize this catalyst with low sulfur coverage. The FTS activity and methane selectivity of the precipitated iron catalyst was inferior to that of the standard fused iron catalyst. High-level sulfur treatment resulted in a catalyst with greater activity and less suppression of methane than a similar treatment did for the fused iron catalyst, possibly because of nonuniform sulfur poisoning.

There are several technical advantages of direct synthesis of aromatic hydrocarbons with low H_2 syngas. The key difficulty of this approach is deactivation of the FTS component because of carbon deposits. Since we observed that sulfur-treated fused iron resisted deactivation, we extended the scope of our project to include studies of aromatics production with dual-function catalysts.

The synthesis of aromatics was performed on several combinations of Fischer-Tropsch and sodium Y-zeolite catalysts in a fixed-bed reactor with H_2/CO ratio = 0.5, 2.0 MPa pressure, and a temperature range of 548 to 700 K. The medium-level sulfur-treated fused iron and sulfur-treated alumina-supported ruthenium were used as the FTS catalyst components and compared with results for the clean fused iron and clean ruthenium catalysts mixed with zeolite. The mixed catalyst containing sulfur-treated iron initially provided high yields of light oxygenates and aromatics with low yields of olefins, but the selectivity declined rapidly, especially with catalysts containing the more acidic low sodium zeolite components. The rapid decrease in aromatic and oxygenate yield and the increase in olefin yield was probably caused by carbon deposition on the surface of the zeolite component. The catalyst reactivity could be prolonged by using a higher zeolite/FTS catalyst ratio and by using zeolites with higher sodium weight loading.

These results with low H_2/CO syngas compare favorably with prior similar studies performed under less severe coking conditions. Additional work with high silica-shape selective zeolite components to extend the catalyst active life is recommended at high syngas conversion using sulfur-treated iron catalysts.

I CLUSTER-DERIVED FTS CATALYSTS

Introduction

The Fischer-Tropsch synthesis (FTS) reaction is essentially a polymerization reaction as shown in reaction (1) and therefore can be analyzed using techniques developed to understand polymer chemistry.

$$CO + H_2 \longrightarrow [-CH_2-]_n + n\ H_2O \qquad (1)$$

The exact details of the mechanism are still the subject of considerable discussion.[1-4] However, it is generally agreed that FTS is a coordination catalyzed polymerization that proceeds by stepwise insertion of monomers into a metal-polymer bond.[5-9] Therefore, it resembles the Ziegler-Natta catalyzed polymerization of alkenes, which is the most frequently studied example of coordination catalyzed polymerization.[10-13] These two types of coordination catalyzed polymerization reactions are examples of the more general polymerization process called chain polymerization. Chain polymerizations proceed in three distinct steps: initiation, propagation, and termination. For coordination catalyzed polymerizations, termination is usually the elimination of the growing chain from the catalyst, and propagation is the insertion of the monomer unit into the metal-polymer bond, even though the exact nature of the monomer unit is not established for FTS. It is less clear if the analogy between Ziegler-Natta and FTS holds for the initiation step. For the Ziegler-Natta reaction, initiation is the generation of the active catalyst. For FTS, the initiation step is not well established but is generally thought to be reduction of CO to an alkyl (methyl) on the catalyst surface. Table I-1 compares these two coordination catalyzed polymerization reactions.

The last line of Table I-1 demonstrates the reason for the comparison: the product distribution is usually described by the

Table I-1

COMPARISON OF FTS AND ZIEGLER-NATTA REACTIONS

	Ziegler-Natta	Fischer-Tropsch
Reactant:	$RCH{=}CH_2$	$CO + H_2$
Product:	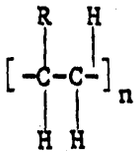	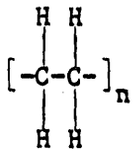
Initiation:	Generate active catalyst	Reduce CO to some active monomer
Propagation:	Monomer insertion	Monomer insertion
	$M{-}R + CH_2{=}CH_2 \longrightarrow M{-}CH_2{-}CH_2R$	$M{-}R + [CH_2] \longrightarrow MCH_2R$
		or
		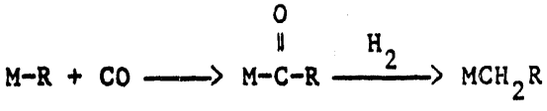
		or
		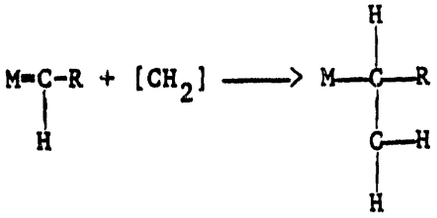
Termination:	β-Elimination (or others) $M{-}CH_2CH_2R \longrightarrow M{-}H + CH_2{=}CH{-}R$	β-Elimination (or others) $M{-}CH_2CH_2R \longrightarrow M{-}H + CH_2{=}CH{-}R$
Product distribution:	Poisson or Schultz-Flory	Schultz-Flory

Anderson-Schulz-Flory (ASF) distribution function for the FTS reaction and by the Poisson distribution function for the Ziegler-Natta reaction. However, the Ziegler-Natta reaction can give product distributions defined by either distribution function depending on the catalyst and polymerization conditions. A clear description of these two distribution functions is given in reference 9. Both are given in terms of mass distribution functions (m_p). The ASF distribution function is

$$m_p = \frac{(1 - \alpha)^2}{\alpha} p\alpha^p \qquad (2)$$

Where α is the probability of chain growth and p is the number of carbon atoms in the growing chain. The average degree of polymerization defined by the ASF distribution is

$$P_n = \frac{1}{1 - \alpha} \qquad (3)$$

The Poisson distribution is

$$m_p = \frac{e^{-\nu}\nu^{(p-1)}}{(p-1)!\ (\nu+1)} \qquad (4)$$

where ν is the average number of growth steps per molecule and is related to average degree of polymerization by

$$\nu = P_n - 1 \qquad (5)$$

The Poisson and ASF distributions are compared in Figure I-1 for the same average degree of polymerization.

As termination reactions become small relative to propagation reactions (i.e., $\alpha \longrightarrow 1$), a condition known as "living polymers," the product distribution is better described by the Poisson distribution.[12] Termination reactions have been virtually eliminated for a few low

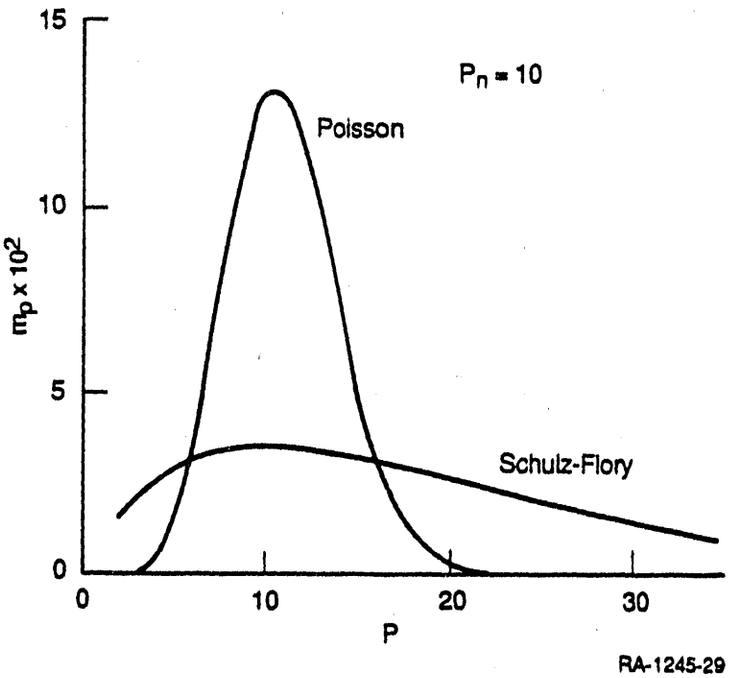

Figure I-1. Comparison of ASF and Poisson distribution for the same average degree of polymerization $P_n = 10$ (from reference 9).

temperature Ziegler-Natta polymerizations,[14] and very narrow product distributions (Poisson) have been observed experimentally for those systems.

However, if termination reactions are eliminated and all other factors held constant, the average number of polymerization steps increases. Extremely high molecular weight polymers would result, as in the case of high-density polyethylene. For Ziegler-Natta reactions, this result is desirable because polyethylene is wanted. However, it is not desirable for FTS reactions in which motor fuel range hydrocarbons are wanted. In Figure I-1, the maximum Poisson distribution and Schulz-Flory distribution is around 10 carbons for an average degree of polymerization (P_n) of 10. King has calculated the effect of P_n on the products of FTS using the ASF distribution function (Figure I-2), which shows that the maximum motor fuel yield is in the range of P_n = 5 to 8.[3] For Ziegler-Natta, P_n can be controlled by limiting the supply of monomer per active catalyst or by quenching at appropriate times after initiation. Neither action is appropriate for FTS operation as a continous process. King discussed alternative ways of limiting P_n that have appeared in the literature.[3] We conclude that to narrow the distribution of products from FTS we must increase the ratio of polymerization reactions to termination reactions (to get a Poisson distribution). However, to maximize the motor fuel yield, the number of polymerization reactions for each product must be limited to less than about 10.

Background

Strategy for Selection of Non-ASF FTS Catalysts

Figure I-3 shows the reaction products observed over a variety of catalysts at the indicated conditions.[15] Ruthenium catalysts have very high chain growth probabilities when operated at low temperatures and high pressures. Pichler et al. have reported the synthesis of polymethylene, whose properties are similar to those of low pressure polyethylene, over an activated ruthenium oxide catalyst at 132°C and

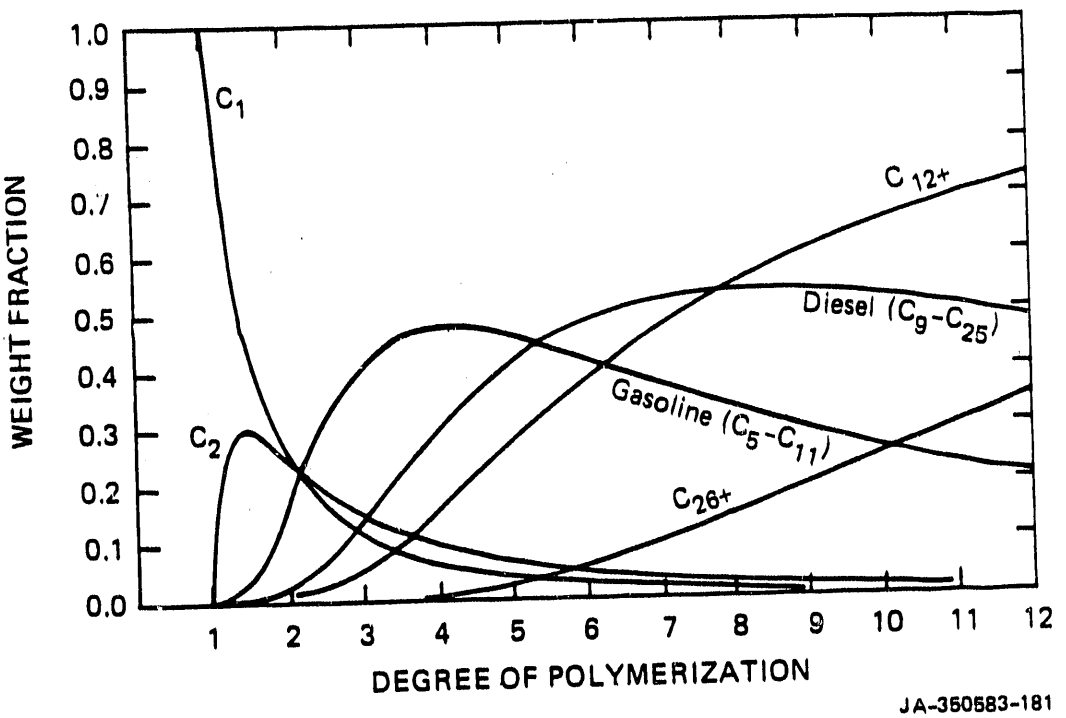

Figure I-2. Effect of average degree of polymerization (P_n) on the product mix for FTS with an ASF distribution (from reference 3).

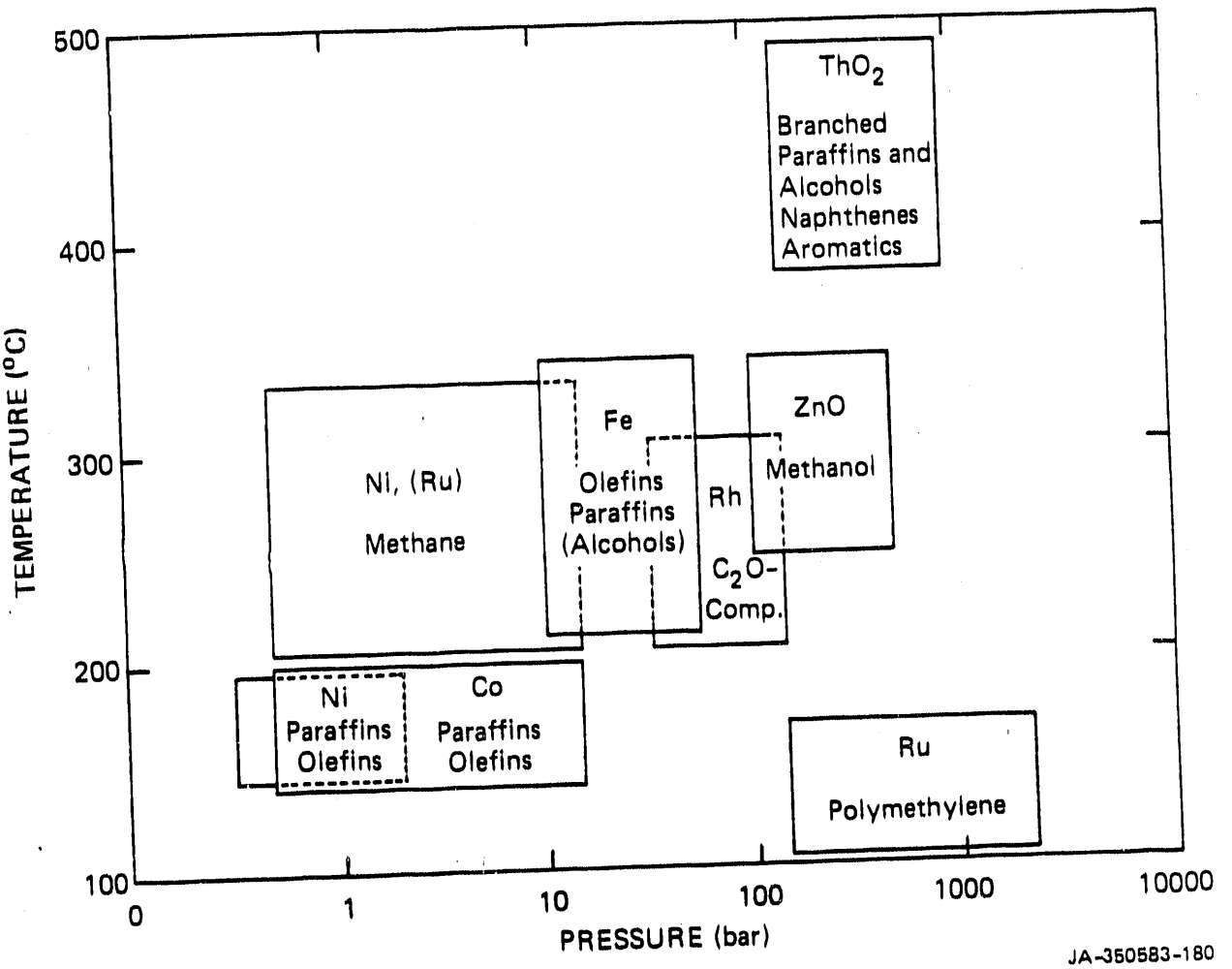

Figure I-3. Operating regimes for FTS catalysts (from reference 15).

1000 atm in a slurry reactor with water as the liquid phase and H_2/CO ratio of 2.[16] The molecular weight of the polymethylene product was reported to be over 100,000. In a similar experiment, Kolbel and coworkers slurried ruthenium metal in water and reacted with CO at 150°C and 200 atm to give parraffin waxes with molecular weight up to 7000.[17] This last reaction is an example of the Kolbel-Engelhardt reaction, which is closely related to FTS because the source of hydrogen is water. Despite the different source of hydrogen, the result is in good agreement with that of Pichler. Madon has also observed product distributions that deviate from ASF, as shown in Figure I-4, over a ruthenium catalyst at more reasonable process conditions of 241°C, 30 atm, and a heterogeneous reactor with space velocity of 193/h.[18] The extreme similarity of Figure I-4 implies that the product distribution observed by Madon is fit best by the Poisson distribution function. These three results strongly imply that over ruthenium catalysts at high pressures the chain termination reactions can be eliminated or significantly reduced so that the distribution approaches Poisson, as observed with Ziegler-Natta catalyzed polyolefin distributions.

Several other researchers have investigated the use of ruthenium as catalyst for FTS. In 1978, D. King compared supported and unsupported Ru and also compared supports.[19] He observed no significant deviations from an ASF distribution operating at 4 atm, 2/1 H_2/CO, and 175°-300°C. However, he reported that the reaction may be "mildly" structure sensitive. Bell and Kellner conducted a thorough kinetic study on alumina-supported Ru at 1-10 atm total pressure, H_2/CO ratio from 1/1 to 3/1, and 500-525 K temperature range.[20] Stowe reported that an Ru on alumina catalyst could be optimized to give a C_{2+} selectivity of 90% and a C_{6+} selectivity of 60%, of which 95% boiled at less than 500°F.[21] F. King and coworkers reported in 1985 a study of low weight loading Ru on alumina (0.3 %) at 210°C, 20-60 atm, and 2/1 H_2/CO ratio, which showed that at high pressures the selectivity to waxes was very high but apparently did not deviate from the ASF distribution.[22] Two reports have appeared on the effect of Ru particle size on FTS product distribution.[23,24] In both cases, hydrocarbon selectivities were greater for larger catalyst particles, although another group found the opposite result.[25]

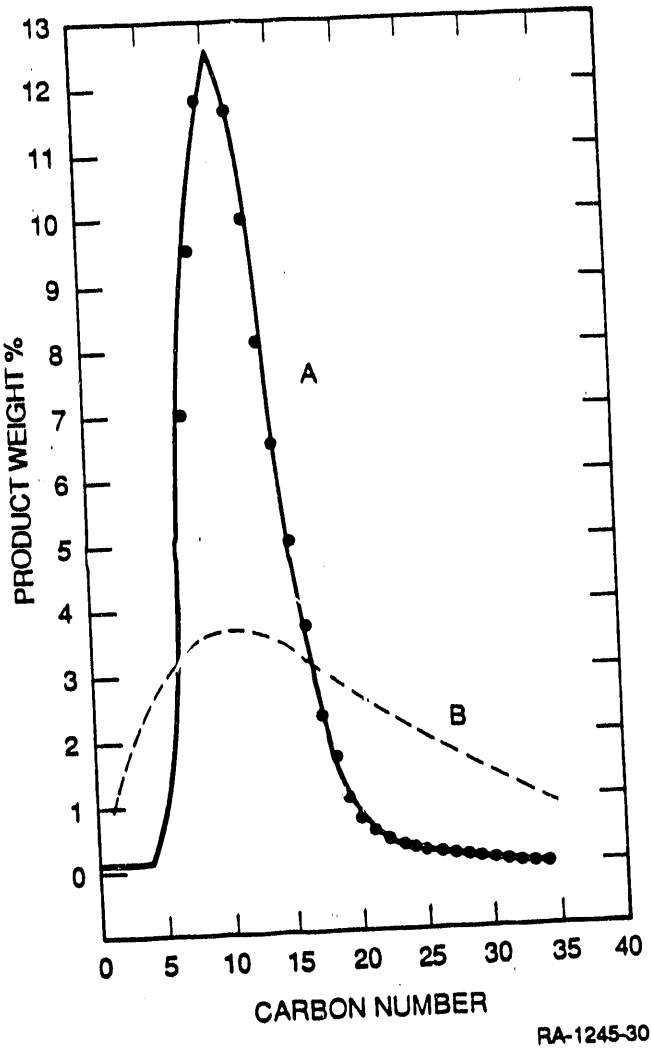

Figure I-4. Comparison of the product distribution (curve A) obtained by Madon over 1% Ru/Al_2O_3 at 241°C, 30 atm, and $H_2/CO = 2$ with the ASF theoretical distribution (curve B) (from reference 18).

Groups at the University of Tokyo and Tokyo Institute of Technology have studied the effect of promoters and particle size on supported Ru catalysts.[25-28] A group at Nagoya University has been studying the effect of nontraditional promoters such as rare earths and early transition metals.[29-33] They have found very high selectivities for C_5 through C_{15} hydrocarbons with rare earth and vanadium-promoted ruthenium catalysts. A second group at the University of Tokyo has been studying Ru-Pt bimetallic catalysts that selectively produce isoalkanes but with ASF product distribution.[34-36]

In 1979 Jacobs published a classical paper claiming that non-ASF distribution has been observed using Ru catalysts supported on zeolites.[37] He proposed that this effect was due to shape selectivity of the zeolite support. His results with Ru were rapidly confirmed for Fe[38] and Co[39] catalysts on zeolite supports. After further study, he changed the reason for non-ASF distributions in the FTS reaction from shape selectivity to an effect of the metal particle size.[40] He and Nijs developed an expanded ASF model that accounted for metal particle size and gave the observed non-ASF distributions by imposing a chain growth limitation related to the particle size.[41] Tkatchenko studied Fe, Ru, and Co on Y-zeolite and attributed selectivity for low-molecular-weight hydrocarbons to small metal particles.[42] Basset and coworkers reported non-ASF distributions on highly dispersed iron catalysts that disappeared as the catalysts aged because of sintering of the metal particles.[43] FTS studies over zeolite supported metals have continued in many laboratories in recent years with mixed results: some researchers have observed non-ASF distributions and others have not.[44-49] References 48 and 41 are most interesting. Lee and Ihm showed that the method of production of the metal particle on the zeolite affected the distribution; catalysts prepared from metal carbonyl precursors demonstrated selectivity.[48] Jacobs carefully studied an iron catalyst prepared from iron pentacarbonyl and Na-Y zeolite.[49] He was able to show that non-ASF distributions were observed only before the steady state, while the metal was being reduced. Once the metal was reduced, it agglomerated into larger particles that gave ASF distributions.

Jacobs and Van Wouwe critically reviewed the literature of non-ASF FTS reactions.[50] They concluded that it is very difficult to show that any reported deviations are real and result from mechanistic considerations rather than experimental artifacts. They suggested several explanations for the deviations and showed mathematically what the effect of each might be. The suggested effects include wax deposition, transient operation, sampling artifacts, secondary reactions, and mechanistic effects. The wax deposition theory is similar in concept to the encapsulation theory for deviations observed in Zeigler-Natta catalysis, which has been discounted.[51] However, for FTS, this effect was calculated by Dictor and Bell[52] with results that closely predict the experimental observations. The transient model has also been studied theoretically in detail.[53]

Since Jacobs's review, several articles have appeared reporting non-ASF distributions. Deviations over ruthenium catalysts were reported by several authors. Leith reports that for ruthenium supported on Y-zeolites, the hydrocarbon product distribution depends on particle size--larger particles give higher activity and higher hydrocarbons.[54] However, a reexamination of his data does not support his conclusion (Table I-2). His data indicate a very poor correlation of activity with particle size as measured by H_2 desorption. For any pair of catalysts using the same support, where differences in particle size were observed in the used catalysts, the activity was <u>greater</u> for smaller particles but the percent of C_{5+} was lower. Fukushima et al. studied Ru on SiO_2 by <u>in situ</u> FTIR techniques[55] and reached the same conclusion as Leith.[56]

Deviations from ASF have been reported for a number of other catalysts. Fujimoto et al.[56,57] report yields of 85% C_2-C_4 paraffins with less than 16% methane from a hybrid catalyst of a physical mixture of Pd/SiO_2 and Y-type zeolite. Fu and Bartholomew report that cobalt supported on alumina results in catalysts whose activity depends linearly on particle size[58] but have no significant deviations from ASF product distributions. Researchers at Mobil have reported the selective production of ethane over a dual-function catalyst composed of HZSM-5 zeolite containing Cr and Zn.[59] The selective formation of ethane has

Table I-2

LEITH'S DATA FOR Ru-Y CATALYZED FTS

Catalyst	Fresh Particle Size (nm)	Used Particle Size (nm)	Activity (mol s^{-1} g^{-1} Ru)	< $\%C_5$
RuMgY-I	4.3	4.9	160.2	23.4
RuNaY-I	4.9	4.6	72.9	19.2
$RuNH_4Y$-I	4.0	3.2	163.8	24.5
RuMgY-II	1.4	2.6	245.2	10.9
RuLaY-I	2.1	2.0	339.6	24.8
RuLaY-II	1.6	2.0	284.8	10.2
RuNaY-II	1.2	2.0	91.9	6.2
$RuNH_4Y$-II	2.3	1.7	247.6	15.4

also been reported by Iwasawa and Ito using a surface-confined mononuclear molybdenum catalyst on silica.[60] Their results are in distinct contrast to those of Somorjai et al., who studied CO hydrogenations over molybdenum single crystals and foils, which yielded primarily methane.[61]

Review of Synthesis Methods

A promising approach to preparing multifunctional catalysts was the unique process of surface confining, which permits the preparation of high-dispersion, high-activity catalysts through the reaction of organometallic compounds with support surfaces. Because the size, configuration, and metal composition of the homogeneous cluster (the catalyst precursor) can be defined a priori, these important parameters of the resulting catalysts are also well defined.

In the surface-confining process, functionalities on the metal cluster precursors are reacted with hydroxyl groups on the surface of the support to produce a surface-bound cluster. This technique has been used to prepare high-dispersion, high-activity catalysts for a wide variety of

reactions including oxidation, olefin metathesis, hydrogenation, reforming, hydrodenitrogenation, and FTS.

Surface-confined organometallic catalysts are prepared from two types of precursors: metal carbonyl clusters and metal hydrocarbyl complexes. Metal carbonyls can be reacted with supports as illustrated in reactions (6) and (7).

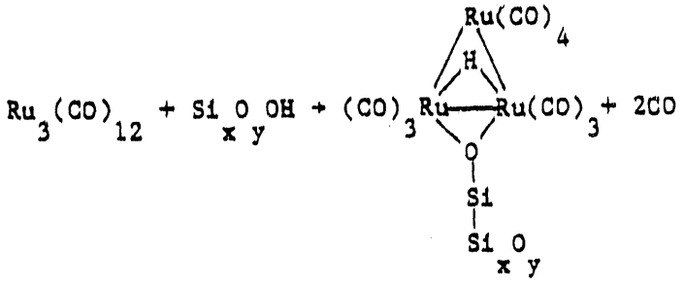

(6)

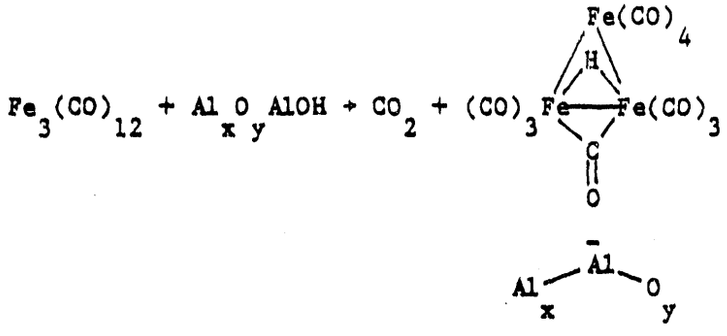

(7)

Metal hydrocarbyl complexes can be surface confined as shown in reaction (8).[62]

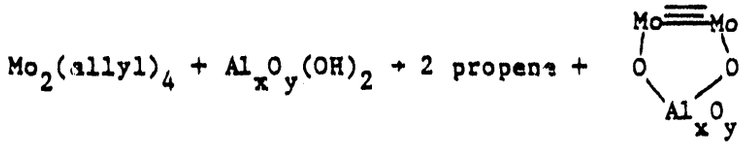

(8)

The preparation of surface-confined catalysts by reaction of organometallic compounds with supports is a rapidly expending area of research that has been the subject of several recent reviews. Researchers in North America and Western Europe have, for the most part, focused their attention on preparing surface-confined catalysts from the reactions of metal carbonyls with supports. The technique of preparing surface-confined catalysts by reacting metal hydrocarbyl complexes with supports has been extensively explored by Russian and Japanese researchers.

This method of catalyst preparation offers significant advantages over traditional impregnation techniques. For example, because the size, configuration, and exact metal composition (for intermetallics) of the organometallic cluster precursor can be designed before confinement, the initial surface-confined particle is totally defined. This feature is particularly useful for mixed-metal catalysts.

Selective control of particle size is a second major advantage of the use of surface-confined catalysts. Catalysts prepared by normal impregnation techniques contain a distribution of particle sizes only partially controllable through the conditions of catalyst preparation. Two problems result from this lack of control. First, the presence of larger clusters can result in a waste of metal in its interior. Second, a distribution of particle sizes can reduce catalyst selectivity. For structure-sensitive catalytic reactions, the particle size distribution can diminish the catalyst's potential selectivity for desired products.

Experimental Results

Synthesis

Surface-confined FTS catalysts were synthesized using a pendant hydrocarbyl functional group that reacts with hydroxyl groups on the surface of an appropriate support material. This work was divided into the following subtasks:

1. Synthesis of hydridocarbonyl ruthenium clusters.

2. Reaction of hydridocarbonyl clusters with alkyl aluminum to give alkyl aluminum carbonyl ruthenium clusters.

3. Reaction of alkyl aluminum carbonyl ruthenium clusters with the support.

4. Synthesis of alkyl complexes of ruthenium.

5. Reaction of alkyl complexes of ruthenium with the support.

Each subtask is described in detail below.

Subtask 1: Synthesis of Hydridocarbonyl Ruthenium Clusters. Three hydridocarbonyl ruthenium clusters, $H_2Ru_3(CO)_{11}$, $H_2Ru_4(CO)_{12}$, and $H_2Ru_6(CO)_{12}$, were synthesized using literature methods. Shore's method[63] was used to synthesize the hexaruthenium clusters.

$$Ru_3(CO)_{12} + Na[Ph_2(CO)] \xrightarrow[25^oC]{THF} 1/2\ Na_2[Ru_6(CO)_{18}] + Ph_2CO + 3\ CO \quad (9)$$

$$Na_2[Ru_6(CO)_{18}] + 2\ HCl \xrightarrow[25^oC]{THF} H_2Ru_6(CO)_{18} + 2\ NaCl \quad (10)$$

The infrared spectrum of $H_2Ru_6(CO)_{18}$ in dicloromethane solution exhibited (n_{CO}) bands at 2058(s), 2052(s), and 2003(w) cm^{-1} as expected. The ^1H NMR of $H_2Ru_6(CO)_{18}$ in CH_2Cl_2 shows a singlet at 8.80 ppm.

We achieved better yields and a purer product for the synthesis of $H_4Ru_4(CO)_{12}$ using our own technique, which involves the direct reaction of $Ru_3(CO)_{12}$ with H_2 in hexamethyldisilazane (HMDS) at elevated temperature.

$$4/3\ Ru_3(CO)_{12} + 2\ H_2 \xrightarrow[135^oC]{HMDS} H_4Ru_4(CO)_{12} + 4\ CO \quad (11)$$

The infrared spectrum of $H_4Ru_4(CO)_{12}$ in cyclohexane solution exhibited the expected CO stretching (n_{CO}) bands at 2081(s), 2067(vs), 2030(m), and 2024(s) cm^{-1}. The ^1H NMR spectrum of $H_4Ru_4(CO)_{12}$ in CH_2Cl_2 showed a singlet at -17.9 ppm.

For the synthesis of $H_2Ru_3(CO)_{11}$, we followed the method reported by Johnson et al.,[64] which entails the reaction of $Ru_3(CO)_{12}$ with sodium borohydride in tetrahydrofuran followed by treatment with acid.

$$Ru_3(CO)_{12} + Na[BH_4] \xrightarrow[25^oC]{THF} Na[Ru_3H(CO)_{11}] + 1/2\ B_2H_6 + CO \qquad (12)$$

$$Na[Ru_3H(CO)_{11}] + HCl \xrightarrow[25^oC]{THF} H_2Ru_3(CO)_{11} + NaCl \qquad (13)$$

The FTIR and NMR results for $H_2Ru_3(CO)_{11}$ indicated the presence of another unknown compound. We also tried Shore's method for the synthesis of this cluster and isolated a less pure compound. Attempts to purify this compound by recrystallization and by column chromatography were not successful. Since we were unable to prepare a pure sample in a reasonable time, we dropped this cluster from the approach.

Subtask 2: Reaction of Hydridocarbonyl Ruthenium Clusters with Alkyl Aluminum. A novel aspect of our approach to the synthesis of strongly bound ruthenium cluster catalysts was the intermediate synthesis of alkyl aluminum ruthenium carbonyl clusters just before reaction with the alumina support. Both the tetraruthenium and the hexaruthenium hydridocarbonyl complexes react readily with triethyl aluminum at room temperature. The reactions were carried out using procedures and techniques published for similar reactions. The reaction stoichiometries were determined by measuring the quantity of ethane produced. Gas chromatography indicated that only ethane was released; no trace of carbon monoxide was detected. Various amounts of ruthenium clusters (from 0.15 to 1.5 mmol) were used to react with excess triethyl aluminum to determine the reaction stoichiometries. For both the tetraruthenium cluster and the hexaruthenium cluster, the results are consistent with the production of one equivalent of ethane.

$$H_4Ru_4(CO)_{12} + Et_3Al \xrightarrow[25^oC]{THF} (Et_2Al)Ru_4(H)_3(CO)_{12} + EtH \qquad (14)$$

$$H_2Ru_6(CO)_{18} + Et_3Al \xrightarrow[25^oC]{THF} (Et_2Al)Ru_6(H)(CO)_{18} + EtH \qquad (15)$$

The reactions were allowed to continue overnight to assure complete reaction. In both cases, the color of the solution changed upon reaction, from yellow [$H_4Ru_4(CO)_{12}$] or purple [$H_2Ru_6(CO)_{18}$] to dark brown. Spectroscopic changes were also observed in the ^1H NMR and IR. These changes are summarized in Table I-3. The reaction of $H_4Ru_4(CO)_{12}$ with Et_3Al in benzene-d_6 was followed by ^1H NMR. New peaks appeared at 5.22 ppm (singlet), 4.10 ppm (AB doublet), and 2.01 ppm (triplet), which are tentatively assigned to the hydride, methylene protons, and methyl protons, respectively, of the $(Et_2Al)Ru_4(H)_3(CO)_{12}$ complex. The infrared spectrum of this new species in THF solution exhibited CO vibrational bands at 2037(m), 2030(m), 2016(s), 1998(s), and 1976(m) cm^{-1}.

Subtask 3: Reaction of Alkyl Aluminum Carbonyl Ruthenium Clusters with the Support. The two alkyl aluminum carbonyl ruthenium clusters, $(Et_2Al)Ru_4(H)_3(CO)_{12}$ and $(Et_2Al)Ru_6(H)(CO)_{18}$, each readily reacted with λ-alumina. The Bronsted acid site density of alumina (1 mmol/g) was determined by titration with ethyl lithium (described in Quarterly Report No. 3). Excess hydroxyl groups were available for reaction with the clusters if the metal loading was less than a few weight percent. The stoichiometries of the surface-confining reaction of the clusters with the supports were again determined by measuring the amount of ethane produced. Again, no carbon monoxide could be detected; only one equivalent of ethane was produced (with respect to the ruthenium cluster used).

$$(Et_2Al)Ru_4(H)_3(CO)_{12} + (AlO)\text{-}OH \quad [support] \xrightarrow[25^oC]{THF} (AlO)\text{-}O\text{-}Al(Et)Ru_4(H)_3(CO)_{12} + EtH \qquad (16)$$

$$(Et_2Al)Ru_6(H)(CO)_{18} + (AlO)\text{-}OH \xrightarrow[25^oC]{THF} (AlO)\text{-}O\text{-}Al(Et)Ru(H)(CO)_{18} + EtH \qquad (17)$$

Elemental analyses of the tetraruthenium cluster and hexaruthenium cluster catalysts on λ-alumina are presented in Table I-4.

Table I-3

FTIR AND NMR SPECTRA OF RUTHENIUM HYDRIDOCARBONYL CLUSTERS

Cluster	FTIR bands (cm^{-1})[a]	NMR peaks (ppm)[b]
$H_4Ru_4(CO)_{12}$	2081(s), 2067(s), 2024(s), 2030(m)	-17.9 (sgl)
$H_2Ru_6(CO)_{18}$	2058(s), 2052(s), 2003(w)	+8.8 (sgl)
$(C_2H_5)_2AlRu_4(H)_3(CO)_{12}$	2016(s), 1998(s), 2037(m), 2030(m), 1976(m)	5.22 (sgl) 4.10 (dbl) 2.01 (tpl)
$(C_2H_5)_2AlRu_6(H)(CO)_{18}$	2059(s), 2025(s), 1993(s), 2044(m), 1972(m), 1960(m), 1947(m)	5.78 (sgl)

[a](s), (m), (w) qualitatively refer to strong, moderate, and weak intensity, respectively, in the FTIR spectra.

[b](sgl), (dbl), (tpl), refer to singlet, AB doublet, and triplet peaks, respectively, in C_6D_6 solvent.

Table I-4

ELEMENTAL ANALYSIS OF RUTHENIUM CLUSTER CATALYSTS SUPPORTED ON λ-ALUMINA

Cluster	Ru	C	H
Ru_4	0.61	5.09	1.04
Ru_6	1.26	9.77	1.84

[a]Balance: Al, O, or Al_2O_3.

Subtask 4: Synthesis of Alkyl Complexes of Ruthenium. A monomeric ruthenium complex $[(allyl)_2Ru(CO)_2]$ was synthesized using literature procedures.[65,66] The procedure for synthesizing this compound is shown in the following equations:

$$Ru_3(CO)_{12} + 3\ (allyl)Br \longrightarrow 3\ (allyl)Ru(CO)_3Br + 3\ CO \quad (18)$$

$$(allyl)Ru(CO)_3Br + 2NaHg \longrightarrow Na^+[(allyl)Ru(CO)_3]^- + NaBr \quad (19)$$

$$Na^+[(allyl)Ru(CO)_3]^- + (allyl)Br \longrightarrow (allyl)_2Ru(CO)_2 + CO + NaBr \quad (20)$$

Allyl bromide reacts with ruthenium carbonyl in high yield to give $(allyl)Ru(CO)_3Br$ in high yield as reported.[66] The bromide can be reduced to the isolatable anion $[(allyl)Ru(CO)_3]^-$ using sodium amalgam. This anion reacts with allyl Grignard to give the desired product $[(allyl)_2Ru(CO)_2]$. A coproduct of the last reaction is carbon monoxide. We collected one equivalent of gas identified as CO by gas chromatography (GC). One reason we quantified the CO was to convince ourselves that we could quantify and correctly identify any CO given off in the subsequent reactions of the clusters with the supports.

Subtask 5: Reaction of Alkyl Complexes of Ruthenium with the Support. Monomeric ruthenium cluster catalysts were prepared on all three support materials, alumina, Na-Y zeolite, and molecular sieve zeolite, by reaction with $(allyl)_2Ru(CO)_2$ in THF solution at 25°C. No evolved gas product (e.g., propylene, propane, carbon monoxide) could be detected for reaction with λ-alumina. Therefore, the metal complex may have simply absorbed on the support.

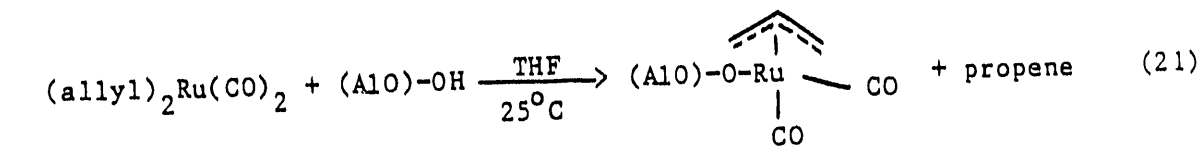

(21)

Elemental analyses of the monomeric Ru catalysts on all supports were performed by a commercial analytical laboratory (Galbraith Laboratory). The results showed ruthenium loadings ranging from 0.31 wt% for Ru/Na Y-zeolite to 0.37 wt% for Ru/λ-alumina.

Characterization

The supported catalysts were characterized by elemental analysis, FTIR, temperature-programmed desorption (TPD), and synthesis reaction stoichiometry. During the synthesis reaction, we measured loss of one ethylene per cluster and no loss of H_2 or CO. Therefore, the resulting supported catalysts were very similar in structure to the starting complexes. The FTIR confirms this. The diffuse reflectance FTIR of the alumina-supported hexameric cluster is shown in Figure I-5 as an example (the carbonyl stretching region is shown by the Kubelka-Munk expression). Three carbonyl stretching bands are observed at 2033, 2027, and 1970 cm^{-1}. These peaks are shifted by ~23 cm^{-1} from their position for the unsupported cluster. The peaks are approximately equal in intensity for the supported cluster, in contrast to the pattern of two strong and one weak observed in the spectra of the unsupported cluster.

The catalysts were analyzed by TPD in situ in the FTS reactor. The catalysts were tested from 300 to 573 K in a helium or hydrogen carrier gases at 0.167 K/s or 0.083 K/s. Figure I-6 shows the evolution of

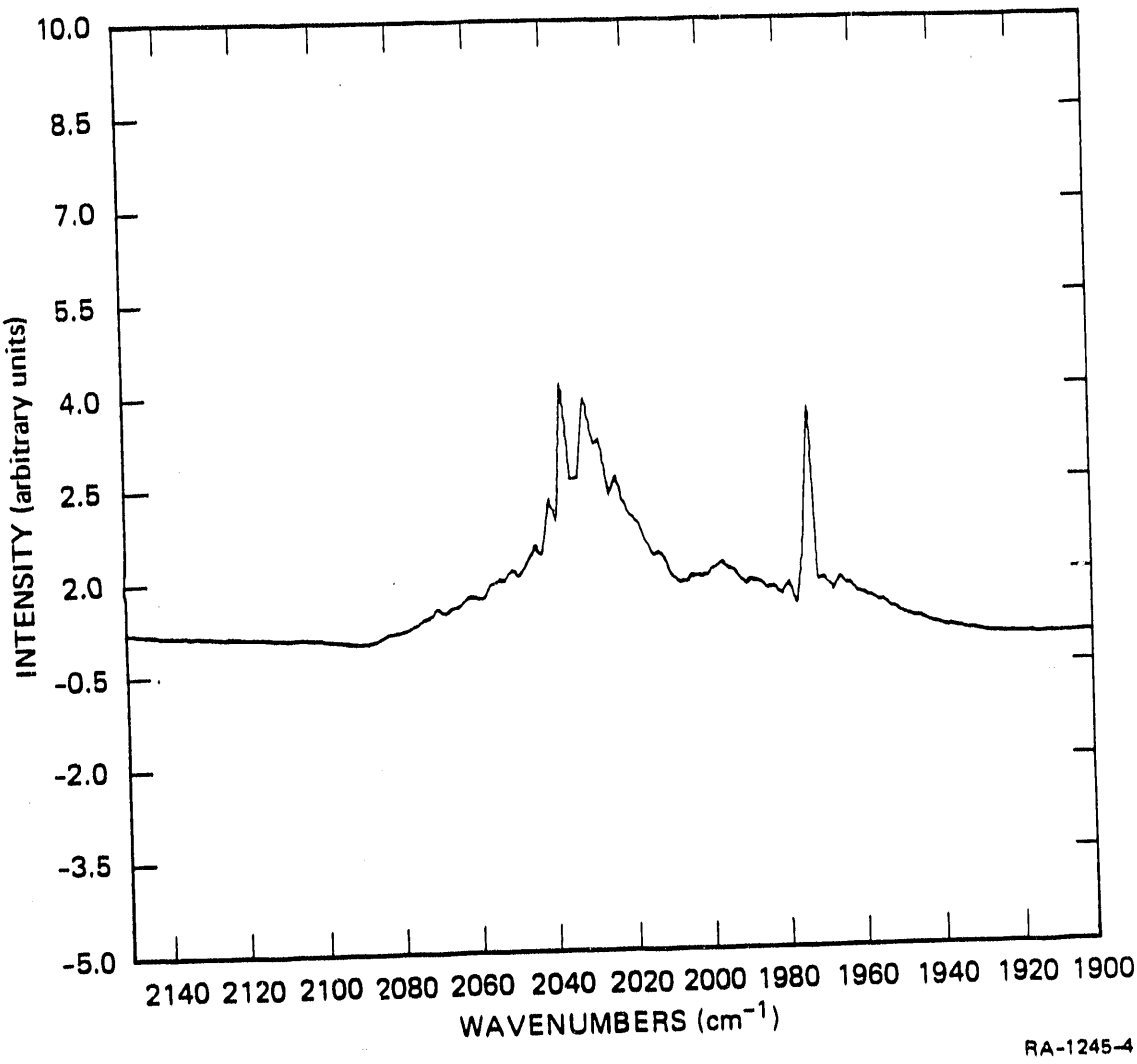

Figure I-5. Diffuse reflectance FTIR spectra for alumina-supported ruthenium hexameric carbonyl cluster catalyst before activation.

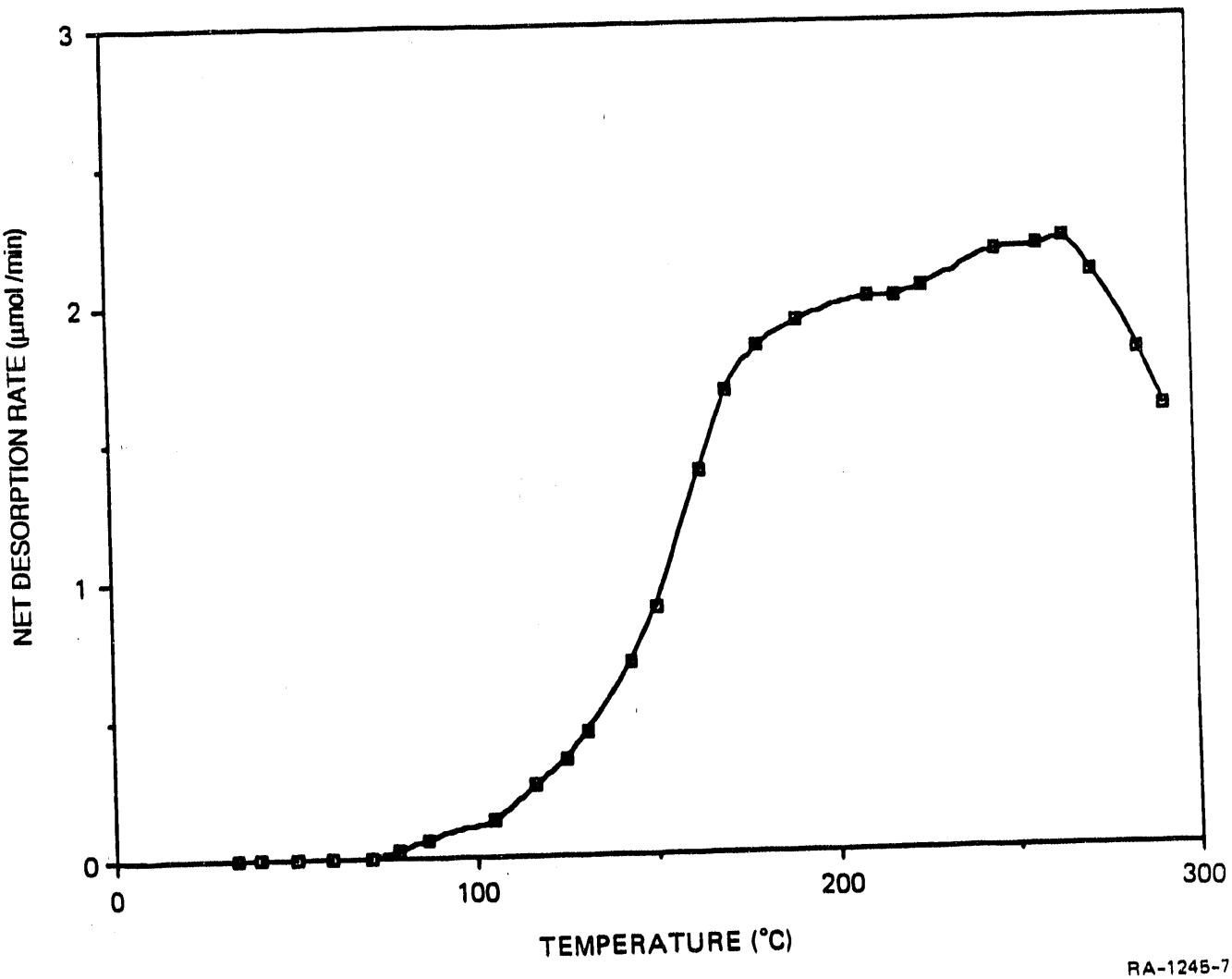

Figure I-6. Temperature-programmed desorption of Mass 28 for surface-confined ruthenium hexamer cluster catalyst.

Mass 28 starting at approximately 100°C at 0.167 K/s from the hexameric cluster catalyst in helium. This curve is indicative of continued reaction with the support upon heating. Most catalysts studied at 0.083 K/s in He showed onset of ethene evolution at approximately 433 K. At higher temperatures, C_1 and C_3 hydrocarbons were detected. TPD results are summarized in Table I-5. Temperature-programmed reaction (TPR) of all of these catalysts was also performed in 0.1 MPa hydrogen at 0.167 K/s. Methane was detected, and the reaction appeared to go to completion, indicating complete removal of the carbonyl ligands. Subsequent to activation, the catalyst was unloaded from the reactor and examined by FTIR to determine structural changes and sent for elemental analysis to

Table I-5

He TPD OF RUTHENIUM CLUSTER CATALYSTS
AT 5°/min UP TO 300°C

Catalyst	Temperature (°C)	Ethane or Ethylene (ppm)	Propane or Propylene (ppm)
Ru_5/5 Å mol, sieve	300°C	23.16	
Ru_6/Al_2O_3	250°C	44.31	
Ru_4/5 Å mol, sieve	250°C	56.61	
Ru_4/Na-Y zeolite	200°C	31.4	
Ru_4/Al_2O_3	200°C	47.0	
Ru/5 Å mol, sieve	260°C		35.9
Ru/LZY-52 zeolite	286°C		170.5
Ru/Al_2O_3	240°C		100.2

determine extent of changes in metal loading. Figure I-7 shows the FTIR of the hexameric cluster on alumina after He TPD to 300°C. Three broad bands are observed in the region from 2090 to 1910 cm^{-1}. The intensities of these absorptions are considerably smaller than observed for the

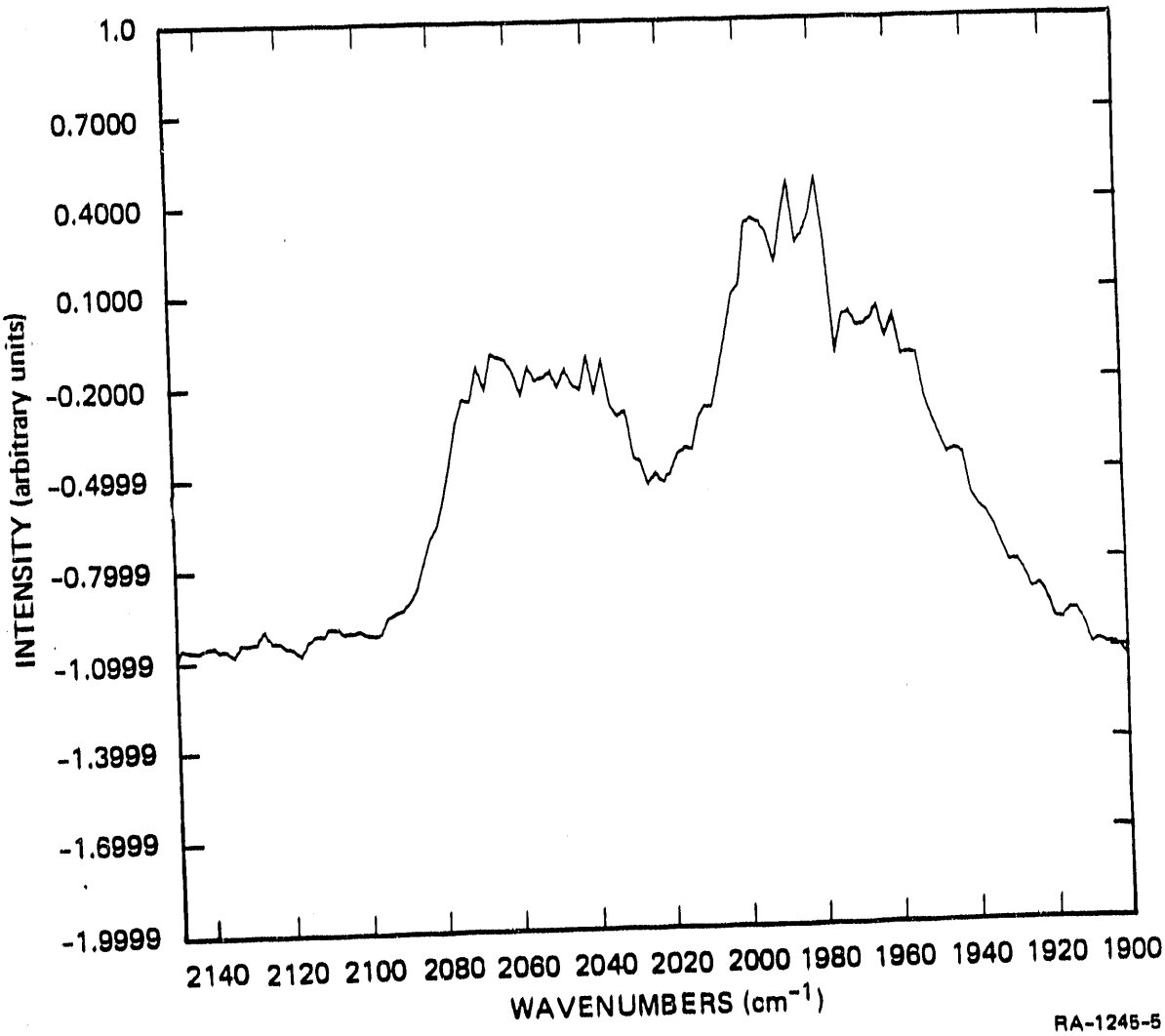

Figure I-7. Diffuse reflectance FTIR spectra for alumina-supported ruthenium hexameric carbonyl cluster catalyst after TPD.

sample before TPD, indicating loss of CO ligands. The loss of terminal CO stretching bands is most noticeable in the FTIR spectra, but new CO bridging bands appear. These changes in the FTIR spectra are indicative of major changes in structure caused by heating.

Catalysis

Fixed-Bed Reactor. A continuous flow quartz microreactor (Figure I-8) was used for FTS reaction studies. The catalyst sample (0.2 to 0.5 g) was placed on a fritted quartz disk located inside the reactor. Gaseous reactants fed to the reactor were purified: syngas, by passage through a molecular sieve trap cooled by dry-ice acetone; hydrogen, by diffusion through a Pd-Ag thimble; and helium, by passage through an oxygen trap. A quartz-sheathed chromel-alumel thermocouple situated in the catalyst bed continuously monitored the reactor temperature.

The FTS reaction was conducted with 0.1 MPa syngas. Syngas compositions of 2/1 and 1/1 (H_2/CO) were used. Reaction temperatures of 550 K and 573 K were used. A gas hourly space velocity of up to 12,000 was used to maintain approximately 10% conversion of carbon monoxide. The effluent from the reactor was continuously monitored by a quadrupole mass spectrometer and two gas chromatographs. The mass spectrometer and the automated two-column gas chromatograph (Carle) were used to follow the yield of methane, ethane, ethylene, carbon dioxide, and the overall CO conversion rate. Aliquots (0.1 mL) were withdrawn from the effluent of the reactor and injected into a second temperature-programmable gas chromatograph (Hewlett-Packard) with a wide-bore capillary column operating at 390 K and a flame ionization detector for analysis of higher hydrocarbons. The product distribution up through carbon number C_{12} could be measured with the dual GC system. The entire sampling system was wrapped with heating tape to prevent condensation of higher hydrocarbons.

The hydrocarbon reaction rate R is defined as the number of nanomoles of carbon monoxide converted into C_1 through C_{10} hydrocarbon per gram of catalyst per second. The selectivity S is defined as the

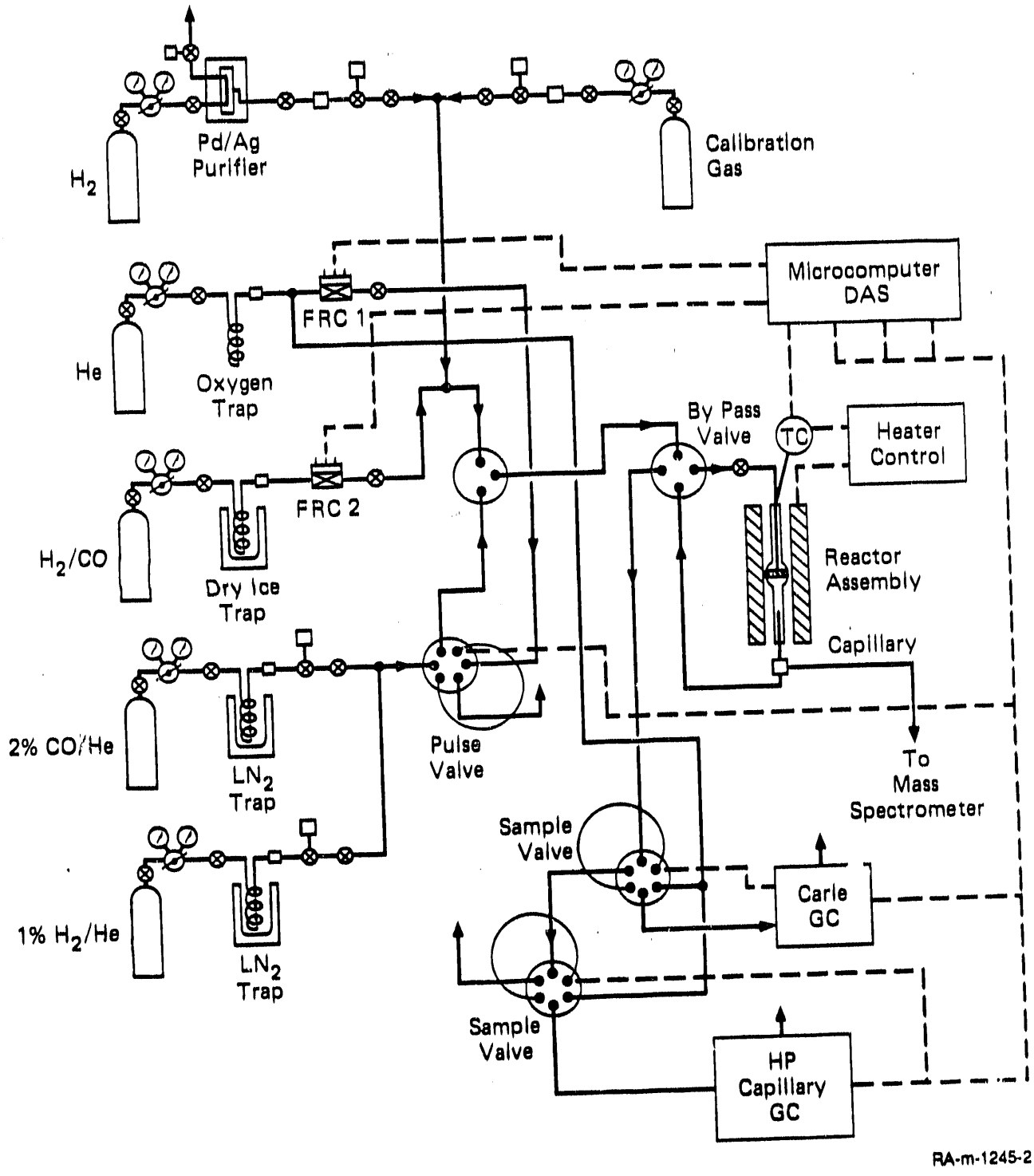

Figure I-8. Catalyst characterization and testing apparatus.

ratio of the rate of formation of methane relative to the overall hydrocarbon reaction rate for C_1 through C_{10} products (on a carbon-atom basis).

At 573 K using 2/1 H_2/CO synthesis gas, the ruthenium catalysts have very high selectivity for methane. The organometallic derived catalysts were more active than the conventional Ru catalyst. The activity at 523 K and 1/1 H_2/CO is summarized in Table I-6.

Slurry-Phase Reactor. The FTS activity and selectivity in the slurry phase were examined for four catalysts: the allyl-derived Ru monomer on a molecular sieve support, the aluminum-hydridocarbonyl-derived Ru_4 cluster catalyst on an Na-Y zeolite support, a conventional Ru catalyst on alumina, and the fused iron standard catalyst (Table I-7). The reactor set-up was similar to that used by Huff and Satterfield.[67] In a 300-mL slurry reactor, 2 g of powdered catalyst was used with 50 g of n-octocosane wax ($n\text{-}C_{28}H_{58}$, 99%, Alfa Chemical) with 1:1 $CO:H_2$ syngas at 60 atm and 483 K (10 K) for 48 h. The gas outlet was connected to a high temperature trap (100°C). The hydrocarbon distribution of the product gas up through C_4 was directly analyzed periodically by capillary GC with FID detection. Condensation in the sample lines precluded observation of hydrocarbon above butane.

The liquid product distribution was analyzed by FIMS after the synthesis run. We were unable to detect higher hydrocarbons from any of these slurry runs because of the high concentration of the n-octocosane. (Calibration of the FIMS technique using FTS wax provided by Professor Satterfield of MIT is described in Section II.[68])

Discussion

The organometallic derived catalysts showed activity similar to that observed for the conventional ruthenium catalyst in fixed-bed tests at 523 K as shown in Table I-6. The most active catalysts were the tetrameric ruthenium cluster on alumina and sodium Y-zeolite, followed by the monomeric ruthenium on 5-Å molecular sieves. However, under these conditions all the catalysts gave distributions that were not

Table I-6

FTS PERFORMANCE OF RUTHENIUM CLUSTER AND CONVENTIONAL RUTHENIUM CATALYSTS

Catalyst	Ru/Na-Y Zeolite 0.31 wt% Ru	Ru_4/Na-Y Zeolite 0.61 wt% Ru	Ru_6/Na-Y Zeolite 0.20 wt% Ru	Ru/5A Molecular Sieve 0.37 wt% Ru	Ru_4/5A Molecular Sieve 0.49 wt% Ru	Ru_6/5A Molecular Sieve 0.19 wt% Ru	Ru/Al_2O_3 0.35 wt% Ru	Ru_4/Al_2O_3 0.61 wt% Ru	Ru_6/Al_2O_3 1.2 wt% Ru	Conventional Ru/Al_2O_3 0.50 wt% Ru
Temperature (K)	523	523	523	523	523	523	523	523	523	523
Pressure (MPa)	0.01	0.01	0.01	0.1	0.1	0.1	0.1	0.1	0.1	0.1
H_2/CO ratio	1	1	1	1	1	1	1	1	1	1
Run duration (h)	24	16	20	24	24	24	24	19	22	24
Product rate[a] (nmol/s/g cat)										
CO_2	2.31	2.96	3.68	3.16	2.25	2.73	1.09	2.73	4.03	2.1
C_1	3.54	7.63	0.78	12.19	6.68	4.41	2.82	12.67	9.23	6.32
C_2	0.47	0.994	0.158	0.81	0.81	0.87	0.51	1.19	0.87	0.65
C_3	0.55	1.044	0.27	0.57	0.7	0.56	0.594	1.05	0.76	0.684
C_4	0.22	0.392	0.104	0.155	0.24	0.19	0.198	0.33	0.29	0.23
C_5	0.77	0.138	0.012	0.029	0.091	0.053	0.058	0.12	0.114	0.081
C_6	0.75	0.066			0.047	0.028	0.022	0.068	0.073	0.04
C_7	0.48	0.033			0.032	0.0088	0.007	0.031	0.039	0.019
C_8	0.26	0.017			0.016	0.004	0.005	0.015	0.021	0.008
C_9					0.0091			0.0053	0.0073	0.004
C_{10}					0.0074			0.0043	0.0058	
TOTAL	8.39	15.77	2.382	16.29	12.605	9.117	6.93	20.958	15.983	11.51
Chain Growth Factor[b]	0.57	0.48		0.23	0.46	0.39	0.37	0.45	0.43	0.47
Olefin to Paraffin Ratio[c]	2.02	1.2		1.4	0.77	1.3	3.2	1.1	1.1	1.3
Methane Selectivity[d]	45	52	36	77	56	52	44	61	63	58

[a] GHSV = 600 h^{-1}; Product rate for each carbon number includes n-paraffins and α- and β-olefins; total product rate is on a carbon-atom basis.

[b] Average chain growth parameter (α) for C_{3+} hydrocarbons.

[c] Average olefin to paraffin ratio for C_2 to C_6 hydrocarbons.

[d] C_1 rate/(total rate) x 100%.

Table I-7

RESULTS OF SLURRY REACTOR FTS EXPERIMENTS

Catalyst	Clean Fused Iron	Ru_4/Na-Y Zeolite 0.61 wt% Ru	Ru/5A Molecular 0.37 wt% Ru	Conventional Ru/Al_2O_3 0.50 wt% Ru
Temperature (K)	493	493	493	493
Pressure (MPa)	6.9	6.9	6.9	6.9
H_2/CO ratio	1	1	1	1
Run duration (h)	48	48	48	48
CO_2	90.932	15.932	0.262	1.094
C_1	11.629	9.031	0.536	0.24
C_2	6.211	2.215	0.106	0.0063
C_3	5.91	1.349	0.041	0.022
C_4	3.23	0.568	0.0176	0.0187

[a]GHSV = 600 h^{-1}; Product rate for each carbon number includes n-paraffins and α- and β-olefins; total product rate is on a carbon-atom basis.

[b]Average chain growth parameter (α) for C_{3+} hydrocarbons.

[c]Average olefin to paraffin ratio for C_2 to C_6 hydrocarbons.

[d]C_1 rate/(total rate) x 100%.

significantly different from that of ASF. The methane selectivity was in the range of 36 to 77 mol%. To more closely approach the condition of "living polymers," we had to increase the pressure. This was done in a slurry reactor at approximately 60 atm. We compared a clean fused iron and a conventional ruthenium catalyst to the tetraruthenium on Y-zeolite and the mononuclear ruthenium on 5-Å molecular sieves (Table I-7). Of the four catalysts tested, the iron and the Ru_4/Na-Y-zeolite showed very high activity, whereas the mononuclear Ru and the conventional Ru showed very low activity. Only the conventional Ru showed high chain growth probabilities and low methane selectivities that would be expected for slurry reactions. In no case could we observe any wax products in the slurry by FIMS after 48 h.

Unfortunately, the results of the slurry reactor experiments neither deny nor verify the hypothesis that the cluster catalysts can produce a narrowed FTS product distribution. The FIMS analysis of slurry liquid samples at the end of the experiments was not adequate even to resolve the high-molecular-weight product distribution for the conventional catalysts, and we could not have expected to measure the product distribution in the C_{12+} range for the cluster catalysts. Additional slurry runs with much longer reaction time (at least 200 h) must be performed in future work to test the cluster hypothesis. However, the low chain growth factor and the presence of light alkanes in the gaseous product indicates that we may not have reached the state of "living polymers."

References

1. M. E. Dry and J. C. Hoogendoorn, Catal. Rev. 23, 265 (1981).

2. M. E. Dry, "The Fischer-Tropsch Synthesis," in Catalysis Science and Technology, J. B. Anderson and M. Boudart, Eds. (Springer-Verlag, 1981), p. 159.

3. D. L. King, J. A. Cusumano, and R. L. Garten, Catal. Rev. 23, 203 (1981).

4. A. T. Bell, Catal. Rev. 23, 203 (1981).

5. C. K. Rofer-DePoorter, Chem. Rev. 31, 447 (1981).

6. P. Biloen and W.M.H. Sachtler, Adv. Catal. 30, 165 (1981).

7. H. H. Starch, N. Golumbic, and R. B. Anderson, The Fischer-Tropsch Synthesis (Wiley, 1951).

8. G. Henrici-Olive and S. Olive, J. Mol. Catal. 24, 7 (1984).

9. G. Henrici-Olive and S. Olive, The Chemistry of the Catalyzed Hydrogenation of Carbon Monoxide (Springer-Verlag, 1984).

10. V. A. Zakharov, G. D. Bukatov, and Y. I. Yermakov, Adv. Polym. Sci. 51, 63 (1983).

11. V. Zucchini and G. Cecchin, Adv. Polym. Sci. 51, 103 (1983).

12. K. W. McLaughlin and C.A.J. Hoeue, Polym. Prep. 27, 257 (1986).

13. G. Henrici-Olive and S. Olive, Adv. Polym. Sci. 15, 1 (1974).

14. Y. Doi, S. Ueki, and T. Keii, Macromolecules 12, 814 (1979).

15. M. Roper, "Fischer-Tropsch Synthesis," in Catalysis in C_1 Chemistry, W. Keim, Ed. (D. Reidel, 1983), p. 41.

16. V. H. Pichler, B. Firnhaber, D. Kioussis, and N. Dowallace, Makromol. Chem. 70, 12 (1964).

17. V. H. Kolbel, W.H.E. Muller, and H. Hammer, Makromol. Chem. 70, 1 (1964).

18. R. J. Madon, J. Catal. 57, 183 (1979).

19. D. L. King, J. Catal. 51, 386 (1978).

20. C. S. Kellner and A. T. Bell, J. Catal. 70, 418 (1981).

21. R. A. Stowe and C. B. Murchison, Hydrocarbon Processing, p. 95 (June 1984).

22. F. King, E. Shutt, and A. I. Thomson, Platinum Met. Rev. 29, 146 (1985).

23. M. Audier, J. Klinowski, and R. E. Benfield, J. Chem. Soc. Chem. Commun., p. 626 (1984).

24. K. J. Smith and R. C. Everson, J. Catal. 99, 349 (1986).

25. Z.-Z. Lin, T. Okuhara, and M. Misono, Chem. Lett. p. 913 (1986).

26. T. Okuhara, T. Enomoto, H. Tamura, and M. Misono, Chem. Lett., p. 1491 (1984).

27. T. Enomoto, K. Kaba, T. Okuhara, and M. Misono, Bull. Chem. Soc. Jpn. 60, 1237 (1987).

28. Y. Doi, H. Miyake, and K. Soga, J. Chem. Soc. Chem. Commun. p. 347 (1987).

29. T. Mori, A. Miyamoto, N. Takahashi, M. Fukagaya, H. Niizuma, T. Hattori, and Y. Murakami, J. Chem. Soc. Chem. Commun., p. 678 (1984).

30. T. Mori, S. Taniguchi, Y. Mori, T. Hattori, and Y. Murakami, J. Chem. Soc. Chem. Commun. p. 1401 (1987).

31. N. Takahashi, T. Mori, A. Miyamoto, T. Hattori, and Y. Murakami, Appl. Catal. 38, 61 (1988).

32. N. Takahashi, T. Mori, A. Miyamoto, T. Hattori, and Y. Murakami, Appl. Catal. 38, 301 (1988).

33. N. Takahashi, T. Mori, A. Furuta, S. Komai, A. Miyamoto, T. Hattori, and Y. Murakami, J. Catal. 110, 410 (1988).

34. T. Tatsumi, Y. G. Shul. T. Sugiuna, and H. Tominaga, Appl. Catal. 21, 119 (1986).

35. Y. G. Shul, T. Sugiura, T. Tatsumi, and H. Tominaga, Appl. Catal. 24, 131 (1986).

36. Y. G. Shul, Y. Arai, T. Tatsumi, and H. Tominaga, Bull. Chem. Soc. Jpn. 60, 2335 (1987).

37. H. H. Nijs, P. A. Jacobs, and J. B. Uytterhoeven, J. Chem. Soc. Chem. Commun., p. 180 (1979).

38. D. Balliuet-Tkatchenko, G. Coudurier, H. Mozzanega, and I. Tkatchenko, Fund. Res. Homogeneous Catal. 3, 257 (1979).

39. D. Fraenkel and B. C. Gates, J. Am. Chem. Soc. 102, 2478 (1980).

40. H. Nijs, P. A. Jacobs, and J. B. Uytterhoeven, J. Chem. Soc. Chem. Commun., p. 1095 (1979).

41. H. H. Nijs and P. A. Jacobs, J. Catal. 65, 328 (1980).

42. D. Balliuet-Tkatchenko, N. D. Chau, H. Mozzanega, M. C. Roux, and I. Tkatchenko, ACS Symp. Ser. 152, 187 (1981).

43. F. Hugues, P. Bussiere, J. M. Basset, D. Commercoc, Y. Chaurin, L. Bonneviot, and D. Olivier, Proc. 7th Int. Congr. Catal., Tokyo, 1980, T. Seiyama and K. Tanabe, Eds. (Elsevier, 1981), p. 418.

44. Y. W. Chen, H. T. Wang, and J. G. Goodwin, Jr., J. Cataly. 85, 499 (1984).

45. R. K. Ungan and M. C. Baird, J. Chem. Soc. Chem. Commun. p. 643 (1986).

46. T.-A. Lin, L. H. Schwartz, and J. B. Butt, J. Catal. 97, 177 (1986).

47. J. B. Butt, J.-A. Lin, and L. H. Schwartz, J. Catal. 97, 261 (1986).

48. D.-K. Lee and S.-K. Ihm, J. Catal. 106, 386 (1987).

49. T. Bein, G. Schmiester, and P. A. Jacobs, J. Phys. Chem. 90, 4851 (1986).

50. P. A. Jacobs and D. Van Wouwe, J. Mol. Catal. 17, 145 (1982).

51. K. McLaughlin, Dow Chemical, private communication.

52. R. A. Dictor and A. T. Bell, Ind. Eng. Chem. Process Des. Dev. 22, 678 (1983).

53. E. Peacock-Lopez and K. Kindenberg, J. Phys. Chem. 88, 2270 (1984).

54. I. R. Leith, J. Catal. 91, 283 (1985).

55. T. Fukushima, K. Fujimoto, and H. Tominaga, Appl. Catal. 14, 95 (1985).

56. K. Fujimoto, T. Nobusawa, T. Fukushima, and H. Tominaga, Bull. Chem. Soc. Jpn. 58, 3164 (1985).

57. K. Fujimoto, H. Saima, and H. Tominaga, J. Catal. 94, 16 (1985).

58. L. Fu and C. H. Bartholomew, J. Catal. 92, 376 (1985).

59. C. D. Chang, J. N. Miale, and R. F. Socha, J. Catal. 90, 84 (1985).

60. Y. Iwasawa and N. Ito, J. Catal. 96, 613 (1985).

61. M. Logan, A. Gellman, and G. A. Somorjai, J. Catal. 94, 60 (1985).

62. Y. I. Yermakov, B. N. Kuznetsov, and V. A. Zakharov, Catalysis by Supported Complexes (Elsevier, 1981).

63. A. A. Bhattacharyya, C. C. Nagel, and S. G. Shore, Organometallics 2, 1187 (1983).

64. B.F.G. Johnson, J. Lewis, P. R. Raithby, and G. Suss, J. Chem. Soc. Dalton Trans., p. 1356 (1978).

65. G. Sbrana, G. Braca, F. Piacenti, and P. Pino, J. Organomet. Chem. 13, 240 (1968).

66. E. W. Abel and S. Moorhouse, J. Chem. Soc. Dalton Trans., p. 1706 (1973).

67. G. A. Huff, Jr. and C. N. Satterfield, Ind. Eng. Chem. Fundam. 21, 479 (1982).

68. H. G. Stenger, H. E. Johnson, and C. N. Satterfield, J. Catal. 86, 1477 (1984).

II SULFUR-TREATED CATALYSTS

Introduction

An important property of improved Fischer-Tropsch synthesis (FTS) catalysts is low selectivity for the production of light alkanes (paraffin hydrocarbons), especially methane. Production of light alkanes causes several inefficiences in the production of synthetic fuels in addition to the lower yield of gasoline or middle distillate range hydrocarbons. Light alkane products require additional processing steps, such as separation and steam re-forming or thermal cracking before they can be recovered and converted into syngas for recycle or converted into higher value products. These steps necessitate operational and capital investment expenses well beyond the market value of the light alkanes. Reduction in light alkane yield therefore directly reduces the costs associated with these ancillary processing steps.

Dry[1] has described commercial FTS operation at elevated temperature and moderate pressure that gives methane yields down to 10 wt% and total light alkanes in yields from 20 to 30 wt%. As a result of our current investigation, we believe that low-level sulfur pretreatment of new catalyst formulations, such as dual-function catalysts, could directly give motor fuel range hydrocarbons and light olefins in yields well above 80 wt% with a corresponding decrease in light alkane yield. Iron FTS catalysts and other metal catalysts with desirable FTS activity can be treated with controlled amounts of sulfur to selectively inhibit the formation of methane. This approach to development of improved FTS catalysts has several advantages:

- Only selectivity characteristics of the metal crystallite surfaces would be altered; physical properties, such as pore-size distribution, and chemical properties, such as acid-base character, would remain unchanged.

- Any heterogeneous supported metal FTS catalyst can, in principle, be treated with low levels of sulfur.

- Low levels of sulfur may reduce the coking tendencies of FTS catalysts in addition to altering the product distribution.

- Since sulfur is a ubiquitous component of coal and coal processing technology, no environmental or undesirable synergistic catalytic effects would be introduced by treatment with very low levels of H_2S.

Two problems might accompany low-level sulfur treatment:

- Uniform fractional adsorption of sulfur on metal surfaces within a porous catalyst is extremely difficult because of the strong affinity of such surfaces for chemisorbed sulfur.

- Enhancement of selectivity may be offset by a large decrease in activity for the formation of desirable hydrocarbon products; indeed, high coverage by sulfur is a poison for FTS and for methanation.

Selective poisoning of methane production could result in an FTS process with a high yield of hydrocarbons in the motor fuel range. High-molecular-weight waxes can be suppressed by operating at elevated temperatures with a dual-function catalyst. Higher operating temperature could also mitigate any decline in activity caused by the sulfur treatment.

The success of selective methane poisoning depends on the actual kinetic details of the much studied FTS reaction mechanism. There is some evidence that methane and higher molecular weight FTS products are formed through parallel reaction pathways and that methane yield does not always follow the polymerization statistical distribution. Commercial FTS catalysts often follow the polymerization distribution, with the exception of methane.[1,2] The lower methane production rate may result from differences in the stability and termination rates for adsorbed methyl and alkyl species. Consequently, depending on the degree of polymerization, the product distribution can vary from 100% methane (methanation) to a predominance of high-molecular hydrocarbons weight. High temperature and low pressure operation favors the production of methane, whereas low temperature and high pressure operation favors the

production of waxes. Some catalysts, such as nickel and the noble metals, favor methanation, whereas other catalysts,[3] such as ruthenium and cobalt, favor waxes. In general, all are constrained by the Anderson-Schultz-Flory (ASF) product distribution. Improved catalyst performance, e.g., suppressed methane and light alkane production, in combination with changes in operating conditions, e.g., higher temperature with low H_2/CO ratio syngas, may narrow the product distribution curve to substantially improve the yield of usable liquid fuels. Catalysts selectively poisoned by controlled quantities of sulfur may represent such improved FTS catalysts.

Background

Selective Poisoning of FTS Catalysts

Sulfur is a well-known poison for the FTS reaction. However, as pointed out in the review of Madon and Shaw,[4] unexplained observations indicate that small quantities of sulfur can enhance the activity and alter the selectivity of the catalyst. Herington and Woodward[5] reported that the light hydrocarbon yield for a thoria-promoted cobalt catalyst supported on kieselguhr declined, whereas the heavy hydrocarbon yield increased with introduction of H_2S. Increased heavy hydrocarbon production was also noted when H_2S was introduced to the potassium-promoted catalyst under methanation conditions (300°C). Similar observations were reported by Fischer and Meyer[6] for Ni and by King[7] for Co with CS_2 as the poison. Anderson et al.[8] reported an increase in the yield of hydrocarbons in the liquid fuel range after adding small quantities of sulfur to iron catalysts possessing small particle size.

These observations are supported by the more recent evidence that sulfur adsorption strongly decreases the methanation activity of metal surfaces. Dalla Betta[9] reported that 10 ppm H_2S reduced the stationary state methanation activity of Ru and Ni several orders of magnitude. In studies with more carefully controlled sulfur-poisoned metal surfaces, Bartholomew et al.[10] found that the methanation activity declined as the square of unpoisoned sites. Similar and stronger poisoning influence was

reported by Goodman and Kiskinova[11] for the methanation activity of single-crystal Ni and Ru surfaces. However, these studies did not systematically measure the effect of controlled sulfur adsorption on the selectivity of metals for higher molecular weight products under more favorable FTS conditions (higher pressure and lower temperature).

The effect of sulfur poisoning on activity and selectivity during FTS has generally been systematically investigated under transport-limited sulfur poisoning conditions and at H_2S levels well above those necessary to completely cover the active metal surfaces.[4] In these selective poisoning experiments, probably only a very small portion of the total metal surface area of the catalysts was fractionally covered with sulfur, the case for which the selectivity would be most affected. The majority of the surface area would be either clean or completely covered with a monolayer of sulfur. If the entire metal surface area were uniformly covered with low levels of chemisorbed sulfur, the FTS selectivity might be significantly altered.

More recent work by Satterfield and Stenger[12] and by Matsumoto and Satterfield[13] with dibenzyl thiophene-poisoned fused iron in a slurry reactor and our own results with H_2S pretreated fused iron in a fixed-bed reactor have shown significantly decreased methane yield and increased olefin selectivity relative to clean fused iron catalysts.

Uniform Sulfur Adsorption on FTS Catalysts

Our approach was to carefully treat iron and ruthenium catalysts with sulfur so that uniform controlled adsorption could occur separately, before FTS reaction. As our own work has shown,[14,15] the great thermodynamic stability of chemisorbed sulfur ensures that the sulfur is not removed during the subsequent FTS reaction.

The essentially irreversible chemisorption of sulfur to metal surfaces results in poisoning for very low gas phase concentrations of sulfur-bearing gas. It has been long known that levels of H_2S lower than necessary for the formation of metal sulfides still result in complete poisoning, given adequate stoichiometric exposure time. Measurements of

the thermodynamic properties of chemisorbed sulfur on FTS catalysts, including Ni,[16] Fe,[14] Ru,[15] and Co,[14] have shown that extremely low levels of sulfur-bearing gas are required before the adsorption process with H_2S becomes reversible (Table II-1). At FTS temperatures, the ratio of H_2S/H_2 is less than 0.001 ppb for equilibrium with chemisorbed sulfur on iron at 70% of the capacity of the surface to adsorb sulfur.[14] The reversible adsorption levels or threshold poisoning levels for the other metals is even lower. Correlations of the heat of formation of chemisorbed sulfur as a function of bulk sulfide heat of formation and the empirical relation between the coverage and chemical potential of adsorbed sulfur[17] allow an estimate to be made for sulfur coverage as a function of metal, temperature, and gas phase chemical potential of sulfur. All metal catalysts, given some uncertainty owing to the unknown effect of promoters and FTS intermediates, irreversibly chemisorb sulfur for all practical FTS conditions.

Therefore, substantial transport limitations must exist within the pores and even through a catalyst bed because of the very low levels of gas-phase sulfur. The rates of sulfur adsorption at 500 K appear adequate to quickly poison a metal crystallite surface, given any practical gas phase concentration. Thus, few metal crystallites can exist with fractional adsorbed atomic sulfur coverage under ordinary poisoning conditions. Crystallites near the exterior surface of a porous catalyst particle and those located upstream in a fixed bed are completely poisoned, whereas those downstream remain essentially free of chemisorbed sulfur. Those catalysts for which sulfur exposure caused a change in selectivity undoubtedly contained considerable gradients in the adsorbed sulfur coverage. This nonuniformity lessens the effect of sulfur coverage on FTS product selectivity.

Experimental Results

Catalyst Preparation

A doubly promoted (potassium and copper) precipitated iron catalyst was prepared from aqueous solutions of copper(II)nitrate

Table II-1

SULFUR CHEMISORPTION THERMODYNAMICS FOR IRON, COBALT, AND RUTHENIUM

Metal	Temp (K)	PH_2S/PH_2 for Fractional Sulfur Coverage, 0.05	0.10	0.20	0.50	0.75	1.00
Fe	500	6.6×10^{-15}	1.3×10^{-14}	2.7×10^{-14}	5.4×10^{-11}	3.6×10^{-8}	2.1×10^{-5}
	600	6.4×10^{-13}	1.3×10^{-12}	2.5×10^{-12}	2.6×10^{-9}	8.9×10^{-7}	2.8×10^{-4}
	800	1.9×10^{-10}	3.8×10^{-10}	7.6×10^{-10}	3.2×10^{-7}	4.9×10^{-5}	6.8×10^{-3}
	1000	5.8×10^{-9}	1.2×10^{-8}	2.3×10^{-8}	5.7×10^{-6}	5.5×10^{-4}	4.7×10^{-2}
Co	500	6.1×10^{-16}	1.2×10^{-15}	2.4×10^{-15}	1.8×10^{-12}	3.5×10^{-10}	6.1×10^{-8}
	600	1.8×10^{-13}	3.6×10^{-13}	7.3×10^{-13}	2.1×10^{-10}	1.8×10^{-8}	1.4×10^{-6}
	800	2.3×10^{-10}	4.5×10^{-10}	9.0×10^{-10}	7.9×10^{-8}	2.5×10^{-6}	6.9×10^{-5}
	1000	1.6×10^{-8}	3.2×10^{-8}	6.5×10^{-8}	2.8×10^{-6}	4.8×10^{-5}	7.2×10^{-4}
Ru	500	2.3×10^{-26}	4.3×10^{-25}	1.5×10^{-22}	7.0×10^{-15}	1.7×10^{-8}	4.1×10^{-2}
	600	3.4×10^{-23}	5.1×10^{-22}	1.2×10^{-19}	1.4×10^{-12}	1.1×10^{-6}	9.0×10^{-1}
	800	3.1×10^{-19}	3.5×10^{-18}	4.7×10^{-16}	1.1×10^{-9}	2.1×10^{-4}	4.2×10
	1000	7.3×10^{-17}	7.1×10^{-16}	6.7×10^{-14}	5.7×10^{-8}	4.9×10^{-3}	4.3×10^{2}

Source: J. Chem. Phys. 74, 5877 (1981); J. Chem. Phys. 76, 1162 (1982).

[$Cu(NO_3)_2 \cdot 3H_2O$, Alfa Products, puratronic grade] and iron(III)nitrate ($Fe(NO_3)_3 \cdot 9H_2O$, Alfa Products, puratronic grade] in the required ratio at 353 K. The mixed nitrate solution was then slowly added to hot sodium carbonate solution with vigorous stirring over a period of several minutes until the pH reached 7 to 8. The precipitate was collected by centrifugation and washed with 1000 mL of deionized water. Alkali was added by stirring the precipitate with dilute potassium carbonate solution. The catalyst was then dried at 373 K for 24 h. The final weight ratio was $Fe:Cu:K_2CO_3 = 100:0.1:2$. The precipitated iron catalyst was ground and screened to 0.043-0.14 mm. The catalyst was reduced at 623 K for 16 h with hydrogen gas at a gas hourly space velocity (GHSV) of 3×10^4 h^{-1}.

A fused iron catalyst was obtained from United Catalysts Inc. (C73-1-01) as 1.5 x 3.0 mm granules and was crushed and screened to 0.3-0.5 mm. The catalyst was reduced as recommended in 100 mL min^{-1} of flowing hydrogen and programmed from 533 K to 766 K over 29 h.

An unpromoted cobalt catalyst was prepared from an aqueous solution of cobalt(II)nitrate [$Co(NO_3)_2 \cdot 6H_2O$, Alfa Products, puratronic grade] by the method of incipient wetness on Harshaw AL-0104 alumina (BET surface area = 88 m^2/g) and crushed and screened to 0.3-0.5 mm. The catalyst was then dried in air at 400 K for 24 h. The final weight ratio was $Co:Al_2O_3 = 1:10$.

An unpromoted ruthenium catalyst was prepared from an aqueous solution of ruthenium chloride ($RuCl_3$) by the method of incipient wetness on Harshaw AL-0104 alumina crushed and screened to 0.3-0.5 mm. The catalyst was then dried in air at 400 K for 24 hours. The final weight ratio was $Ru:Al_2O_3 = 2:100$.

Sulfur Treatment of Precipitated Iron Catalyst

Sulfur treatment of the precipitated iron catalyst was performed in a gas recirculation system as shown in Figure II-1. After catalyst reduction *in situ* in 100-kPa hydrogen at 623 K for more than 16 h, aliquots of 0.96 mol% H_2S/H_2 were injected into the recirculation loop at 723 K, and the change in the gas-phase concentration of hydrogen sulfide

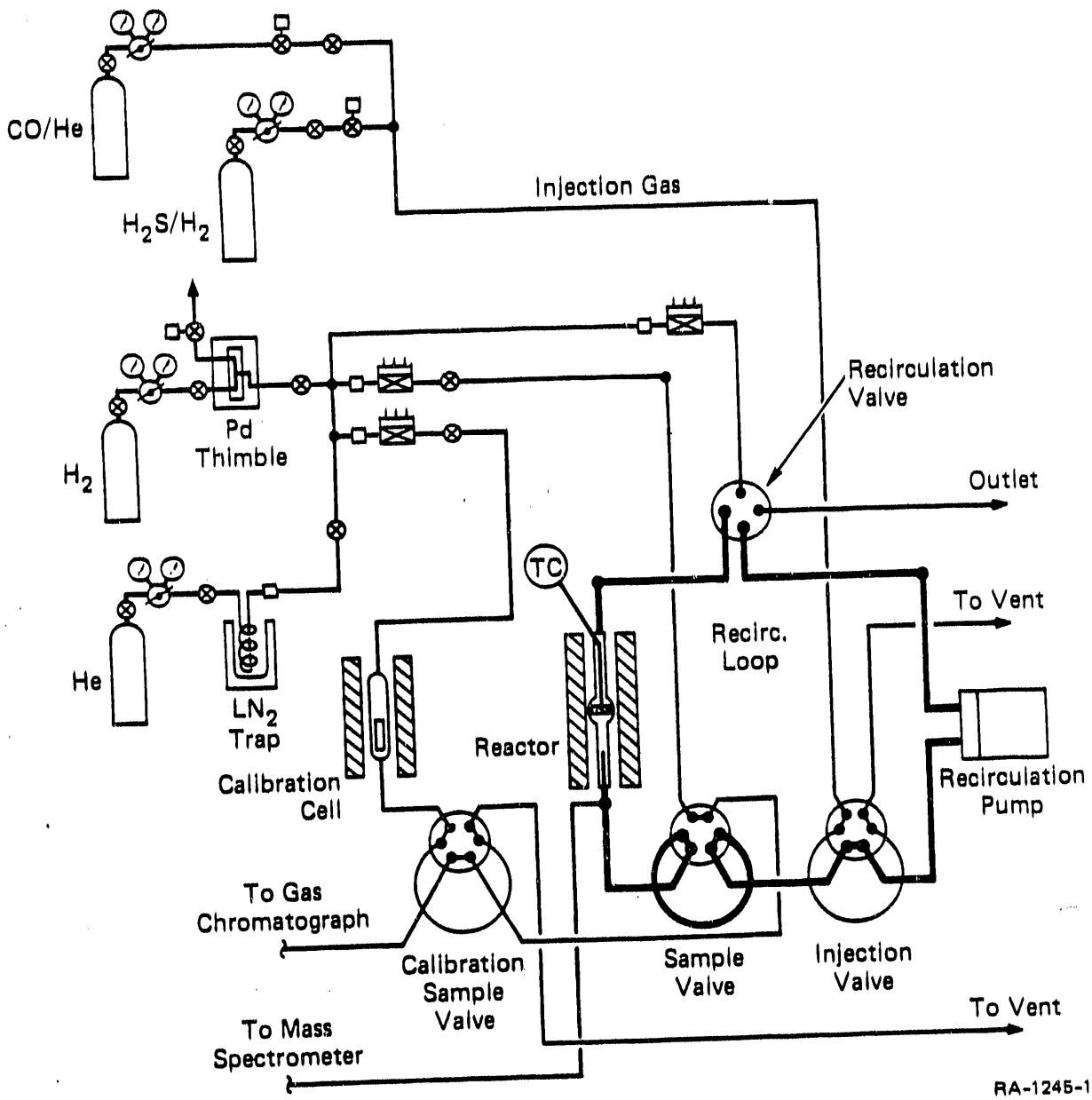

Figure II-1. FTS catalyst sulfur treatment system.

with time was closely monitored. Approximately 39.3 μmol of hydrogen sulfide was adsorbed at saturation, corresponding to a reduced metal surface area of about 6.7 $m^2\ g^{-1}$. The catalyst was exposed to the gaseous mixture for 24 h at 723 K to ensure equilibration. The H_2S gas was flushed with pure hydrogen after cooling to 423 K. Comparison of our data with previously published isosteres on iron powder[14] indicates that our iron catalyst had reached approximately 100% of saturation coverage (i.e., about 1.0 adsorbed sulfur atoms per iron surface atom). The catalyst was then removed from the recirculation system and immediately reduced at 623 K in 100-kPa hydrogen in the FTS testing apparatus.

Sulfur Treatment of Fused Iron Catalyst

Sulfur treatment of the fused iron catalyst was performed in a gas recirculation system, as described previously. After catalyst reduction in situ in 100-kPa hydrogen and temperature programming to 766 K over 29 h, aliquots of 3080 ppm H_2S/H_2 were pulsed into the recirculation loop at 723 K, and the change in the gas-phase concentration of hydrogen sulfide with time was closely monitored. Approximately 140 μmol of hydrogen sulfide was injected into the system, corresponding to a reduced metal surface area of about 8 $m^2\ g^{-1}$. The catalyst was equilibrated with the gaseous mixture for 24 h at 723 K. Gas-phase hydrogen sulfide concentrations were measured over a range of temperatures, and the isostere was plotted in Figure II-2. Comparison of our data with previously published isosteres on iron powder[14] indicates that our iron catalyst had reached approximately 100% of saturation coverage (i.e., about 1.0 adsorbed sulfur atoms per iron surface atom). The catalyst was then removed from the recirculation system and reduced at 573 K in hydrogen in the FTS testing apparatus immediately before we began the catalytic studies.

A special pretreatment procedure was developed for uniform fractional adsorption of sulfur below half saturation coverage because partial sulfur coverage on the metal surfaces within a porous catalyst is extremely difficult to produce owing to the strong affinity of such

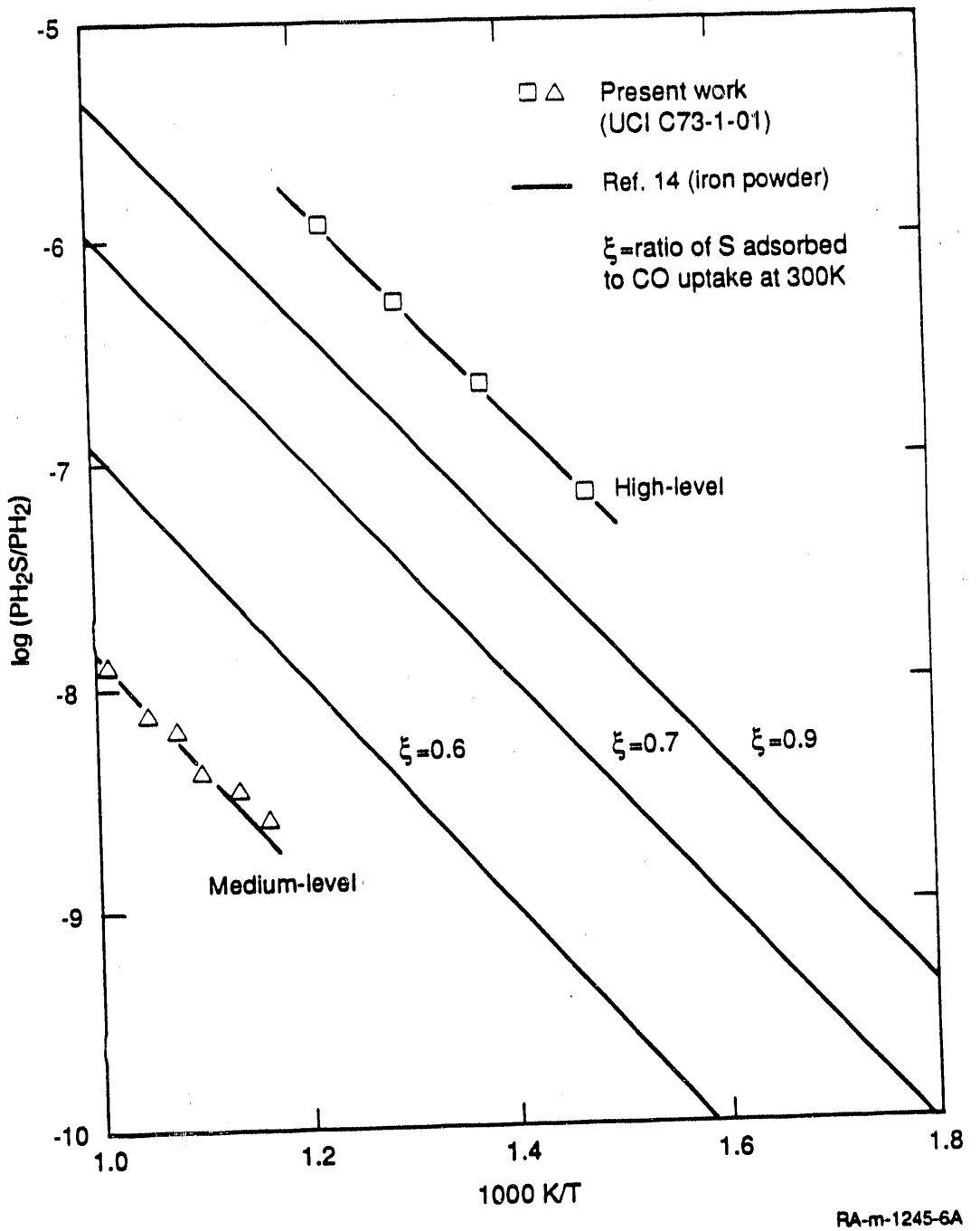

Figure II-2. Sulfur chemisorption isosteres on fused iron and iron powder.

surfaces for chemisorbed sulfur. A low uniform level of sulfur coverage was achieved by slowing the rate of dissociative chemisorption of H_2S on the catalyst surface by the presence of a passivating layer containing a readily removed adsorbate so that surface reaction, rather than pore diffusion, limited the net rate of sulfur uptake. The reduced fused iron catalyst was passivated by CO adsorption, dissociation, and disproportionation to CO_2 at 473 K. Aliquots of 100-kPa CO were injected into the closed gas recirculation loop containing 1 g of the reduced fused iron catalyst, while the $CO-CO_2$ ration was followed with an on-line mass spectrometer. Approximately 200 μmol of carbon monoxide was injected, corresponding to two monolayers of adsorbed CO. Some CO_2 evolution was observed, and most of the CO was consumed during passivation.

Following passivation, aliquots of 0.96% H_2S/H_2 were injected into the closed recirculation loop at 473 K, while the gas-phase H_2S concentration was monitored with a sensitive photoionization detector. Approximately 200 μmol of hydrogen sulfide was injected into the system, representing approximately 0.4 monolayer sulfur capacity of the catalyst. The gas-phase H_2S concentration slowly fell to 15 ppm after 2 h. The system was then flushed with pure hydrogen at 343 K. The deposited carbon, iron carbide, and adsorbed CO were removed by temperature-programmed reaction (TPR) to 873 K in 100-kPa flowing hydrogen. Methane, but no hydrogen sulfide, was observed during the TPR, indicating that chemisorbed sulfur was irreversibly bound during the removal of the passivating layer.

The catalyst was held at 825 K in recirculating hydrogen for 12 h to allow local microscopic surface diffusion and equilibration. Gas-phase hydrogen sulfide concentrations were measured over a range of temperatures and the final sulfur chemisorption isostere was determined (Figure II-2). Compared with isosteres for fractional monolayer sulfur coverage on powdered iron[41], the medium-level sulfur-treated fused iron catalyst had approximately 0.5 monolayer sulfur coverage. The BET surface area of the freshly reduced catalyst (30 $m^2\ g^{-1}$) and medium-level sulfur-treated catalyst (7 $m^2\ g^{-1}$) showed a factor of four reduction in

surface area. The catalyst was further passivated by CO adsorption at room temperature before removal from the recirculation system and transfer to the FTS testing system. The catalyst was reduced in flowing hydrogen at 523 K before FTS testing, as described below.

A low-level sulfur-treated fused iron catalyst (20% monolayer sulfur coverage) was successfully prepared by the technique used to prepare the 50% monolayer sulfur-treated catalyst. The catalyst was heated to only 873 K to avoid sintering, and no isostere was measured. The BET surface area of the low-level sulfur-treated catalyst (17 $m^2\ g^{-1}$) showed a 20% reduction compared with the freshly reduced catalyst.

Sulfur Treatment of Cobalt Catalysts

The alumina-supported cobalt FTS catalyst was treated with H_2S until sulfur was chemisorbed to a coverage of about one-half saturation. Following a more severe passivation procedure (exposure to 99.5% CO at 523 K), the rate of sulfur adsorption at 425 K was slowed to about 0.4 monolayers per hour in a recirculating stream of 30 ppm H_2S in 100-kPa H_2. After reduction at 773 K, the catalyst was characterized by H_2 and CO chemisorption and tested for FTS performance.

A fully sulfided (100% monolayer sulfur coverage) cobalt catalyst was also prepared as a titration of the total active metal surface area. This high-level sulfur-treated cobalt catalyst was also tested for FTS activity and methane selectivity. Approximately 18 μmol of H_2S was injected into the recirculation system at 773 K, corresponding to a metal surface area of 22.5 $m^2\ g^{-1}$. The catalyst was equilibrated overnight at 773 K, the gas-phase H_2S concentration was measured over a range of temperatures, and the isostere was plotted in Figure II-3. Comparison of our data with previously published isosteres on cobalt powder[14] indicates that our cobalt catalyst reached approximately 90% of saturation coverage.

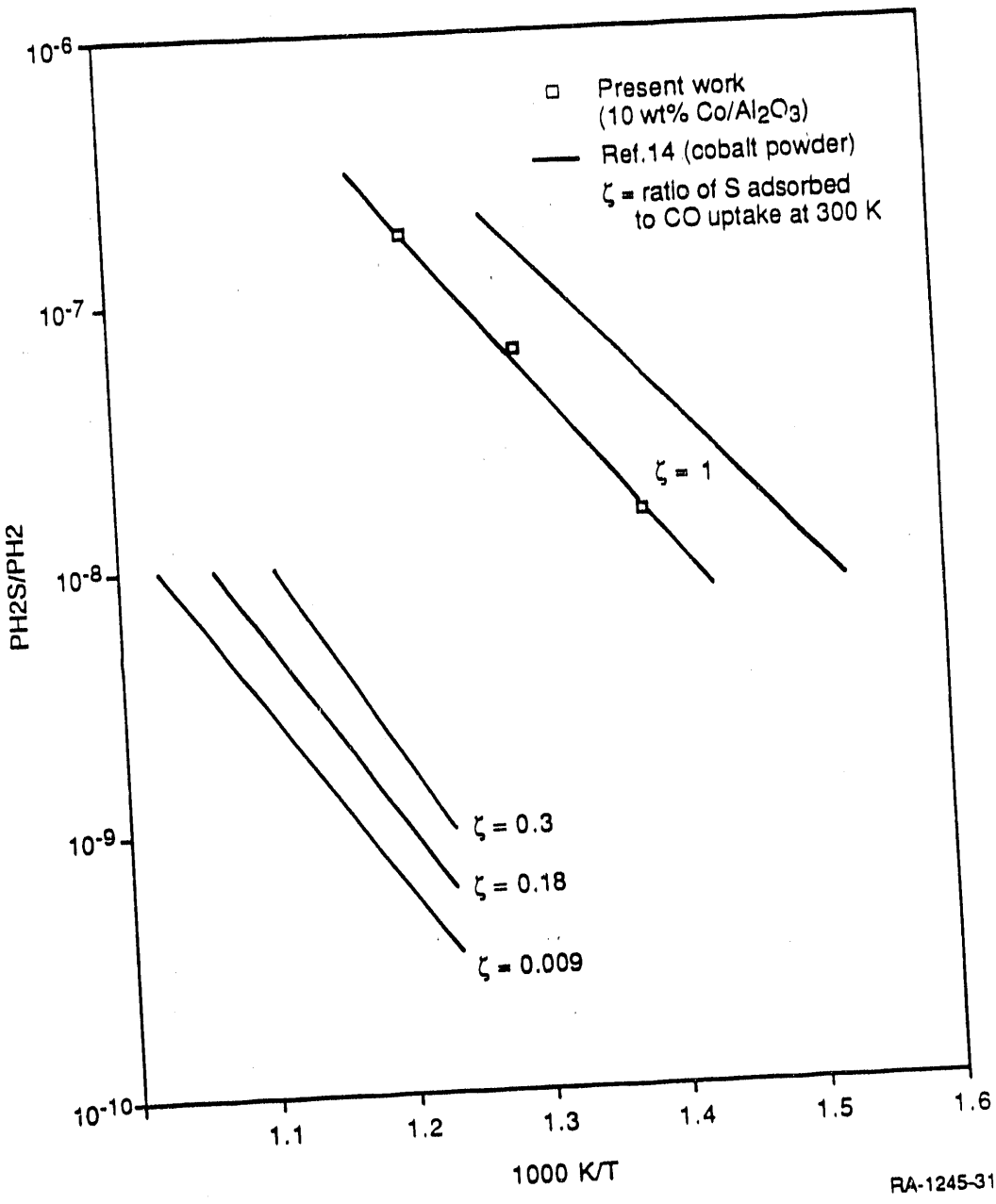

Figure II-3. Sulfur chemisorption isosteres on cobalt/Al_2O_3 and cobalt powder.

Characterization and Testing of FTS Catalysts

Experimental Procedures. The reactant gases included a 33.5% carbon monoxide in hydrogen mixture and a 50.2% carbon monoxide in hydrogen mixture, with metal carbonyls removed by passage through a molecular sieve trap cooled by dry-ice/acetone. The hydrogen used for pretreatment of the catalysts was purified by diffusion through a Pd-Ag thimble, and 99.99% pure helium was further purified with a commercial oxygen-trap.

A continuous flow quartz microreactor was used for FTS reaction studies. The catalyst sample (0.2-0.5 g) was placed on a fritted quartz disk located inside the reactor. The reactor was heated by a resistance furnace and maintained at the desired temperature by an automatic temperature controller. A Chromel-Alumel thermocouple was situated in the catalyst bed to measure the reaction temperature. A schematic diagram of the FTS testing apparatus is shown in Figure II-4.

Effluent from the reactor was continuously monitored by a quadrupole mass spectrometer and two gas chromatographs. The mass spectrometer and the automated two-column gas chromatograph (Carle) were used to follow the methane and hydrocarbon yields up to C_3 and the overall CO conversion rate. Aliquots of samples were injected into a second programmable gas chromatograph (Hewlett-Packard) equipped with a subambient control system, a wide-bore capillary column, and a flame ionization detector. Hydrocarbon products up through carbon number C_{15} were measured, and light olefins and paraffins were separated.

The entire downstream flow and sampling system were heated to about 523 K to prevent condensation of high-boiling waxy products. The experimental configuration permitted sampling of the reactor inlet and outlet gas mixtures by the mass spectrometer and gas chromatograph. The FTS product distribution and synthesis gas conversion were determined from the difference between the inlet and outlet concentrations.

All the FTS experiments were conducted under differential conditions with a maximum CO conversion of 5%. The hydrocarbon reaction rate R is defined as the number of nanomoles of carbon monoxide converted into C_1

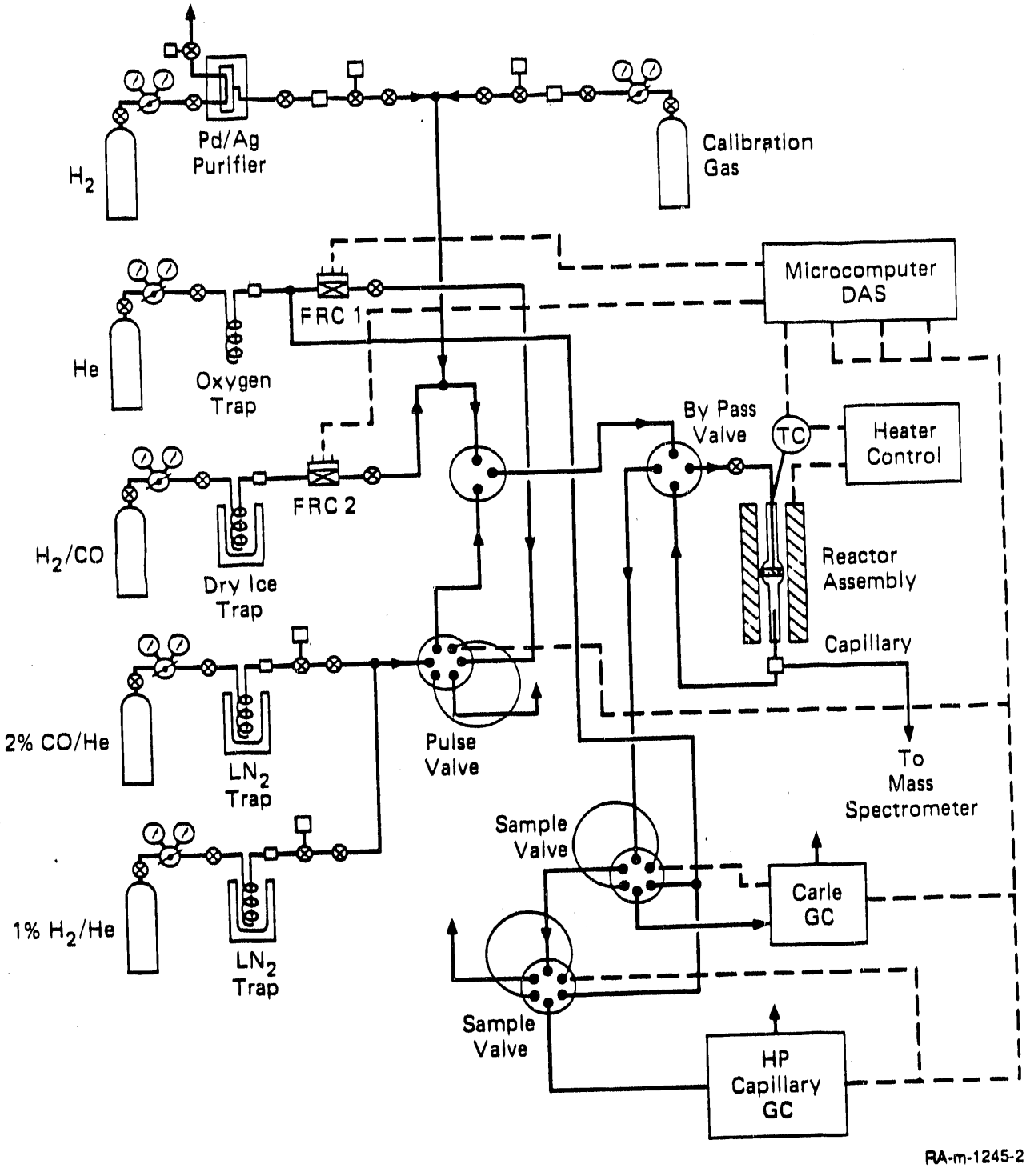

Figure II-4. Catalyst characterization and FTS testing apparatus.

through C_{10} hydrocarbon per gram of catalyst per second. The selectivity S is defined as the ratio of the rate of formation of methane relative to the overall hydrocarbon reaction rate for C_1 through C_{10} products (on a carbon-atom basis). A list of experimental parameters for FTS catalyst testing is included in Table II-2.

FTS Testing of Clean and Sulfur-Treated Fused Iron Catalysts. Fixed-bed FTS tests were performed at 1-atm (0.1 MPa) with 2:1 and 1:1 H_2:CO feedgas ratio for a series of clean and sulfur treated fused iron catalysts (Table II-3). As expected, the sulfur treatment greatly reduced the overall activity of the fused iron catalyst with 2:1 H_2:CO synthesis gas at 573 K after 22 h. The medium-level sulfur-treated showed only 8% and the high-level sulfur-treated fused iron catalysts showed only 2% of the activity of the clean catalyst. However, both sulfur treatments reduced the methane selectivity of fused iron from about 40% (C atom basis) to about 14%, thereby partially offsetting the reduced rates for C_2 and higher hydrocarbons. In addition, the high-level sulfur-treated catalyst produced almost exclusively light olefins with a chain growth factor of only approximately 0.25. These results were encouraging so additional tests were performed with 1:1 H_2:CO synthesis gas.

At 573 K and 100 kPa with 1:1 H_2:CO synthesis gas, the clean fused iron catalyst after 2 h on stream produced hydrocarbons at a rate of 26 μmol g^{-1} s^{-1} with a chain growth probability factor of 0.43 (Figure II-5) an a methane selectivity of 39% at 573 K. The methane selectivity increased to 63% as the clean catalyst deactivated after 24 h to a total hydrocarbon rate of roughly 10% of its projected initial rate (Table II-3). The activity of the clean fused iron catalyst could be restored temporarily to its original value by TPR in 1-atm hydrogen up to 773 K. This effect implicated carbon deposition as the cause for deactivation of the clean fused iron catalyst, as could be expected for low-H_2 synthesis gas; and at 548 K, the clean catalyst had a chain growth probability of 0.48 with a 27% selectivity toward methane and no obserable deactivation.

Table II-2

EXPERIMENTAL PARAMETERS FOR FTS CATALYST EVALUATION

Parameter	Range
Catalyst weight	0.5 to 1.0 g
Feed gas composition	33.51 vol% CO, bal. H_2 50.2 vol% CO, bal. H_2
Feed gas flow rate	2.5 to 20 mL/min
Pressure	0.1 to 2.0 MPa
Temperature	525, 550, 575 K
CO conversion	0.05 to 0.1 mol/mol feed
Run duration	2 to 50 h
Product analysis	CO, CO_2, H_2, CH_4, C_nH_{2n+2}, C_nH_{2n}

Table II-3

FIXED-BED FTS PERFORMANCE OF CLEAN AND SULFUR-TREATED FUSED IRON CATALYSTS AT 1-ATM

Catalyst	Clean Fused Fe					Low-Level Sulfur-Treated Fused Iron			Medium-Level Sulfur-Treated Fused Iron		High-Level Sulfur-Treated Fused Iron	
Temperature (K)	548	573	573	548	573	548	573	573	573	573	548	573
H_2/CO Ratio	1	1	1	2	2	1	1	2	1	2	1	2
Run Duration (h)	23	2	22	24	22	22	22	24	24	24	24	20
Product Rate[a] (nmol/g/s)												
C_1	5.03	9.32	4.54	11.21	57.8	1.56	3.21	10.66	1.79	1.52	0.60	0.24
C_2	2.49	3.05	0.70	5.20	24.1	0.99	2.19	4.50	2.20	1.91	0.47	0.72
C_3	1.44	1.72	0.31	2.86	5.37	0.54	1.17	2.42	1.20	0.96	0.22	0.13
C_4	0.63	0.62	0.10	1.24	2.46	0.22	0.47	0.83	0.46	0.46	0.07	0.055
C_5	0.28	0.22	0.03	0.51	1.19	0.08	0.17	0.22	0.12	0.20	0.01	0.006
C_6	0.15	0.11	0.02	0.23	0.52	0.04	0.07	0.102	0.05	0.058	—	—
C_7	0.12	0.09	0.004	0.14	0.26	0.03	0.06	0.044	0.02	—	—	—
C_8	0.05	0.02	—	0.08	—	0.01	0.02	0.025	0.01	—	—	—
C_9	0.01	0.01	—	—	—	0.003	0.003	—		—	—	—
C_{10}	0.01	0.01	—	—	—		0.002	—		—	—	—
TOTAL	20.60	25.78	7.56	40.7	139.2	6.97	14.85	21.8	12.79	11.41	2.56	2.4
Chain Growth Factor[b]	0.48	0.43	0.36	0.50	0.47	0.43	0.45	0.52	0.39	0.42	0.24	0.25
Olefin to n-Paraffin Ratio[c]	2.2	1.4	3.9	15	—	11.7	3.5	4.8	7.35	21.9	—	>20
Methane Selectivity[d]	27	39	63	30	42	25	24	35.7	15.7	14	26	18

[a] GHSV = 600 h^{-1} and P = 0.1 MPa; Product rate for each carbon number includes n-paraffins and α- and β-olefins; total product rate is on a carbon-atom basis.

[b] Average chain growth parameter (α) for C_{3+} hydrocarbons.

[c] Average olefin to paraffin ratio for C_2 to C_6 hydrocarbons.

[d] C_1 rate/(total rate) x 100%.

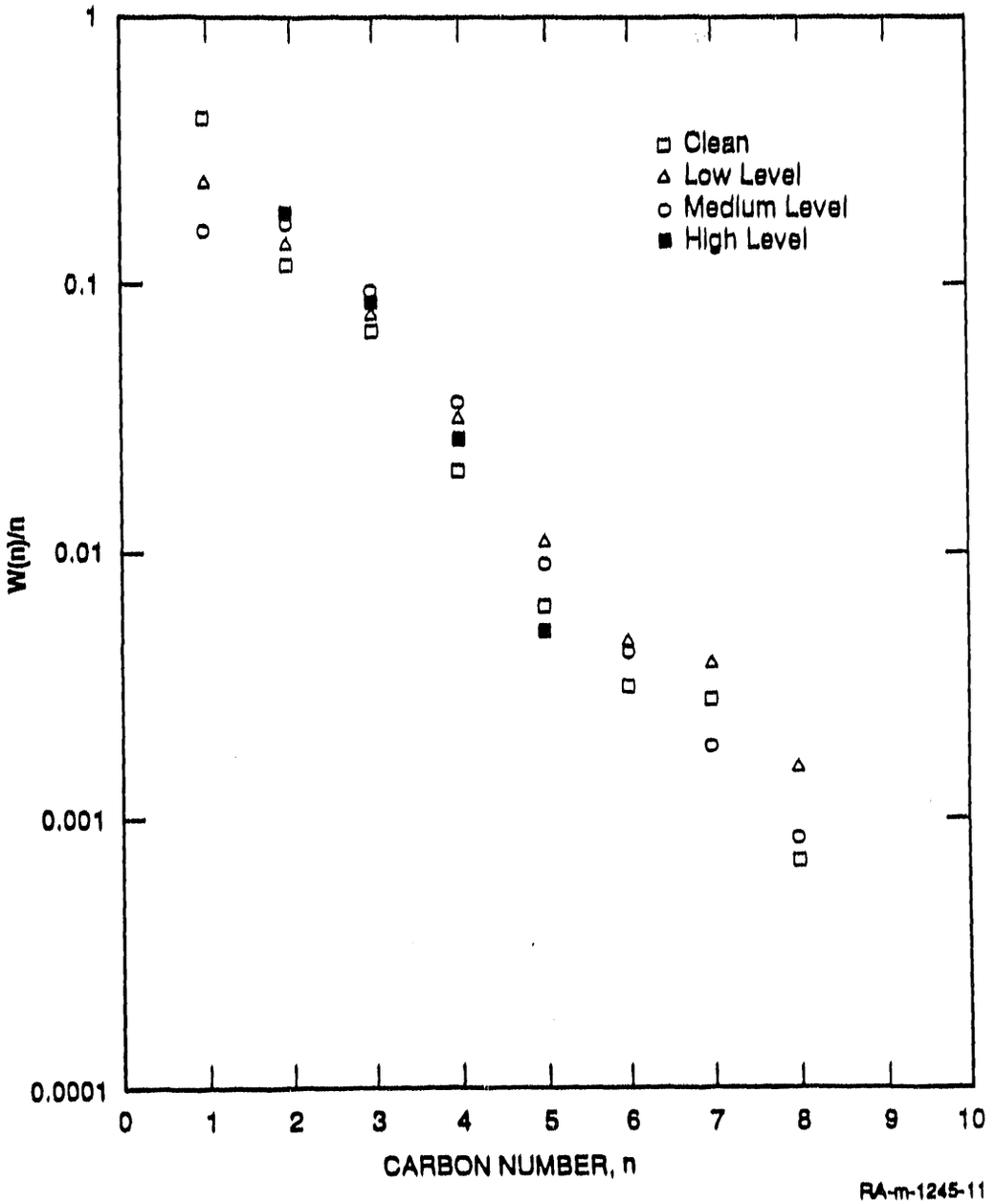

Figure II-5. Schulz-Flory plot of the hydrocarbon product distribution for clean and sulfur-treated fused iron catalysts at 573 K, 100 kPa, and $H_2/CO = 1$.

Unlike the clean catalyst, which deactivated to one-tenth of its original (after 2 h) activity with H_2:CO = 1:1 synthesis gas at 573 K, the sulfur-treated catalysts maintained their activity throughout the 24-h synthesis run. The activity of the low-level sulfur-treated catalyst was about one-third the activity of the clean catalyst at 548 K, but at 573 K under steady state conditions (24 h), it was twice as active as the clean catalyst with superior reduced methane selectivity. The medium-level sulfur-treated catalyst showed about the same activity as the low-level catalyst at 573 K in 1:1 H_2:CO synthesis gas but with a further reduction in methane selectivity. The high-level sulfur-treatment substantially reduced the activity of the fused iron catalyst with a very poor chain growth factor.

The sulfur-treated catalysts demonstrated preferential suppression of methane formation and preferential olefin production. Compared with the early (2 h) FTS performance of the clean catalyst, the low-level sulfur-treated fused iron catalyst demonstrated nearly a twofold (Figure II-6) and the medium-level sulfur-treated catalyst, nearly a threefold reduction in methane selectivity at 573 K (Figure II-7). The selectivity toward methane at 14% for the medium-level sulfur-treated catalyst (50% monolayer sulfur coverage) and 18% (Figure II-8) for the high-level sulfur-treated catalyst (100% monolayer sulfur coverage) as compared with 39%, initially (after 2 h) and 63% at steady-state (after 22 h) for the untreated catalyst. The ratio of alkenes to alkanes was very high at about 20 for both sulfur-treated catalysts (Figures II-7 and II-8). The chain growth probability for C_2 to C_{10} hydrocarbons was reduced slightly as the amount of sulfur chemisorbed on the catalyst's surface increased (Figure II-5).

The series of sulfur-treated fused iron catalysts showed a minimum in methane selectivity (Figure II-9) at roughly 50% saturation coverage. The olefin production rate showed little change from that of the clean catalyst, but the paraffin production rate (including methane) dropped significantly. If only C_2 to C_{10} total hydrocarbon rates were considered, the activity of the medium-level sulfur-treated catalyst in H_2:CO = 2:1 synthesis gas at 573 K was 11% of the clean catalyst, and the activity of the high-level sulfur-treated catalyst was 1.3%; with H_2CO = 1:1 synthesis

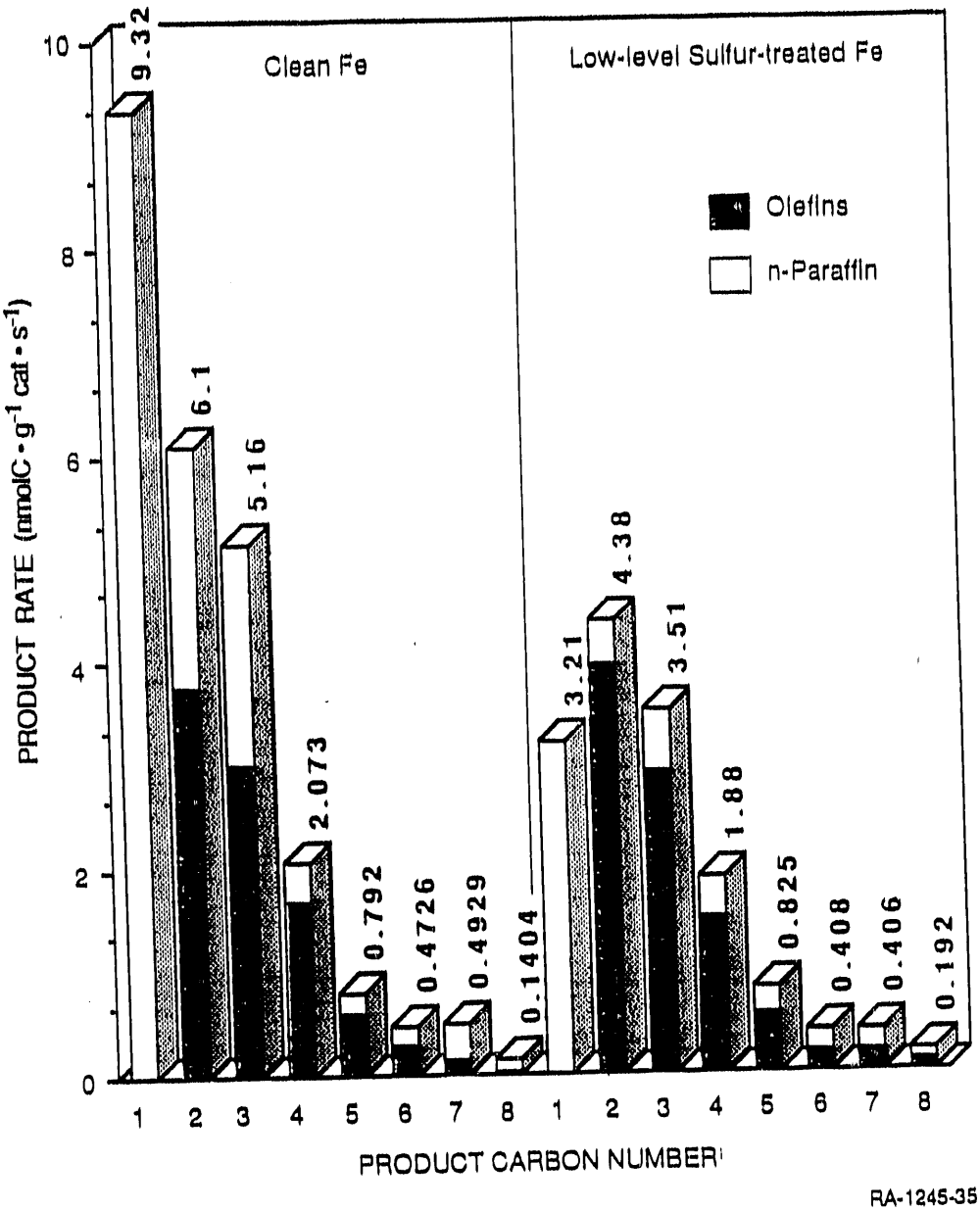

Figure II-6. Fischer-Tropsch synthesis at 573 K, 100 kPa, and H_2/CO ratio = 1, on clean and low-level sulfur-treated fused iron catalysts after 22 h. Rates are in nmoles carbon per gram catalyst per second.

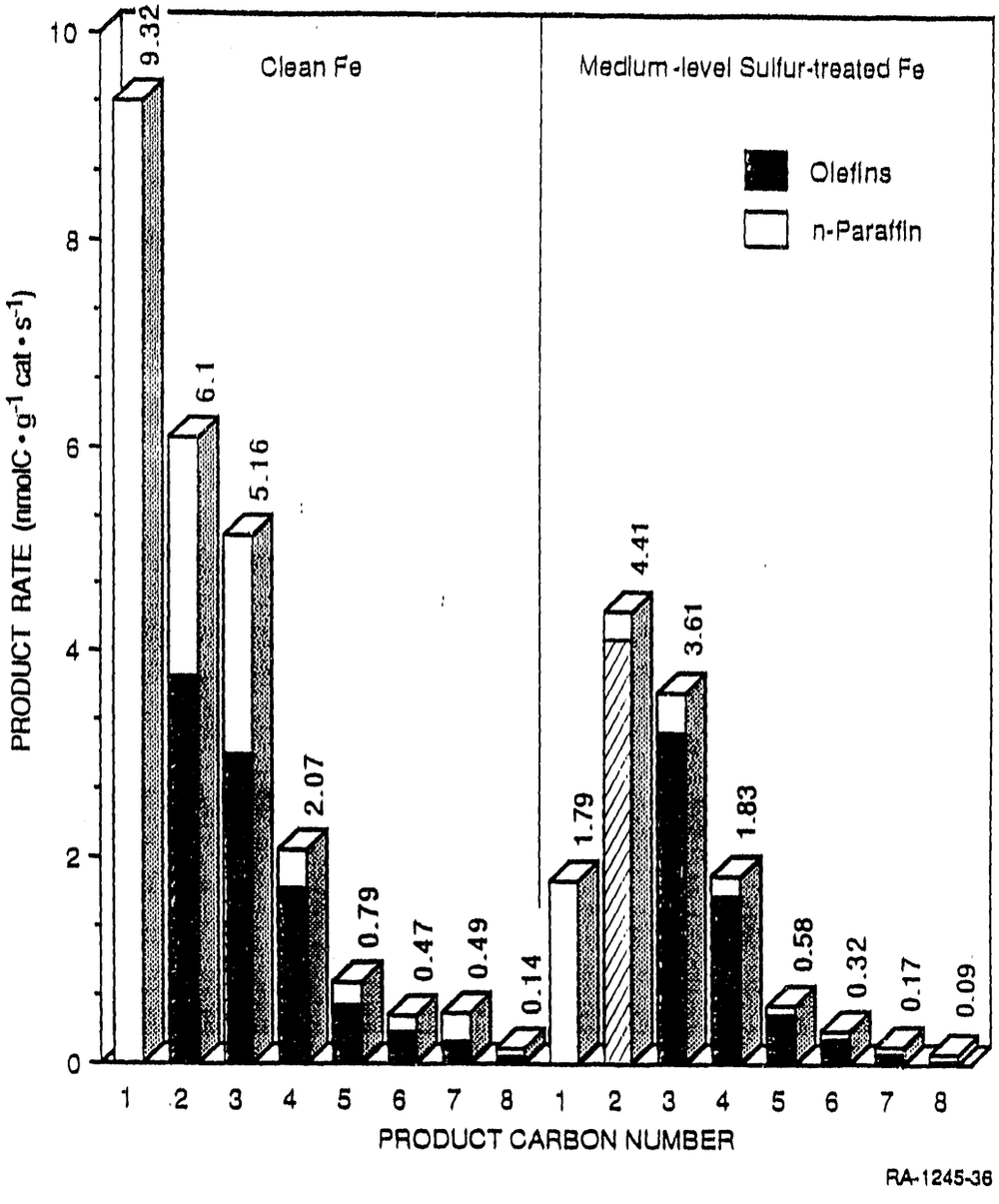

Figure II-7. Fischer-Tropsch synthesis at 573 K, 100 kPa, and H_2/CO ratio = 1, on clean and medium-level sulfur-treated fused iron catalysts after 24 h. Rates are given in nmoles carbon per gram catalyst per second.

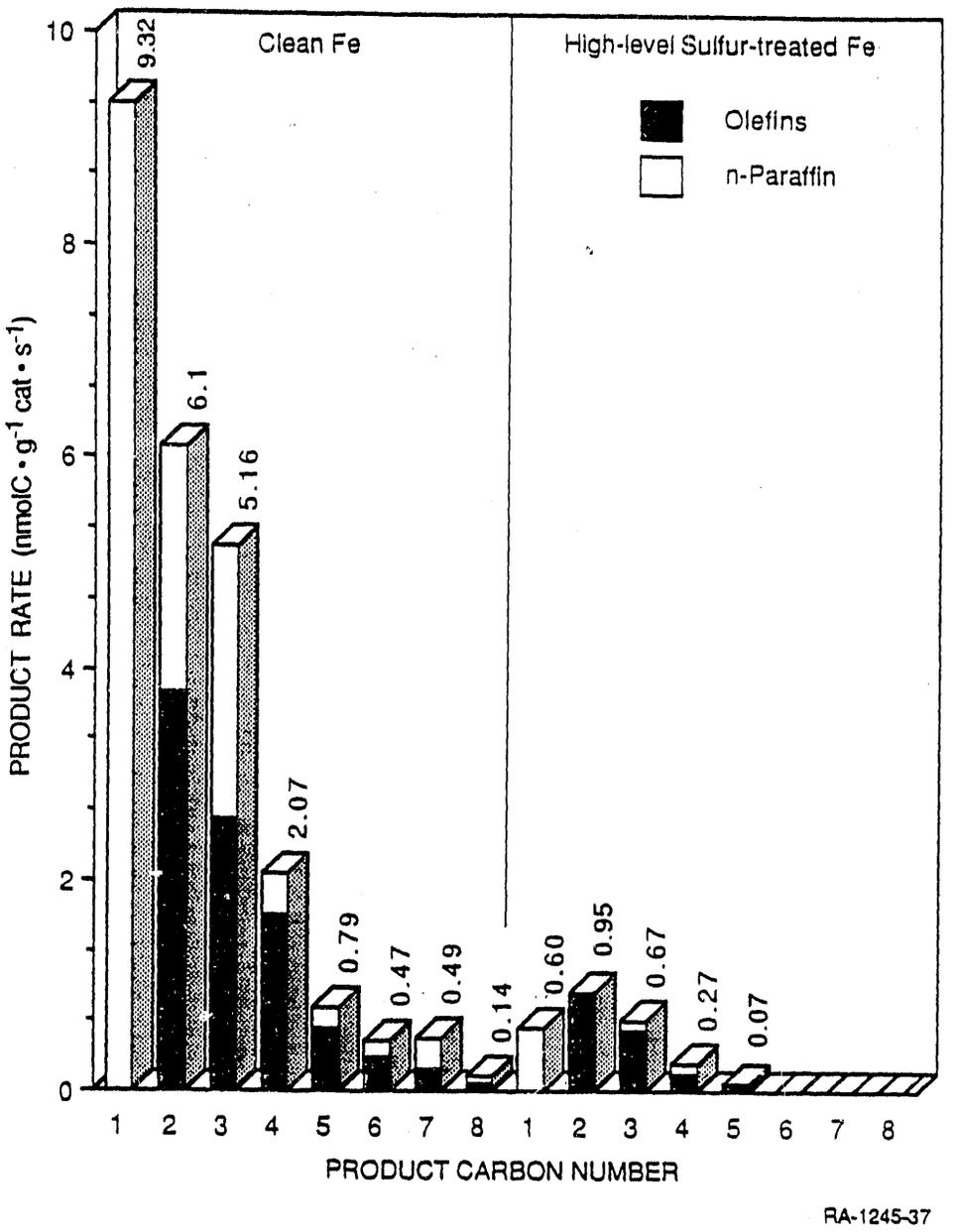

Figure II-8. Fischer-Tropsch synthesis at 573 K, 100 kPa, and H_2/CO ratio = 1, on clean and high-level sulfur-treated fused iron catalysts after 24 h. Rates are given in units nmoles carbon per gram catalyst per second.

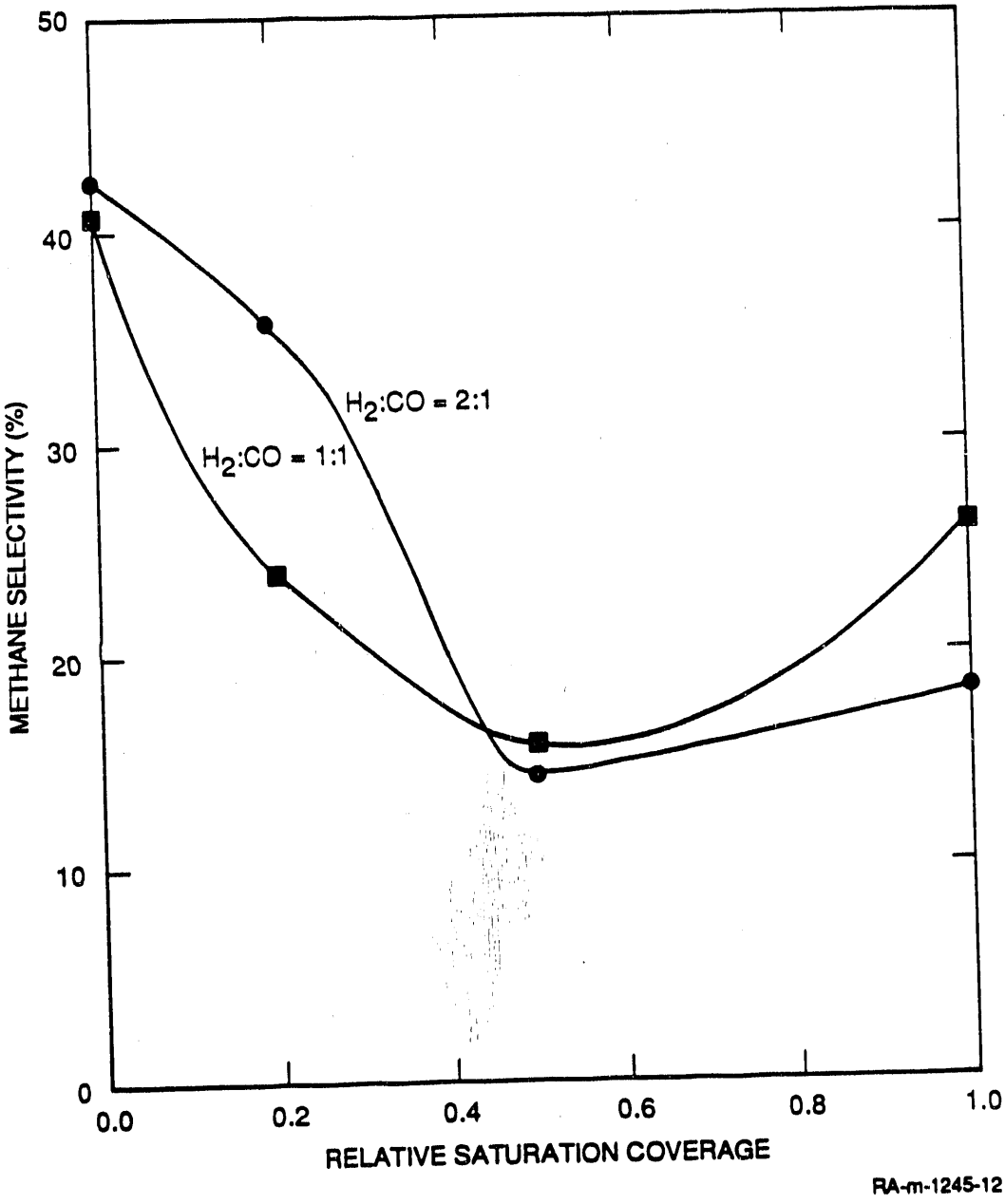

Figure II-9. Fischer-Tropsch synthesis at 573 K and 100 kPa on fused iron catalysts.

gas, the low- and medium-level sulfur-treated catalysts were comparable or superior to the deactivating clean fused iron (Figure II-10).

FTS Testing of Clean and Sulfur-Treated Cobalt Catalysts. The clean cobalt catalyst had higher FTS activity than the fused iron catalyst (Table II-4). The clean cobalt catalyst was 30 times higher in FTS activity initially than the fused iron catalyst at 548 K and 10 times higher at steady state (after a 24-h synthesis run). The clean cobalt catalyst produced hydrocarbons with a chain growth probability factor of 0.47 and a methane selectivity of 43% at 548 K. The chain growth probability factory increased slightly to 0.54 (Figure II-11), but the methane selectivity remained unchanged as the catalyst deactivated after a 24-h run. (At 523 K, the clean catalyst had a chain growth probability of 0.58 with 45% selectivity towards methane and showed no change with time.) The activity of the clean cobalt catalyst could be restored temporarily to its original value by TPR in 1-atm hydrogen up to 773 K. This effect implicated carbon deposition as the cause of deactivation of the clean cobalt catalyst, as could be expected from low-H_2 synthesis gas. The cobalt catalyst may have deactivated at a lower temperature than fused iron (548 K for cobalt and 573 K for fused iron) because of its greater rate of olefin production under low hydrogen conditions.

Figure II-12 shows the similarity of hydrocarbon product distribution between the clean fused iron and clean cobalt catalysts at 573 K and 548 K, respectively. It is most encouraging that the cobalt catalyst possesses a high olefin to paraffin selectivity (alkene/alkane ratio = 10) for light hydrocarbons and a ten-fold higher activity in its uncontaminated state and at lower temperature than the clean fused iron catalyst.

The medium-level sulfur-treated cobalt catalyst was examined for FTS activity and product distribution with $H_2/CO = 1$ synthesis gas at 100 kPa and 525 K. It showed reduced activity relative to the fresh cobalt catalyst but, unlike the sulfur-treated fused iron catalyst, only a moderate decrease in methane selectivity (Table II-4). The olefin-to-paraffin ratio for light hydrocarbons for the sulfur-treated cobalt

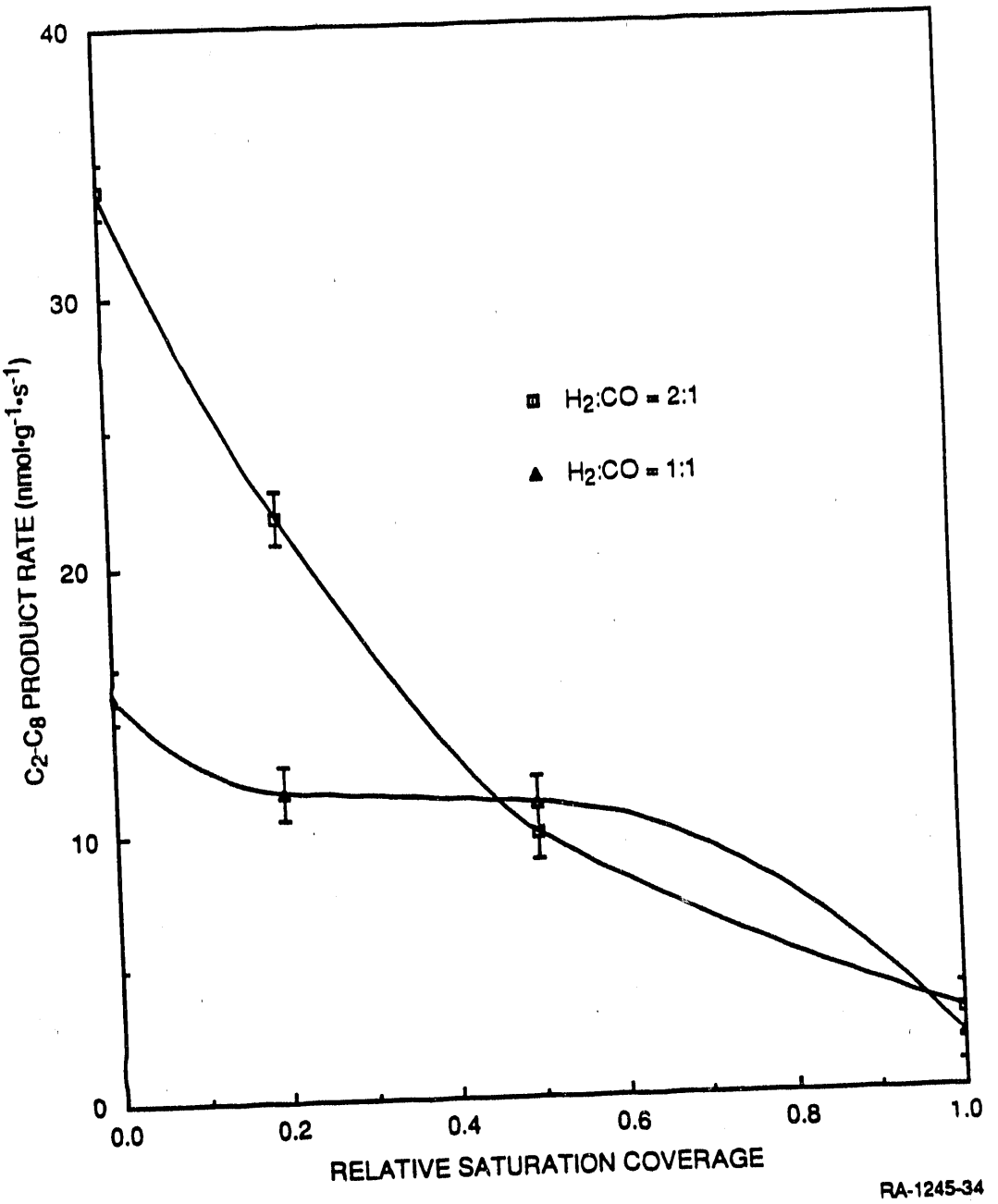

Figure II-10. Effect of sulfur treatment on light hydrocarbon product rate during Fischer-Tropsch synthesis at 573 K and 100 kPa on fused iron catalysts.

Table II-4

FIXED-BED FTS PERFRORMANCE OF CLEAN FUSED IRON AND CLEAN AND SULFUR-TREATED COBALT CATALYSTS

Catalyst	Clean Fused Iron		Clean 10 wt% Co/Al_2O_3			High-Level Sulfur-Treated 10 wt% Co/Al_2O_3	Medium-Level Sulfur-Treated 10 wt% Co/Al_2O_3	
Temperature	548	548	523	548	548	548	523	523
Pressure (MPa)	0.1	2	0.1	0.1	0.1	0.1	0.1	2
H_2/CO Ratio	1	1	1	1	1	1	1	1
Run Duration (h)	23	24	20	2	24	21	23	24
Production Rate[a] (nmol/g/s)								
CO_2	33.53	608.35	33.79	78.75	29.99	2.75	21.64	28.05
C_1	5.03	90.41	113.44	261.97	86.67	2.86	103.57	124.36
C_2	2.49	25.43	9.66	24.41	15.17	1.02	9.42	7.95
C_3	1.44	27.22	14.67	39.86	12.82	0.69	16.65	15.63
C_4	0.63	17.72	8.94	18.95	6.47	0.28	9.54	13.14
C_5	0.28	10.87	4.56	7.32	2.91	0.14	5.44	10.19
C_6	0.15	7.49	2.81	3.55	1.76	0.08	3.15	8.75
C_7	0.12	5.36	1.54	1.62	0.93	0.06	1.73	7.71
C_8	0.05	3.77	0.90	0.75	0.52		1.00	7.06
C_9	0.02	2.99	0.51	0.35	0.26		0.49	7.08
C_{10}	0.01	3.12	0.34	0.22	0.16		0.29	
TOTAL	20.60	518.08	278.09	586.76	221.12	9.69	284.03	517.3
Chain Growth Factor[b]	0.48	0.72	0.58	0.47	0.54	0.49	0.56	0.85
Olefin to Paraffin Ratio[c]	2.2	1.6	3.6	4.2	10.6		0.21	0.93
Methane Selectivity[d]	27	19	45	43	43	32	39	26

[a]GHSV = 600 h^{-1}; Product rate for each carbon number includes n-paraffins and α- and β-olefins; total product rate is on a carbon-atom basis.

[b]Average chain growth parameter (α) for C_{3+} hydrocarbons.

[c]Average olefin to paraffin ratio for C_2 to C_6 hydrocarbons.

[d]C_1 rate/(total rate) x 100%.

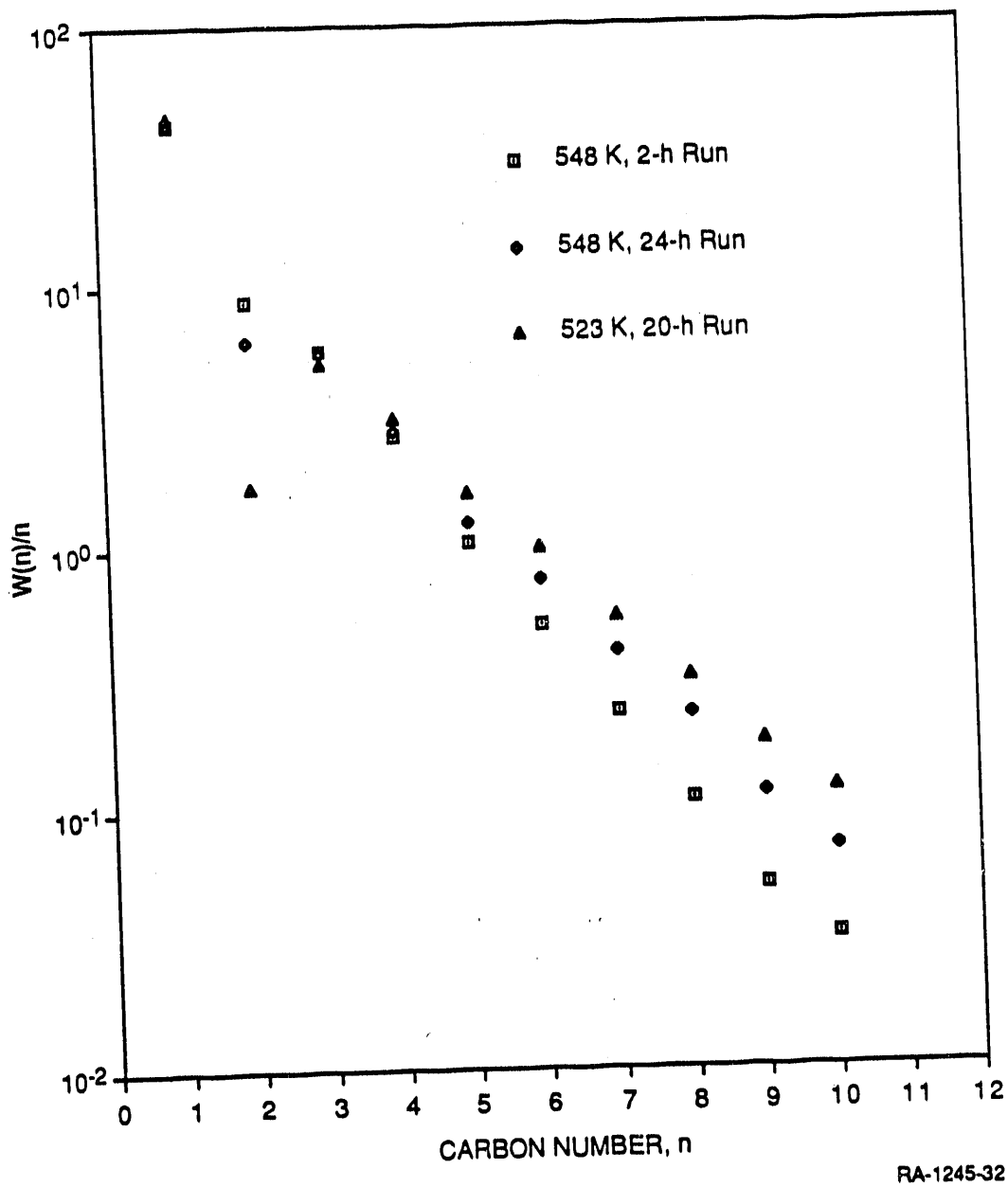

Figure II-11. Schulz-Flory plot of the hydrocarbon product distribution for cobalt on alumina catalyst at 100 kPa and $H_2/CO = 1.0$.

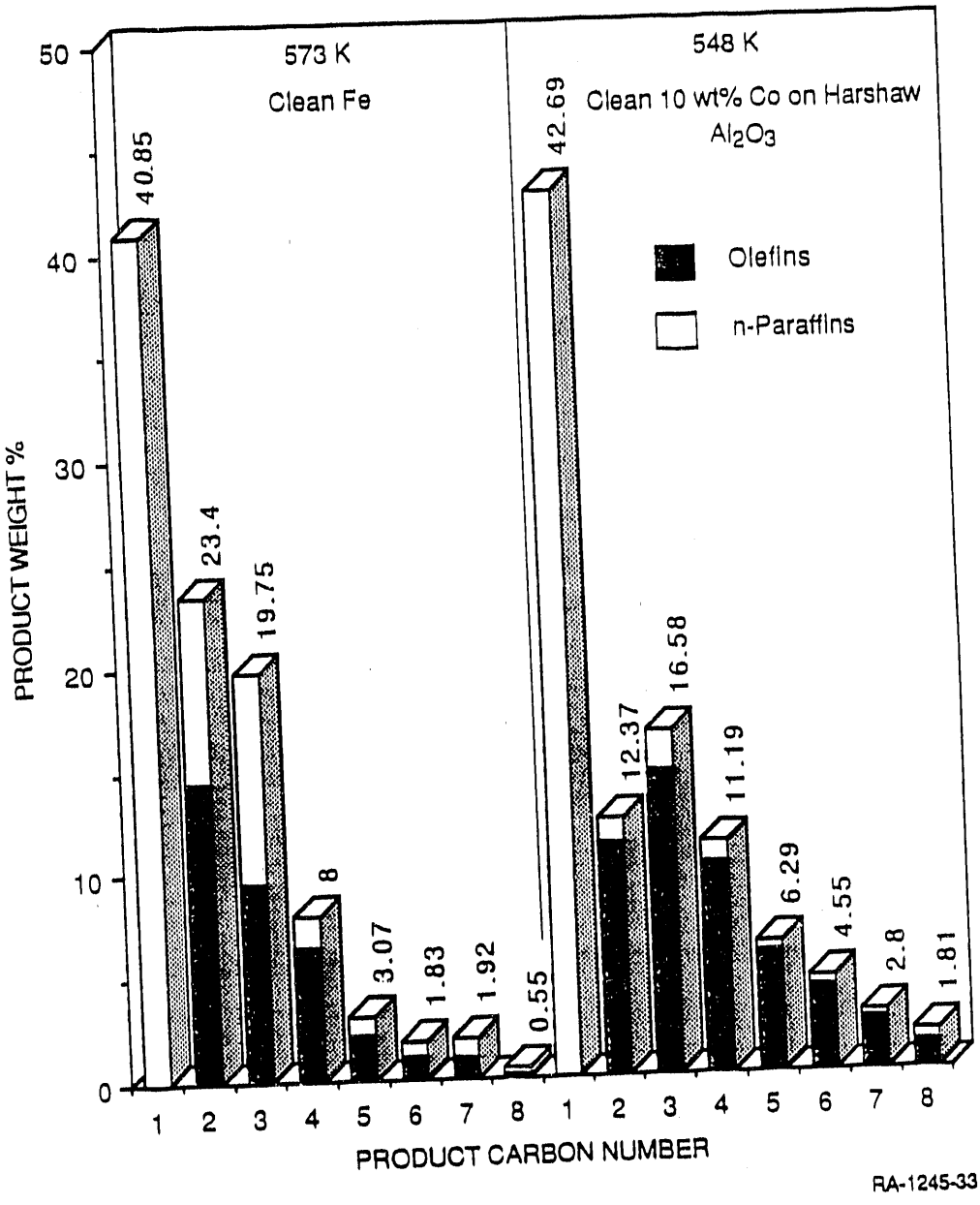

Figure II-12. Fischer-Tropsch synthesis at 100 kPa and H_2/CO ratio = 1 on clean fused iron and clean cobalt catalysts at 573 K and 548 K, respectively.

catalyst was also low (3:1) relative to that of the medium-level sulfur-treated fused iron catalyst (20:1). Unlike the sulfur-treated fused iron catalyst, which showed an increase in olefin selectivity relative to the clean iron catalyst, the sulfur-treated cobalt catalyst showed a decrease in light olefin selectivity compared to that of the clean cobalt catalyst under similar conditions.

Clean and Sulfur-Treated Precipitated Iron Catalysts. The clean and sulfur-treated K- and Cu-promoted precipitated iron catalysts were tested for FTS activity and found to be 68% and 48%, respectively, selective toward methane at 573 K and steady-state conditions. Preparing a sulfur-treated precipitated iron FTS catalyst at a desirable fractional monolayer coverage was difficult because we had no reliable measure of true metal surface area of the potassium-promoted precipitated catalyst. Even at what appeared to be full-saturation sulfur coverage (Θ_S = 1.0), the sulfur-treated precipitated iron catalyst remained more selective toward methane (48%) than fused iron catalysts. No further testing was done on the promoted precipitated iron catalyst because of its instability during sulfur treatment and its high selectivity for methane compared with that of the standard fused iron catalyst.

Evaluation of Improved FTS Catalysts

FTS performance of the medium-level sulfur-treated fused iron catalyst and the fused iron standard catalyst was examined in a fixed bed reactor at 2 MPa and 525 to 575 K. Typically, the CO conversion was about 20%. After 24 h at 575 K, the methane yield of the sulfur-treated fused iron catalyst was 15 wt% at low conversion, whereas the clean fused iron catalyst showed nearly 28 wt% CH_4 under the same reaction conditions (Table II-5). The chain growth parameter (for C_3-C_9) decreased from 0.65 to 0.52 with increased sulfur treatment (Figures II-13 and II-14).

The results for the fixed-bed FTS performance of the medium-level sulfur-treated fused iron FTS catalyst are encouraging. After 24 h, the total hydrocarbon rate at 573 K for the medium-level sulfur-treated catalyst was about 49.6% of the rate of the untreated catalyst. If only C_2 through C_{10} total hydrocarbon rates were considered, the activity of the

Table II-5

FIXED-BED FTS PERFORMANCE OF CLEAN AND SULFUR-TREATED FUSED IRON CATALYSTS AT 20-ATM

Catalyst	Clean Fused Fe		Medium-Level Sulfur-Treated Fused Iron			
Temperature (K)	573	548	573	548	573	548
H_2/CO Ratio	1	1	1	1	2	2
Run Duration (h)	24	24	24	24	24	24
Product Rate[a] (nmol/g/s)						
C_1	332.36	90.41	53.86	7.75	32.55	11.58
C_2	42.44	25.43	43.07	8.27	22.82	9.75
C_3	79.45	27.21	34.70	6.24	16.58	7.04
C_4	47.77	17.72	17.30	3.57	7.81	3.59
C_5	24.56	10.87	6.81	1.27	2.89	1.32
C_6	16.91	7.49	3.80	0.78	1.53	0.75
C_7	10.98	5.36	1.86	0.42	0.77	0.38
C_8	7.28	3.77	1.04	0.24	0.42	0.23
C_9	5.37	2.98	0.65	0.14	0.24	0.13
C_{10}	4.71	3.12	0.37	0.09	0.11	0.09
TOTAL	1201.43	518.08	401.16	75.34	194.85	84.21
Chain Growth Factor[b]	0.65	0.72	0.52	0.54	0.50	0.53
Olefin to n-Paraffin Ratio[c]	1.67	1.58	3.67	5.23	3.34	4.69
Methane Selectivity[d]	28	19	15	11.6	18.6	15.4

[a] GHSV = 600 h^{-1} and P = 20 MPa; Product rate for each carbon number includes n-paraffins and α- and β-olefins; total product rate is on a carbon-atom basis.

[b] Average chain growth parameter (α) for C_{3+} hydrocarbons.

[c] Average olefin to paraffin ratio for C_2 to C_6 hydrocarbons.

[d] C_1 rate/(total rate) x 100%.

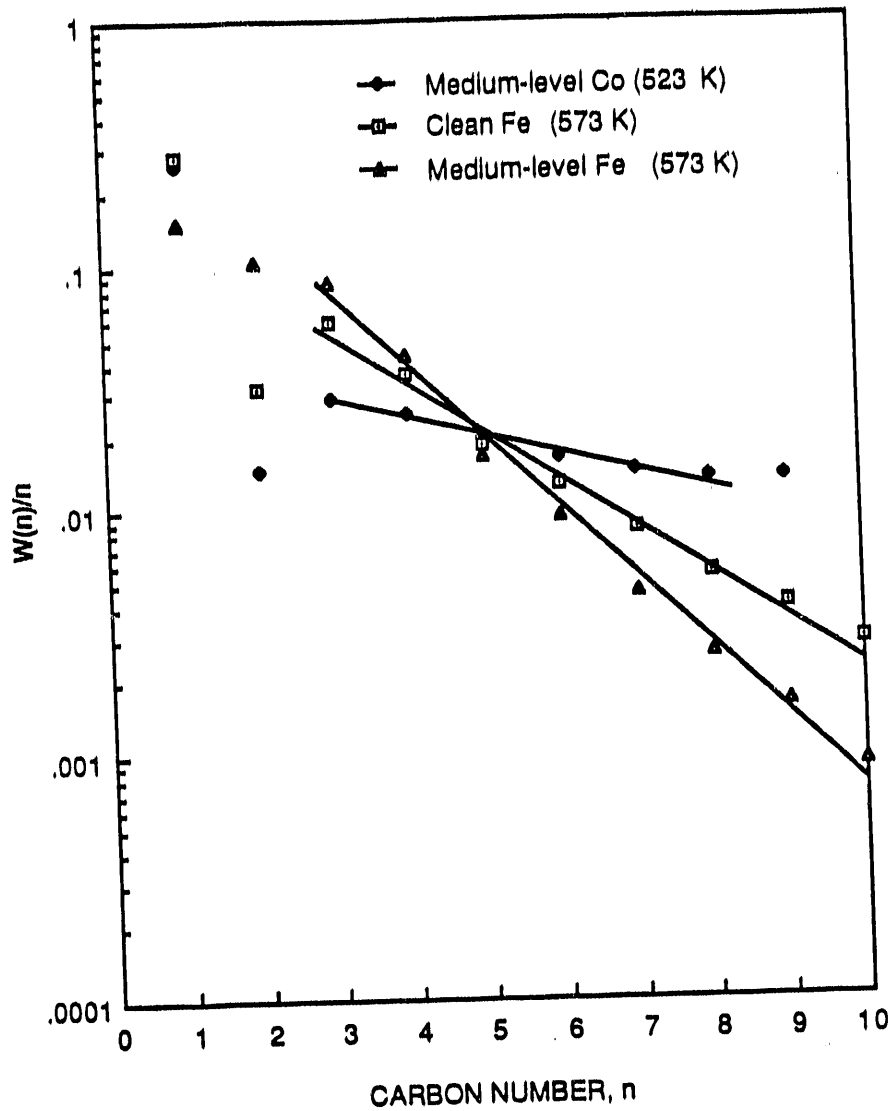

Figure II-13. Schulz-Flory-Anderson plot of the hydrocarbon product distribution for fused clean iron, medium-level sulfur-treated iron, and medium-level sulfur-treated cobalt catalysts at 2 MPa, $H_2/CO = 1$, and 573 K and 523 K, respectively.

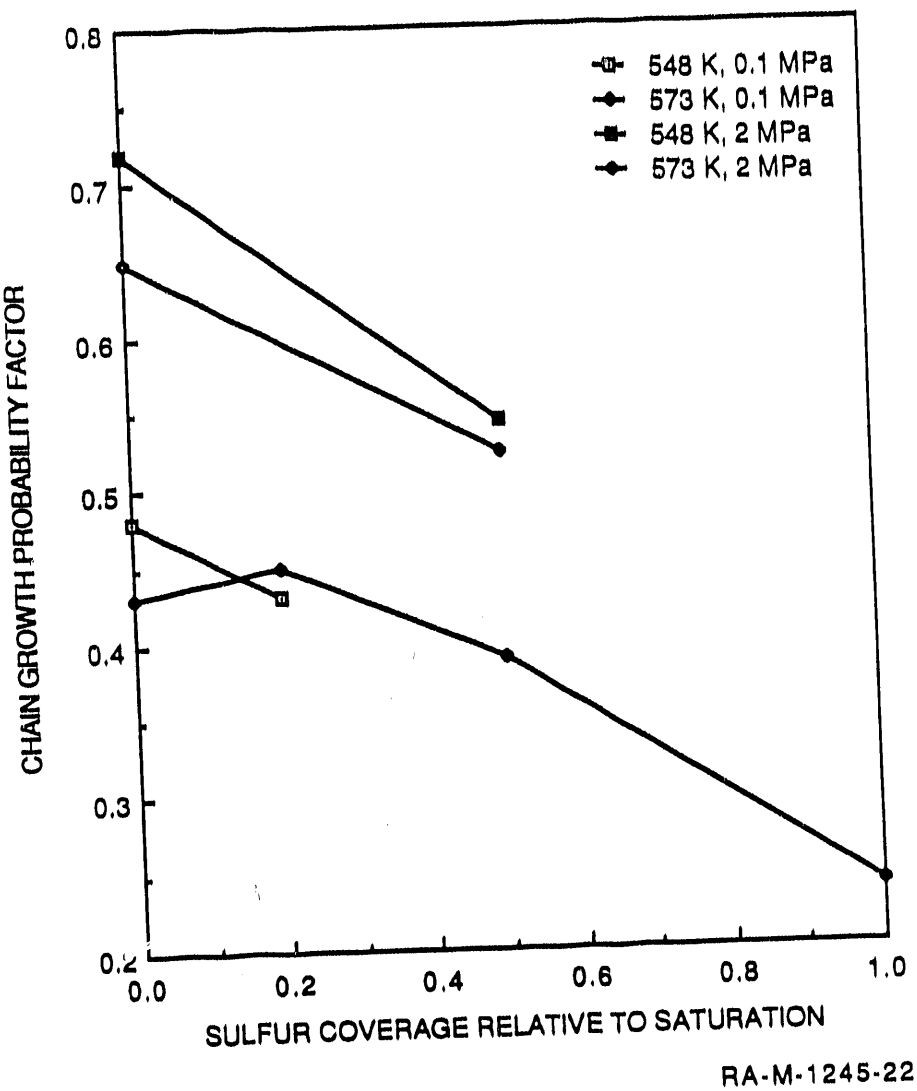

Figure II-14. Chain growth probability factor for clean and sulfur-treated fused iron catalysts with H_2/CO ratio = 1.

medium-level sulfur-treated catalyst was 66.8% of the clean catalyst. The sulfur-treated catalyst shows nearly the same level of improvement in methane selectivity (decreased by a factor of about 2) at 2 MPa as previously found at 100 kPa, with roughly a factor of three decline in overall rate at 575 K.

A hot-wax trap was installed at the exit of the FTS reactor. The trap was designed to collect C_{12+} hydrocarbons when operated at 393 K. The condensed wax was dissolved in toluene and analyzed by FIMS to determine the distribution and chain growth probability factor of higher hydrocarbons. Hydrocarbon wax contains both paraffins and olefins and exhibits chain growth probability of up to carbon number C_{50}. Samples from slurry reactor runs using cobalt and fused iron catalysts were kindly provided by Professor Satterfield of MIT and were used as the comparative standard and calibration for our FIMS data. In using the FIMS technique to analyze the MIT cobalt sample, which was composed almost entirely of normal paraffins, we obtained results (weight %) for C_{30} through C_{45} very similar to the data in the accompanying analysis.[18] Therefore, we were able to obtain the weight fractions of C_{30} and C_{40} in the sample from the hot wax trap for the fixed-bed synthesis run with clean fused iron at 573 K, 2 MPa, and H_2/CO ratio of 1 (Table II-6).

Table II-6

FIMS ANALYSIS OF FTS WAX

Carbon Number	FIMS Result (weight %)	Predicted Value (weight %)
30	3.07×10^{-4}	1.32×10^{-3}
40	4.34×10^{-5}	2.36×10^{-5}

We compared the FIMS results in Table II-6 to the values predicted by extrapolating to the wax range using the calculated (for C_3 through C_9) chain growth probability factor ($\alpha = 0.649$). The FIMS results indicated that a higher probability factor ($\alpha \tilde{=} 0.8$) existed for the wax range than for the light hydrocarbon range.

Discussion

The selectivity of the medium-level sulfur-treated fused iron catalyst with two to threefold reduction in methane yield and nearly 80% olefin selectivity for light hydrocarbons is most encouraging. The two to threefold decrease in activity can be offset by the higher operating temperature; i.e., the sulfur-treated catalyst operating at 573 K has about the same activity for C_{2+} hydrocarbon production as the untreated catalyst at 523 K. The adequate activity, low selectivity for methane, and high selectivity for light olefins make this catalyst a good candidate for FTS in a fluid-bed or fixed-bed reactor operating above 550 K to suppress wax production by lowering the Anderson-Schulz-Flory chain growth parameter.

Matsumoto and Satterfield[13] (at MIT) reported, in a study similar to our high-pressure fixed-bed studies, FTS results with sulfur-treated fused iron catalyst. They used liquid dibenzothiophene as the poison in a slurry reactor operating at 536 K, 1.48 MPa, and H_2/CO ratio of 0.7:1.0, and they observed that methane selectivity of the poisoned fused magnetite catalyst was significantly lower than that of the unpoisoned catalyst and that the olefin to paraffin ratio was higher on the poisoned catalyst than on the clean catalyst. They also reported that methane selectivity increased and olefin to paraffin ratio decreased with increased CO conversion and that neither parameter was substantially affected by temperature or pressure for a given sulfur-treated catalyst.

Comparison of the results of Matsumoto and Satterfield with our results (respectively) is complicated by differences in sulfur treatment methods (injection of dibenzyl-thiophene to the wax solution of freshly reduced and used carburized catalysts versus H_2S exposure to reduced and passivated catalysts), in extent of sulfur adsorption (approximately 1-10

monolayers determined by bulk elemental analysis versus submonolayer measured adsorption), and in reactor configuration (integral continuous stirred slurry reactor versus fixed-bed reactor, differential with respect to reactants). Since the MIT studies of sulfur-exposed freshly reduced catalysts probably resulted in formation of bulk sulfides, we compare only the results for the used carburized catalyst. The amount of sulfur adsorbed was approximately one monolayer, based on the elemental analysis and the leveling of sulfur loading with increased sulfur exposure. This average sulfur loading was about twice the level of our medium-level sulfur-treated catalyst and probably was less uniform. However, the similar change (roughly 50% decrease) in activity suggests comparable local sulfur coverage.

Our study showed that methane selectivity decreased from about 20 wt% to 12 wt% for the medium-level sulfur-treated fused iron catalysts compared with a 30 mol% to 15 mol% decrease in the MIT study, and the methane selectivity was not affected by increasing pressure (Figure II-15). However, in our study, the olefin to paraffin ratio was increased by the sulfur treatment but decreased with increasing pressure (Figure II-16). Their smaller pressure range (from 0.79 to 1.48 MPa compared to our 0.1 to 2 MPa) may explain why Matsumoto and Satterfield observed no pressure effect for methane selectivity or olefin to paraffin ratio. At 548 K and 2 MPa, our methane selectivities were in the same range for the clean C-73 iron catalyst as that reported for slurry reactor studies, e.g., Dictor and Bell,[19] Pennline et al.,[20] and Huff and Satterfield,[21] as well as Matsumoto and Satterfield.[13] Our study showed that the primary products were linear 1-olefins and paraffins with the majority of the olefins being terminal (i.e., α- versus β-olefins). We also observed that the β-olefin/α-olefin ratio increases with increasing carbon number and the olefin to paraffin ratio remains high (unity) in the wax range. These observations are in agreement with slurry results reported by Dictor and Bell.[19]

Sulfur-treated iron FTS catalysts may have beneficial properties in addition to improved product selectivity. One possibility is that the

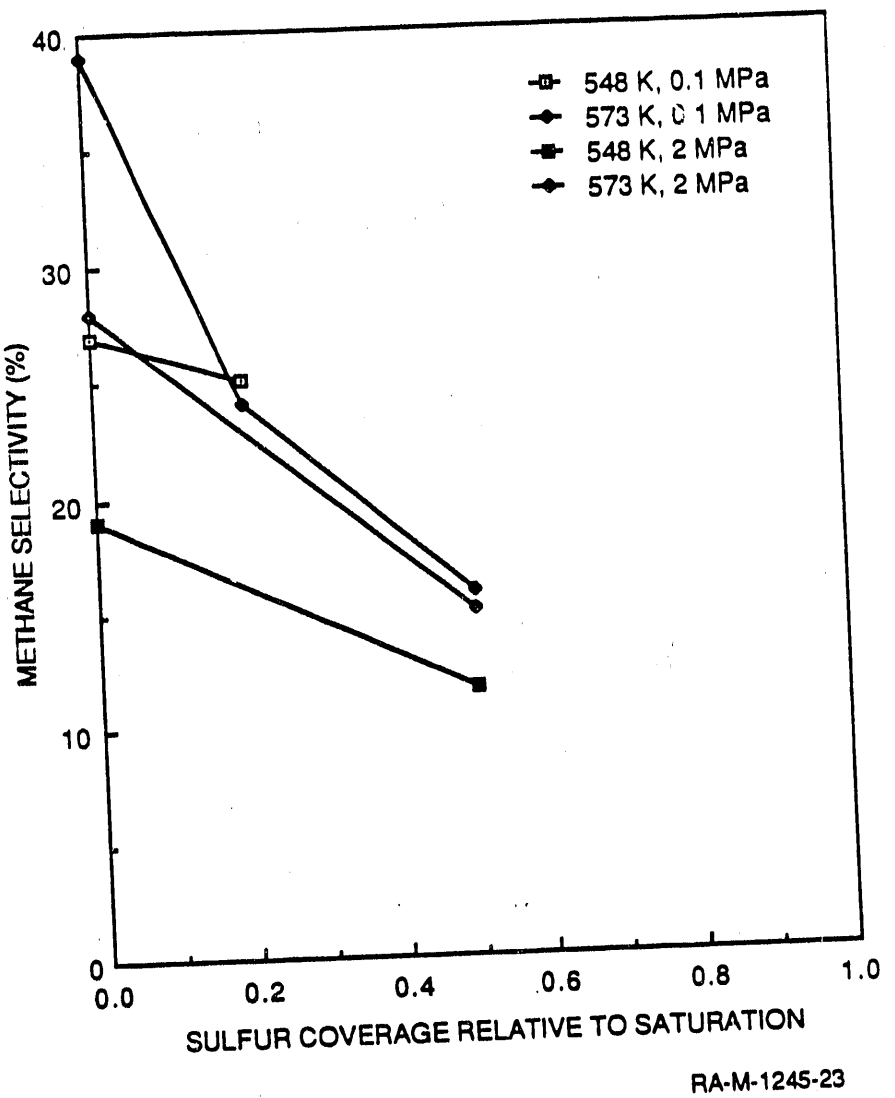

Figure II-15. Methane selectivity for fixed-bed FTS by clean and sulfur-treated fused iron catalysts with H_2/CO ratio = 1.0.

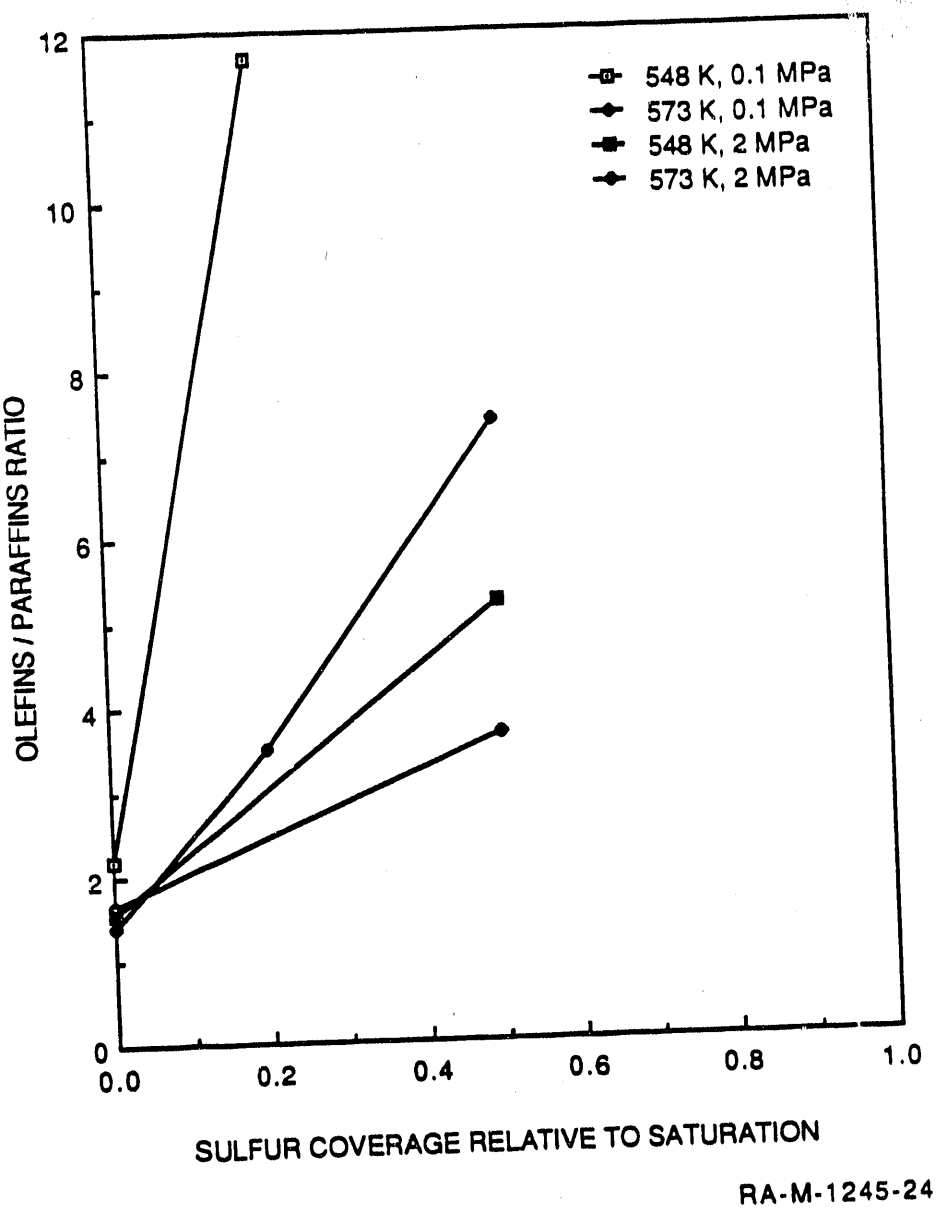

Figure II-16. Light olefin selectivity for fixed-bed FTS by clean and sulfur-treated fused iron catalysts with H_2/CO ratio = 1.0.

activity is more strongly dependent on pressure than for the untreated catalyst. The increased pressure dependence is due to the decreased binding strength of both chemisorbed hydrogen and carbon monoxide because of the presence of uniformly distributed surface sulfur. The reaction order for production of hydrocarbons (dependence of the log FTS rate on log partial pressure) is typically less than 1 for H_2 and less than 1 for CO, indicating that the active surfaces are nearly fully occupatied by adsorbed intermediates. Weakened CO and H adsorption could free reaction sites, thereby increasing the synthesis rate.

Another possible desirable property could be increased coking resistance. Steam re-forming catalysts are known to have increased resistance to coke formation owing to fractional adsorption of (low-level) sulfur. Deposition of catalyst carbon is associated with surface planes of high coordination (those containing steps and ledges), which may be responsible for methane formation and are known to preferentially bind adsorbed sulfur atoms on nickel surfaces. Increased coking resistance could allow FTS reaction with a higher CO-to-hydrogen ratio, perhaps 1:1 or greater, thereby increasing olefin and higher hydrocarbon yields while using less expensive synthesis gas processes following the gasifier.

Recommendations

The effect of increased conversion on methane and olefin selectivity of sulfur-poisoned fused iron must be examined in future work. Matsumoto and Satterfield[13] report that the initial improvements in selectivity noted at low conversion declined with higher CO conversion and at 80% conversion no enhancement in selectivity was observed. They offered no explanation. However, since the CO and especially H_2 levels (with H_2/CO = 0.7 in the feed gas) decline considerably at 80% CO conversion, the actual H_2 levels in the exit gas may have varied owing to the presence of sulfur. Perhaps the change noted[13] in the effect of water vapor on the activity, because of the sulfur treatment, is responsible for the change in selectivity with high CO conversion. Additional work with sulfur-

in selectivity with high CO conversion. Additional work with sulfur-treated C-73 fused iron catalysts at high CO conversion should clarify this phenomenon.

Sulfur treatment with stable manganese-promoted iron catalysts in the absence of alkali promoters should be examined further. The coking resistance of the sulfur treatment also warrants further study.

References

1. M. E. Dry, "The Fischer-Tropsch Synthesis," in Catalysis Science and Technology, J. B. Anderson and M. Boudart, Eds. (Springer-Verlag, 1981), p. 159.

2. M. E. Dry and J. C. Hoogendoorn, Catal. Rev. 23, 265 (1981).

3. S. Novak and R. J. Madon, Ind. Eng. Chem. Fundam. 23, 274 (1984).

4. R. J. Madon and H. Shaw, Catal. Rev. Sci. Eng. 15, 69 (1977).

5. E.F.G. Herington and L. A. Woodward, Trans. Faraday Soc. 35, 958 (1939).

6. F. Fischer and K. Meyer, Gest. Abb. Kennt. Kohle 11, 484 (1934).

7. J. G. King, J. Inst. Fuel 11, 484 (1938).

8. R. B. Anderson, F. S. Karn, and J. F. Shultz, J. Catal. 4, 56 (1965).

9. R. A. Dalla Betta, A. G. Piken, and M. Shelef, J. Catal. 40, 173 (1975).

10. C.H.B. Bartholomew, P. K. Agrawal, and J. R. Katzer, Adv. Catal. 31, 135 (1982).

11. D. W. Goodman and M. Kiskinova, Surface Sci. 105, L265 (1981).

12. C. N. Satterfield and H. G. Stenger, Jr., Ind. Eng. Chem. Process Des. Dev. 24, 407 (1985).

13. D. K. Matsumoto and C. N. Satterfield, Energy and Fuels 1, 203 (1987).

14. J. G. McCarty and H. Wise, J. Chem. Phys. 76, 1162 (1982).

15. J. G. McCarty and H. Wise, J. Chem. Phys. 74, 5877 (1981).

16. J. G. McCarty and H. Wise, J. Chem. Phys. 72, 6332 (1980).

17. H. Wise, J. G. McCarty, and J. Oudar, "Sulfur and Carbon Interactions with Metal Surfaces," Chpt. 1 in Deactivation and Poisoning of Catalysts, J. Oudar and H. Wise, Eds. (Marcel Dekker, 1985).

18. D. K. Matsamoto, private communication.

19. R. A. Dictor and A. T. Bell, Appl. Catal. 20, 145 (1986).

20. H. W. Pennline, M. F. Zarochak, R. E. Tischer, and R. R. Schehl, Appl. Catal. 21, 313 (1986).

21. G. A. Huff, Jr., and C. N. Satterfield, J. Catal. 85, 370 (1984).

III SYNTHESIS OF AROMATIC HYDROCARBONS

Introduction

Single-stage direct conversion of synthesis gas into aromatic hydrocarbons is a demonstrated catalytic process. Combination of acidic synthetic zeolites, such as Mobil's ZSM-5, and FTS catalysts have been shown by Chang et al.[1,2], Seitzer,[3] and Rao et al.[4] to produce benzene, toluene, and mixed xylenes from syngas with high selectivity. Combinations of catalysts selective for methanol synthesis and ZSM-5[5-7] or other zeolites[8] have also been shown by Shamsi et al.,[5] Bruce et al.,[6] and Varma et al.,[7] to produce BTX with high selectivity. The zeolite may synergistically convert the unstable intermediate synthesis products, olefins or alcohols, into the more thermodynamically stable aromatics. However, the advantage of single-stage reaction is generally offset by the disadvantage of nonoptimal operating conditions of sequential reactions. As a consequence, Mobil has developed the methanol-to-gasoline (MTG) process with ZSM-5 to convert syngas into gasoline following conventional methanol synthesis, a commercially established technology.

Single-stage aromatics synthesis has two principal disadvantages: (1) the compromised operating conditions have suboptimal yields and (2) the catalytic active components are deactivated by carbon deposition (coking). FTS or methanol synthesis is thermodynamically favored at low temperature and high pressure, whereas conversion of olefins or alcohols to aromatics is favored at high temperature and low pressure. Low temperature operation (500 K) slows conversion into aromatics, whereas high temperature operation (700 K) tends to produce too much light alkane, especially methane, and also tends to promote rapid deactivation because of carbon deposition on the catalyst. Thus, the synergistic potential of dual-function catalysts to produce high selectivity and high conversion has not been realized, and two-stage processing is currently a more attractive technology.

Direct aromatic hydrocarbon synthesis over a dual-function catalyst with unusually low concentration of hydrogen in the reactant gas has the potential advantages of high aromatic yields, stoichiometrically and thermodynamically limited methane yield, relatively dry product gas, and nearly complete hydrogen consumption. The principal difficulty in processing low hydrogen syngas is the need to suppress the greater tendency for carbon deposition on the catalyst and subsequent catalyst deactivation. In our previous study (Section II), we found the sulfur-treated iron catalysts did not deactivate during FTS synthesis with H_2/CO = 1 syngas. Therefore, we investigated several combinations of zeolites with the the coking-resistant sulfur-treated fused iron catalysts for FTS performance and aromatic hydrocarbon production in a fixed-bed reactor with low hydrogen syngas.

Background

Achieving the goal of efficient single-stage conversion of olefins to aromatics depends on identifying one or more catalysts that use low-hydrogen syngas, especially those that resist formation of deactivating carbon. The single-stage conversion of syngas to aromatic hydrocarbons is a feasible and demonstrated concept. The unique aspect of our approach is the evaluation of catalyst performance under conditions expected to favor relatively severe carbon deposition, i.e., low H_2/CO ratio (0.5) and moderately high temperature. The selection of candidate catalysts is discussed below following a brief review of earlier research on the direct conversion of syngas to aromatics. Finally, carbon deposition is discussed in detail.

Direct Synthesis of Aromatic Hydrocarbons

Several reports of direct conversion of syngas to aromatic hydrocarbons have been published the last decade. Both promoted FTS and methanol synthesis catalyst components with a strongly acidic zeolite component have been examined with varying degrees of success.

In an early study, Chang et al.[1,2] reported results for iron, zirconia, and ZnO/Cr_2O_3 catalysts combined with ZSM-5 molecular sieve zeolite under the conditions $H_2/CO = 1$, 644 K, and 3.5 MPa. Addition of the zeolite produced aromatic hydrocarbons and greatly decreased the olefin selectivity, but yields were only 5 wt% with the balance methane and light alkanes. The ZnO/Cr_2O_3/ZSM-5 catalyst fared better at 700 K and 8.3 MPa, with 70 wt% aromatics, while the ZrO_2/ZSM-5 catalyst at 700 K and 8.3 MPa produced nearly 85 wt% aromatics. Selectivity for aromatics in the C_{5+} fraction was very high (97%) for the last two catalysts.

In general, FTS catalysts tend to form light hydrocarbons at temperatures favorable to conversion of intermediate olefins to aromatics over the zeolite. Low selectivity for aromatics (about 10 wt%) was reported for copper chromite-promoted iron with a Y-type zeolite.[3] Similar results were found for Fe/ZSM-5 and Fe-Co/ZSM-5 bifunctional catalysts.[4] Conversion to aromatics by several 9 wt% Co/ZSM-5 catalysts varied from 8 to 25 wt% selectivity, depending on method of preparation, with physical mixture of components giving the greatest aromatic yield.[5] Thoria-promoted Co/ZSM-5 at 595 K and 2 MPa with $H_2/CO = 1$ gave selectivities[9] approaching 10 wt% with a high yield of methane and moderate deactivation (50% loss in activity after approximately 150 h). Several studies with zirconia[6,7] or MnO_2-promoted[8] Ni-Co alloys with ZSM-5 have shown sustained (>200 h) aromatics production of up to 30 wt% with $H_2/CO = 1$, 523 K, and 0.1 MPa.

However, two-stage conversion currently is the method of choice for FTS routes to aromatics. Superior results were obtained for Ru/ZSM-5[10] and ZrO_2-promoted Ni-Co/ZSM-5[11] combinations in separate reactors because optimal operation of the zeolite requires temperatures at which typical FTS catalysts produce methane and tend to deactivate. A similar situation applies to the well-known and recently commercialized Mobil process using conventional methane synthesis with Cu-ZnO and methanol-to-gasoline (MTG) conversion with ZSM-5.

Direct aromatics production with alcohol/zeolite catalyst combinations has been examined for unpromoted $ZnO-Cr_2O_3$/ZSM-5 (discussed above),[1] Pd-promoted[12] $ZnO-Cr_2O_3$/ZSM-5, and several Pd/zeolite[13] catalysts. The best selectivities of these catalysts were 85 wt% (700 K and 8.3 MPa), 41 wt% (654 K and 2 MPa), and 51 wt% (627 K, 2.1 MPa, H-exchanged mordenite zeolite), respectively. Since the Mobil process with its very high gasoline range (C_{5+}) and aromatic hydrocarbon selectivity sets the standard for two-stage synthesis gas processing, current catalyst performance fails to provide adequate incentive for direct single-stage production of aromatics by this route, i.e., the combination of ZHSM-5 and a methanol synthesis catalyst.

Effect of Promoters in FTS Catalysis

Over the past 60 years, researchers have sought ways to modify conventional FTS catalysts to achieve a narrow product distribution in the gasoline range. A key difficulty is the high yield of light alkanes. More recent work[14,15] has shown that chemical modification of iron FTS catalysts permits formation of light olefins in the C_2 to C_4 range and suppression of methane.

Several investigators have reported that the use of Mn and alkali promoters increases light olefin selectivity of iron FTS catalysts. A manganese, potassium, and zinc-promoted iron catalyst (100 Fe : 100 Mn : 10 ZnO : 4 K_2O) operating at 595 K, 1 MPa, and H_2/CO ratio of 1 can achieve a product distribution of 70.9 wt% C_2 to C_4 olefins. This catalyst appears to be able to operate at a low degree of polymerization without giving the high yield of methane (9.6 wt%) predicted from Shultz-Flory statistics. Abbot et al.[16] have shown that the addition of sodium (Na/Fe = 0.1) and manganese (Mn/Fe = 0.4) to alumina-supported iron catalysts produces a stable catalyst with high selectivity for light olefins and concurrent suppression of methane selectivity. Ratios of olefins/paraffin equal to 5 are observed in the range C_3 through C_5, with methane selectivity reduced to less than 10% at 550 K, 800 kPa, and CO/H_2 ratio of 2. Deckwar et al.[17] observed, at 1.2 MPa, 570 K, and CO/H_2

ratios of 1.68 and 1.87, the product distribution of an Mn/Fe catalyst with C_2 through C_4 hydrocarbon yield of 77.2 wt% and 74.5 wt%, and C_2 through C_4 olefin yield of 57.1 wt% and 50.3 wt% for slurry-phase and fixed-bed reactors, respectively.

Selective poisoning also enhances the selectivity of iron for light olefins, suppresses methane production, and most importantly may greatly inhibit carbon deposition. We have demonstrated (see Section II) that sulfur-treated fused iron preferentially decreased methane formation and increased the olefins to n-paraffin ratio for light hydrocarbons during FTS reaction at 0.1 to 2 MPa, 573 to 593 K, and H_2/CO ratio = 1-2. The ratio of ethylene to ethane was about 15 for the sulfur-treated catalyst. C_3 through C_6 hydrocarbons produced from this catalyst were also highly olefinic, having an average ratio of olefins to n-paraffin of about 10. The product distribution consisted of 69.6 wt% C_2 through C_4 olefins and 75.2 wt% C_2 through C_4 olefins plus paraffins.

Unlike the reduced untreated fused iron catalyst, which deactivated with time on-stream, the medium-level sulfur-treated fused iron catalyst showed continued steady evolution of CO_2 and hydrocarbon products with syngas exposure time. After 24 h, the total hydrocarbon rate at 573 K for the medium-level sulfur-treated catalyst was about half the rate of untreated catalyst. The selectivity of the medium-level sulfur-treated fused iron catalyst with almost a threefold reduction in methane yield and nearly 90% olefin selectivity for the light hydrocarbons was most encouraging. The roughly twofold decrease in activity can be offset by higher operating temperature, that is, the sulfur-treated catalyst operating at 573 K had about the same activity for C_{2+} hydrocarbon production as the untreated catalyst at 523 K. The adequate activity, low methane selectivity, high selectivity for light olefins, and coking resistance of this catalyst make it a good candidate for FTS in a fluid- or fixed-bed reactor operating above 600 K to suppress wax production.

Carbon Deposition

Thermodynamics of syngas conversion can be invoked to predict the catalyst phase and the product distribution for equilibration. The phase diagram[18,19] for iron carbides (Fe_3C and Fe_2C) and iron oxide (Fe_3O_4), given an equilibrated gas mixture at 700 K, shows that under the conditions of the proposed work Fe_3O_4 and both carbides would be stable. The initial feed gas has considerably greater carburizing thermochemical potential than the equilibrated gas; consequently, bulk iron carbides always form during FTS. Iron carbides are also thought to rapidly catalyze formation of filamentous carbon, which can lead to fouling. Thus, operating temperatures are kept below 533 K in fixed beds[20] to avoid catalyst disintegration and plugging of the bed. Studies of the rate of carbon formation for syngas at 1 MPa and 573 K have shown a relationship between P_{CO}/P_{H_2} and the rate of carbon deposition.

A similar situation exists for reduced metal Co and Ni catalysts, except that the Ni oxide (NiO) is always unstable and the carbide (Ni_3C) is typically thermodynamically unstable in the presence of equilibrated gas. Nickel catalysts are capable of operating under severe coking conditions during hydrocarbon steam re-forming. Pretreatment of nickel on magnesium aluminate supports with fractional monolayers of chemisorbed sulfur has shown[21] that operation well into the region of carbon deposition is feasible. At elevated temperature (>500 K), chemisorbed sulfur on single-crystal surfaces has been shown in our laboratory to become locally mobile[22] and to segregate at surface dislocations or randomly occupy high coordination sites on crystal planes. Rostrup-Nielsen[21] has suggested that random distribution of sulfur on metal surfaces inhibits the nucleation and growth of carbon by an ensemble effect; i.e., a group of six or seven associated carbon chemisorption sites may be required for nucleation of carbon. Therefore, random occupation of those sites by adsorbed sulfur atoms at half-coverage could decrease the rate of carbon deposition by two orders of magnitude. In this scenario, FTS of steam re-forming requires ensembles with fewer sites to act as reaction centers (e.g., three adjacent sites) so that the poisoning has much less effect on the desired reactions.

Another explanation of the inhibiting effect of sulfur chemisorption on carbon deposition is selective blockage of high coordination sites. Deposition of catalyst carbon may be associated with surface dislocations, such as steps and ledges, that have high coordination with an adsorbing atom or molecular fragment. Such sites may be responsible for hydrogenation activity (such as methane formation) and may accumulate coke in the same way as noble metal naphtha re-forming catalysts. Note that Pt/Al_2O_3 naphtha re-forming catalysts operate under conditions that greatly favor carbon deposition, yet these catalysts are used for months without regeneration.

Experimental Results

Sulfur Treatment of FTS Catalysts

In our preceding studies with sulfur-treated fused iron catalysts, we found that partially sulfur-covered iron surfaces produced fewer saturated light alkanes than did untreated catalysts and exhibited no observable coking. The medium-level sulfur-treated iron catalysts prepared as described previously were mixed with zeolite and tested at 2 MPa for their ability to produce aromatics in syngas with H_2/CO ratio = 0.5. A new sulfur-treated catalyst, Ru/Al_2O_3, was also prepared for this study using the same sulfur treatment procedure.

Medium-level Sulfur Treatment of Ru/Al_2O_3 Catalyst

The alumina-supported ruthenium FTS catalyst was treated with H_2S until sulfur was chemisorbed to a coverage of about one-half saturation. Following a more severe passivation procedure (exposure to 99.5% CO at 523 K subsequent to 10.4% C_2H_4/He), the rate of sulfur adsorption at 425 K was slowed to about monolayers per hour in a recirculating stream of 10 ppm H_2S in 100-kPa H_2. After removal of the carbon overlayer in 1-atm H_2 at 773 K, the catalyst was removed from the sulfur treatment apparatus, reduced and tested for aromatics sysnthesis performance in the fixed-bed FTS reactor system.

The aromatics synthesis performance of the medium-level sulfur-treated fused iron catalyst, the medium-level sulfur-treated alumina-supported ruthenium, the clean alumina-supported ruthenium, and the fused iron standard catalyst, all in combination with Union Carbide Na-Y zeolites [sodium content: 0.2 wt% (LZY-52), 2.0 wt% (LZY-62), and 10 wt% (LZY-82)] were examined in a fixed-bed reactor at 2 MPa, H_2/CO ratio = 0.5, and 548 to 700 K (Table III-1). The catalyst bed was a physical admixture of the FTS and zeolite catalyst powders (10/14 mesh) of various weight ratios (zeolite/FTS catalyst ratio = 4 or 10) maintained at a constant temperature. Typically, CO conversion was about 20% at a gas hourly space velocity (GHSV) of 1×10^4 to 2×10^4 h^{-1}. GHSV is defined as the hourly flow rate (NTP) of $CO + H_2$ per unit volume of the FTS catalyst component.

After 2 h at 573 K, the methane yield of the sulfur-treated fused iron only and of the Na-Y zeolite combination was 11 and 15 wt%, respectively. The oxygenate (methanol and dimethylether) and aromatic (benzene, toluene, ethylbenzene, and xylenes) yields of the sulfur-treated fused iron, Na-Y zeolite combinations were much greater than the yield of fused iron alone. The amount of oxygenates initially produced (after 2 h) depended heavily on the sodium weight loading of the zeolite of the mixed catalyst (Table III-1). The chain growth parameter, α, decreased substantially from 0.71 to 0.34 with increased oxygenate and aromatic hydrocarbon selectivity. The methane yield remained low and decreased slightly for catalysts with the smallest zeolite component.

However, the combination fused iron and zeolite catalysts were prone to deactivation by carbon deposition in hydrogen-deficient syngas. After 24 hours of synthesis reaction, the product distribution typically resembled that of the sulfur-treated fused iron catalyst alone (Figure III-1). The decreased oxygenate and aromatics yields were nearly matched by the increased olefin yield, suggesting that the zeolite component of the mixed catalyst was deactivated, probably by carbon deposition. Deactivation was most pronounced for the zeolite with low sodium weight

Table III-1

SYNTHESIS OF AROMATICS AND OXYGENATES BY MIXTURES OF SULFUR-TREATED FUSED IRON AND ZEOLITE CATALYSTS

Catalyst	Medium-Level Sulfur Treated Fused Iron	Medium-Level Sulfur-Treated Fused Iron + LZY-82 Zeolite (1:4 by wt)	Medium-Level Sulfur-Treated Fused Iron + LZY-52 Zeolite (1:4 by wt)	Medium-Level Sulfur-Treated Fused Iron + LZY-62 Zeolite (1:10 by wt)	Medium-Level Sulfur-Treated Fused Iron + LZY-52 Zeolite (1:10 by wt)			
Temperature (K)	573	573	573	573	573	650	650	700
Pressure (MPa)	2	2	2	2	2	2	2	2
H_2/CO Ratio	1	0.5	0.5	0.5	0.5	0.5	0.5	0.5
Run Duration (h)	24	2	2	2	2	1.5	23.5	1
Production Rate[a] (nmol/g/s)								
C_1	53.86	262.28	326.62	162.09	165.78	153.32	222.39	193.67
C_2	43.07	63.66	183.18	33.27	62.66	58.13	67.63	59.87
C_3	34.71	106.90	166.96	39.69	31.40	52.06	72.97	56.98
C_4	17.30	53.11	119.34	20.40	15.49	26.98	47.47	25.26
Oxygenates	2.17	451.00	173.49	190.19	176.47	272.47	14.34	205.10
Aromatics	0.03	0.00	59.67	11.21	13.67	54.24	4.72	20.55
TOTAL	401.16	1743.20	2901.80	870.10	950.20	1662.60	1080.10	1199.60
Chain Growth Factor[b]	0.52	0.34	0.71	0.45	0.61	0.56	0.50	0.40
1-Butene to Butane Ratio[c]	0.85	0.00	0.78	0.00	0.07	0.12	0.70	0.06
Methane Selectivity[d]	14.76	11.54	11.53	15.60	15.10	8.58	22.00	14.20
Oxygenate Selectivity	1.24	57.09	15.10	51.71	39.90	38.60	3.61	38.20
Aromatic Selectivity	0.52	0.00	11.90	5.61	6.30	16.80	2.51	8.08

[a] GHSV = 600 h^{-1}; Product rate for each carbon number includes n-paraffins and α- and β-olefins; total product rate is on a carbon-atom basis.

[b] Average chain growth parameter (α) for C_{3+} hydrocarbons.

[c] Average olefin to paraffin ratio for C_2 to C_6 hydrocarbons.

[d] C_1 rate/(total rate) x 100 %.

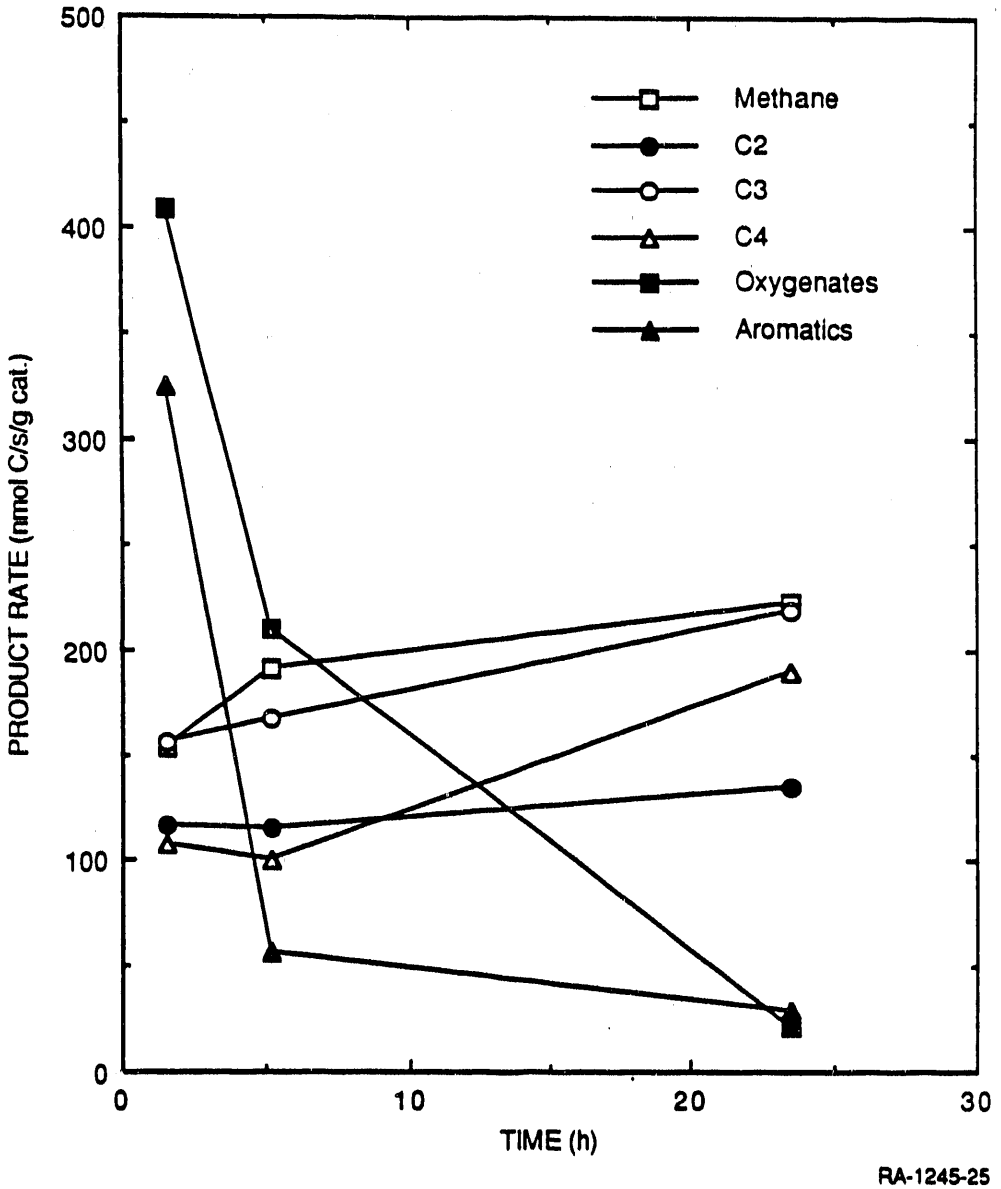

Figure III-1. Aromatic synthesis at 573 K, 2 MPa, H_2/CO ratio = 0.5 on medium-level sulfur-treated fused iron catalyst and LZY-52 zeolite (1:10 wt ratio).

loading. However, the catalysts could be regenerated by reacting the deposited carbon with pure hydrogen at 773 K and 100 KPa for 2 h. To prolong the useful life of the catalyst, especially at higher temperatures, we used a larger amount (10:1 versus 4:1) of a less acidic (higher sodium content, LZY-52) zeolite in combination with the sulfur-treated iron catalyst. This zeolite combination also showed evidence for deactivation in the form of decreased oxygenate and aromatic yields at 650 K (Table III-1).

The mixed catalyst with low sodium (LZY-82) produced predominantly oxygenates, with high conversion of the light olefins. The mixed catalyst with high sodium (LZY-52) produced a mixture of oxygenates and aromatics of roughly equal proportion, with correspondingly lower conversion of the light olefins (Figure III-2). The mixed catalyst with (LZY-62) had a product distribution similar to that of the LZY-52 mixed catalyst (Figure III-3).

The activity of the sulfur-treated alumina-supported ruthenium/Na-Y zeolite catalyst was a factor of ten lower than that of the sulfur-treated fused iron/Na-Y zeolite catalyst at 573 K. However, the oxygenates and aromatics selectivities (28 wt% and 17 wt%, respectively) of the ruthenium/Na-Y zeolite mixed catalysts were roughly the same as that of the fused iron mixed catalyst. The lower activity of the ruthenium mixed catalyst (per unit weight FTS catalyst) was primarily due to its much lower metal weight loading (2.4 wt% Ru) compared to that of the bulk fused iron mixed catalyst. The sulfur-treated ruthenium mixed catalyst showed 50% decreased methane and a factor of two increased oxygenates and aromatics yields at both 573 and 598 K when compared to the clean ruthenium mixed catalyst (Table III-2).

Discussion

The synthesis of aromatic hydrocarbons was performed under differential reactor conditions because of the constraints of maximum catalyst bed volume and minimum controllable syngas flow rate at elevated pressure. As a result, overall conversion of the syngas was limited to

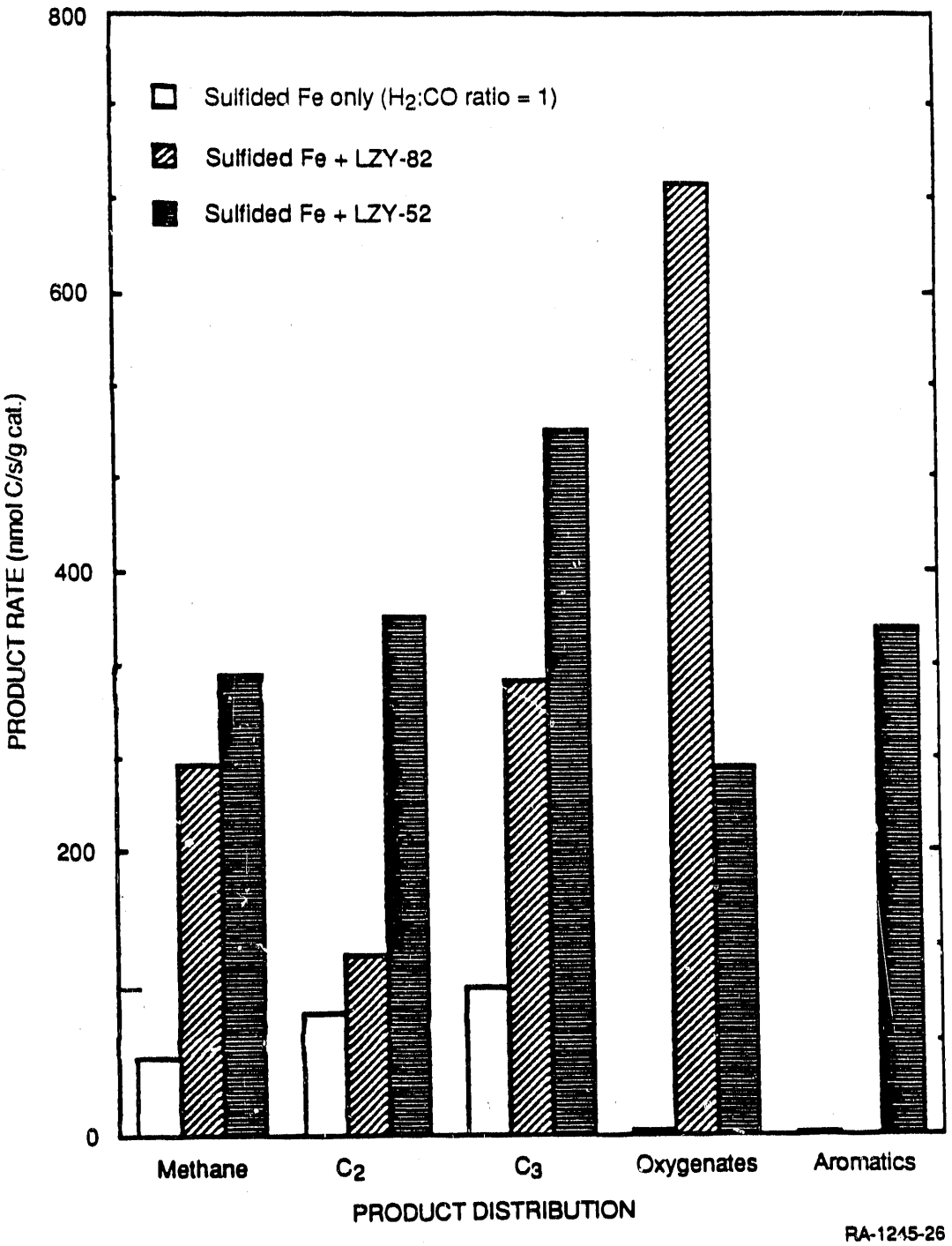

Figure III-2. Aromatic synthesis at 2 MPa, 573 K, H_2/CO ratio = 0.5, on mixed medium-level sulfur-treated fused iron and Na-Y zeolite catalysts (1:4 weight ratio).

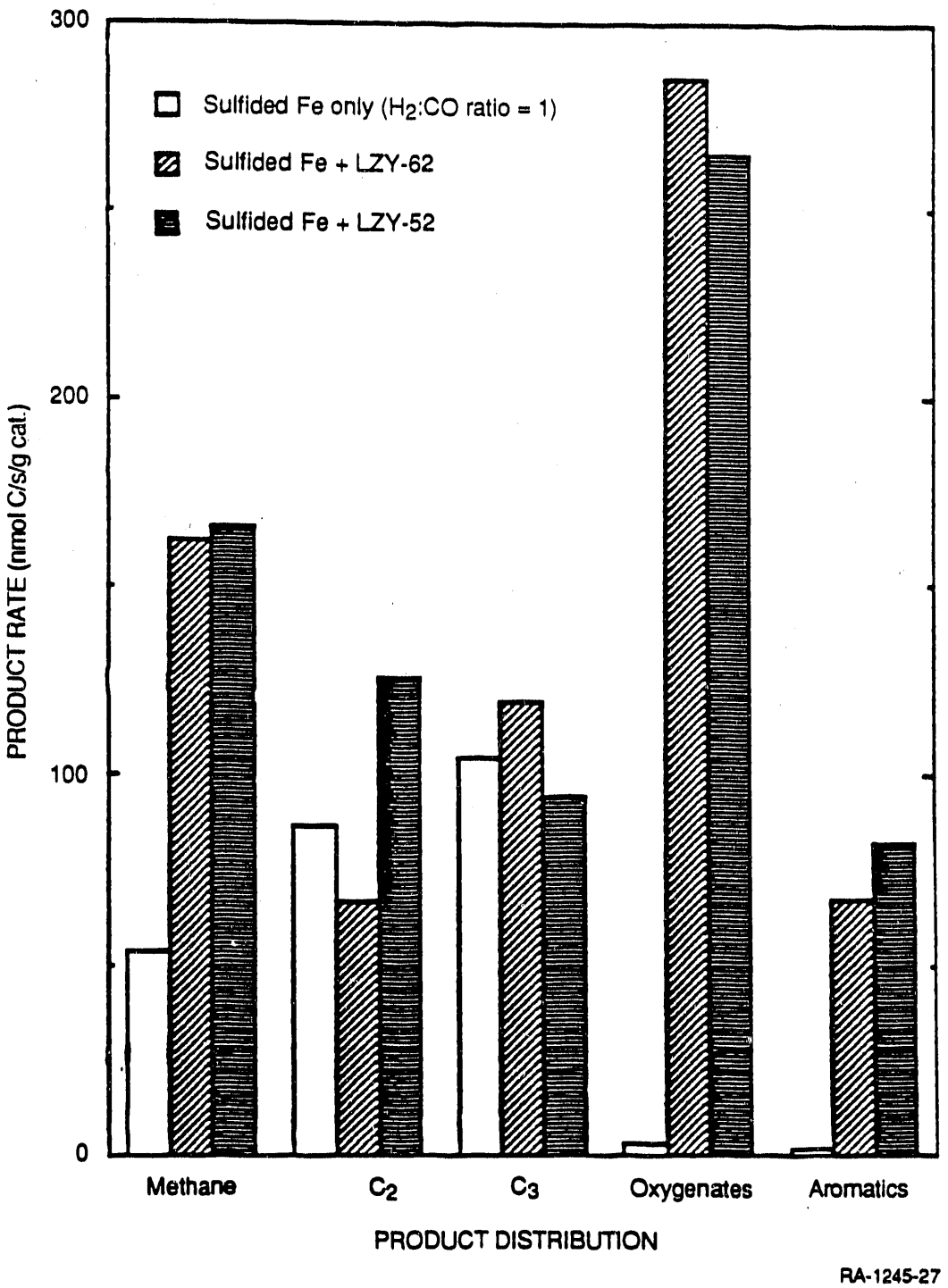

Figure III-3. Aromatic synthesis at 2 MPa, 573 K, H_2/CO ratio = 0.5 on medium-level sulfur-treated fused iron catalyst and Na-Y zeolites (1:10 wt ratio).

Table III-2

SYNTHESIS OF AROMATICS AND OXYGENATES BY MIXTURES OF SULFUR-TREATED RUTHENIUM AND ZEOLITE CATALYSTS

Catalyst	Clean 2.4 wt% Ru/Al_2O_3 + LZY-52 Zeolite (1 to 10 wt ratio)		Medium-level Sulfur-treated 2.4 wt% Ru/Al_2O_3 + LZY-52 Zeolite (1 to 10 wt ratio)	
Temperature (K)	598	573	598	573
Pressure (MPa)	2	2	2	2
H_2/CO ratio	0.5	0.5	0.5	0.5
Duration (h)	2	2	2	2
Product rate[a] (nmol/s/g cat)				
C_1	22.96	5.20	23.44	10.32
C_2	2.37	0.55	2.55	1.14
C_3	1.72	0.89	2.33	1.56
C_4	1.11	0.84	1.56	1.42
Oxygenates	1.83	1.31	4.63	7.27
Aromatics	0.20	0.54	0.89	2.03
TOTAL				
Chain Growth Factor[b]	0.48	0.55	0.50	0.66
1-Butenes to Butane Ratio[c]	0.44	0.73	0.52	0.62
Methane Selectivity[d]	50.90	26.30	37.90	16.10
Oxygenates Selectivity	9.70	15.60	17.80	27.50
Aromaties Selectivity	2.10	13.50	7.64	16.80

[a]GHSV = 600 h^{-1}; Product rate for each carbon number includes n-paraffins and α- and β-olefins; total product rate is on a carbon-atom basis.

[b]Average chain growth parameter (α) for C_{3+} hydrocarbons.

[c]Average olefin to paraffin ratio for C_2 to C_6 hydrocarbons.

[d]C_1 rate/(total rate) x 100%.

20% and was relatively insensitive to temperature (Table III-1). The aromatics yield increased threefold with a corresponding decrease in methane yield by increasing the reactor temperature from 573 K to 650 K (Figure III-4). However, an additional increase in reactor temperature to 700 K resulted in more rapid deactivation of the zeolite catalyst without additional enhancement in aromatics selectivity or syngas conversion.

The yield of aromatics in the synthesis product using the mixed sulfur-treated iron and zeolite catalyst may have been limited by low conversion of the syngas. The presence of unreacted hydrogen and product water vapor perhaps inhibited the dehydrocyclization reaction and favored the formation of dimethylether and methanol, which can be considered intermediates for aromatic hydrocarbons on zeolite catalysts such as HZSM-5.[1,2] The acidic properties of the low-sodium zeolite enhanced oxygenate and aromatic hydrocarbon formation but also enhanced cracking and led to more rapid deactivation of the catalyst.

Since the strong acidic sites in the zeolite are responsible for the formation of aromatics by the dehydrocyclization of the C_6 olefins, the observed decrease in oxygenates and aromatics selectivity with time can be attributed to the progressive deactivation of these sites by coking. The deactivation of the zeolite component of the catalyst resulted in loss of isomerization and dehydrocyclization activity to formed aromatics and isoparaffins. Using of a higher weight ratio of zeolite to FTS catalyst in the mixed bed mode prolonged the activity and increased oxygenates and aromatics selectivity.

The consumption of light olefins, which are essential building blocks for aromatics, to form oxygenates effectively decreased the selectivity of aromatics in the product. The formation of aromatics may be the rate-limiting step of overall conversion of methanol to aromatics on HZSM-5.[1] The cracking and hydrogenolysis of intermediate olefin products apparently led to low aromatics yield and to carbon deposition on the zeolite components of the mixed catalyst.

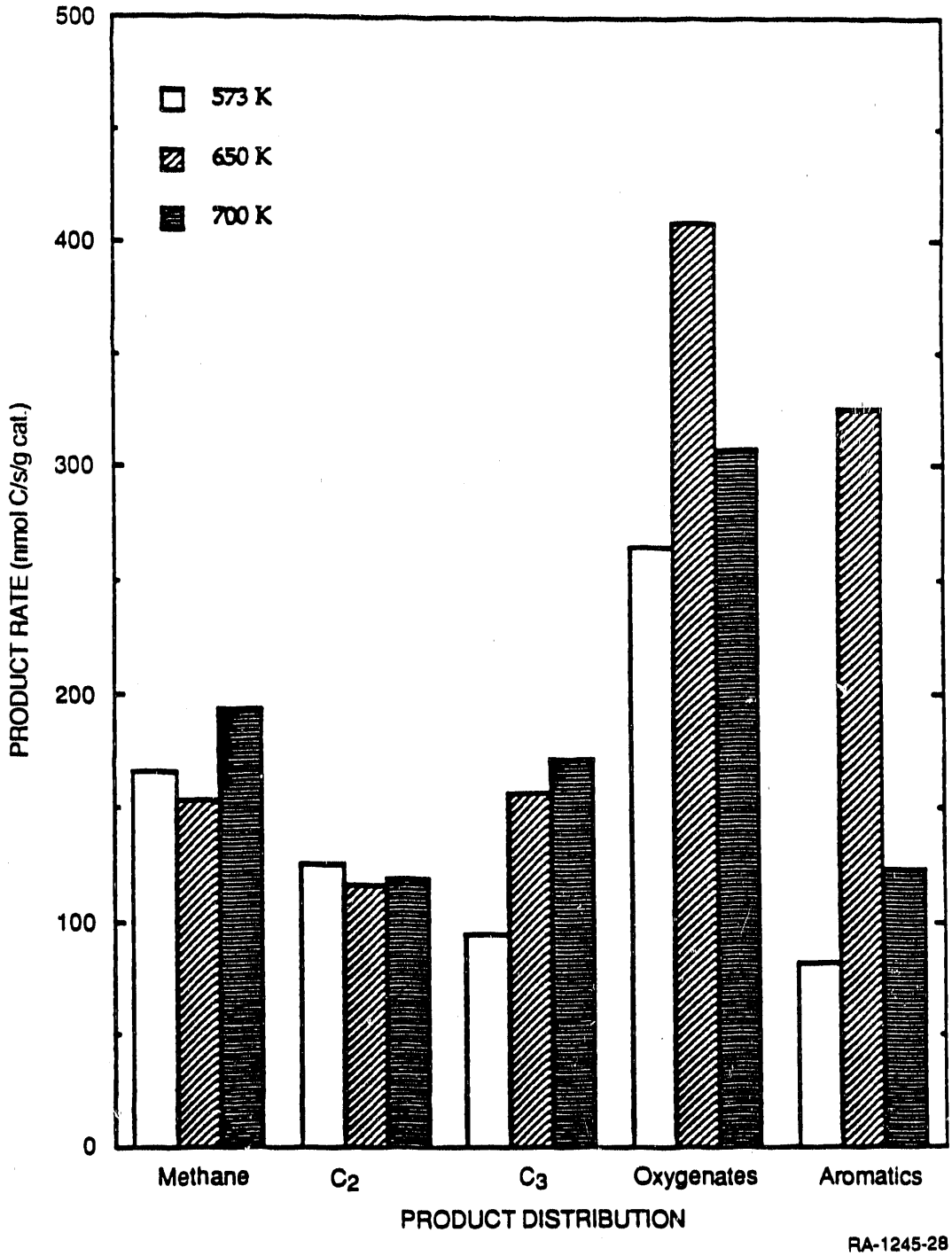

Figure III-4. Effect of temperature on the synthesis of oxygenates and aromatics at 2 MPa and H_2/CO = 0.5 with medium-level sulfur-treated fused iron catalyst and LZY-52 zeolite (1:10 wt ratio).

Conclusions and Recommendations

Combinations of low and moderate sodium exchanged Y zeolites with a coking-tolerant sulfur-treated fused iron catalyst readily convert FTS product olefins into alcohol and aromatic products in a fixed-bed reactor at 2 MPa pressure, 573 to 650 K temperature, and low CO conversion (<10%). Similar results have been obtained at lower temperature and higher H_2/CO ratio (1.0). We had expected coking of the FTS component of the catalyst to be important at the higher temperatures and lower hydrogen syngas used in our study. Despite the high coking conditions at $H_2/CO = 0.5$ and 650 K, the FTS component did not deactivate and continued to produce relatively high FTS rates. Deactivation of the sodium Y-zeolite function was observed, however.

Our selection of the zeolite component was not optimal, and a more systematic search for a coking-tolerant acid catalyst is recommended. The addition of Na to the acidic Y zeolite we used was apparently insufficient to prevent moderately rapid coke formation (around 2 h). The sodium may also have contributed to the high selectivity for oxygenates, since it has been recently shown that Pd with an alkali exchanged ZSM-5 support generates high oxygenate yields in syngas.[23]

Clearly, shape selectivity is important in reducing coking rates. A small-pore high-silica zeolite that can reject coke precursors is a more desirable choice than Y or X silica-alumina zeolites. ZSM-5 is generally regarded as having low coking tendency because of its low Al content and its small pore sizes. Rare earth exchanged ZSM-5 class zeolites may have more optimal coking resistance and acidity sufficient to effect rapid rates of conversion of olefins to aromatics. The CO and, especially, hydrogen conversion must also be increased to improve the hydrocarbon selectivities. Producing high yields of aromatics without rapid acid deactivation may not be possible because of coking. Coke formation may simply parallel aromatics production. Acceptable rates of conversion of olefin intermediates to aromatics may simply require high acidity (which generally means greater Al content in the zeolite), which in turn results in unacceptable deactivation rates.

References

1. C. D. Chang, W. H. Lang, and A. J. Silvestry, J. Catal. 56, 268 (1979).

2. C. D. Chang and W. H. Lang, Mobil Oil, U.S. Patent 4180516 (1979).

3. W. H. Seitzer, Suntech, U.S. Patent 4139550 (1979).

4. U.S. Rao, R. J. Gormley, H. W. Pennline, L. C. Schneider, and R. Obermyer, ACS Div. of Fuel Chem. Preprints 25(2), 119 (1979).

5. A. Shamsi, U. Rao, R. J. Gormley, R. T. Obermyer, R. R. Schehl, and J. M. Stencel, Ind. Eng. Chem. Prod. Res. Dev. 23, 513 (1984).

6. L. Bruce, G. T. Hope, and J. F. Mathews, Appl. Catal. 9, 351 (1984).

7. R. L. Varma, K. Jothimurugesan, N. N. Bakhshi, J. F. Mathews, and S. H. Ng, Can. J. Chem. Eng. 64, 141 (1986).

8. R. L. Varma, D.-C. Liu, J. F. Mathews, and N. N. Bakhshi, Can. J. Chem. Eng. 63, 72 (1985).

9. H. W. Pennline, V.U.S. Rao, R. J. Gormley, and R. B. Schehl, ACS Div. Fuel Chem. Preprints 28, 164 (1983).

10. T. J. Huang and W. O. Haag, ACS Symposium Series 152, 307 (1981).

11. R. L. Varma, N. N. Bakhshi, J. F. Mathews, and S. H. Ng, Ind. Eng. Chem. Res. 26, 183 (1987).

12. T. Inui, T. Hagiwara, and Y. Takegami, Sekiyu Gukkaishi, 27, 228 (1984).

13. K. Fujimoto, Y. Kndo, and H.-O. Tominaga, J. Catal. 87, 136 (1984).

14. B. Bussemeier, C. D. Frohring, G. H. Horn, and W. Kluy, German Offen. 2,518,964 and 2,536,488 assigned to Ruhrchemie AG (1976).

15. R. Malessa and M. Baerns, Ind. Eng. Chem. Res. 27, 279 (1988).

16. J. Abbot, N. J. Clark, and B. G. Baker, Appl. Catal. 26, 141 (1986).

17. W. D. Deckwar, Y. Serpemen, M. Ralek, and B. Schmidt, Ind. Eng. Chem. Process Des. Dev. 21, 222 (1982).

18. S. Schechter and H. Wise, J. Phys. Chem. 83, 2107 (1979).

19. M. P. Manning and R. C. Reid, Ind. Eng. Chem. Process Des. Dev. 16, 358 (1977).

20. M. E. Dry, Applied Industrial Catalysis 3, 167 (1983).

21. J. Rostrup-Nielsen, presention at the 10th North American Meeting of the Catalysis Society (to be published in Appl. Surf. Sci., 1987).

22. B. J. Wood, C. M. Ablow, and H. Wise, Appl. Surf. Sci. 18, 429 (1984).

23. R. T. Thomson and E. E. Wolf, Appl. Catal. 41, 65 (1988).

END

DATE
FILMED
5/20/92